

Graduate School of
Systemic Neurosciences
LMU Munich

Lee Simon-Vermot

22 12 2017

**Association Between
Resting-State Functional Connectivity,
Glucose Metabolism And
Task-Activation Of Neural Networks**

Dissertation der Graduate School of Systemic Neurosciences
der Ludwig-Maximilian Universität München

**ASSOCIATION BETWEEN RESTING-
STATE FUNCTIONAL CONNECTIVITY,
GLUCOSE METABOLISM AND TASK-
ACTIVATION OF NEURAL NETWORKS**

Dissertation at the Graduate School of
Systemic Neurosciences

Submitted by: Lee Simon-Vermot 22.12.2017

Defended on: 04.05.2018

First supervisor & reviewer: Prof. Dr. Michael Ewers

Second supervisor & reviewer: Prof. Dr. med. Axel Rominger

Third reviewer: Dr. Kathrin Koch

External reviewer: Dr. David Bartrés-Faz

ABSTRACT

The brain is organized into several large-scale functional networks. Such networks are primarily characterized by intrinsic functional connectivity, i.e. temporally synchronous activity between the different brain regions of a network. The functional connectivity of networks can be identified via functional MRI during resting state, i.e. without engaging the subject in a particular task. Resting-state fMRI is thus less demanding on the subject and therefore of particular interest from a clinical point of view to detect alterations in brain function. Applied to neurodegenerative disease including Alzheimer's disease, resting-state fMRI has shown alterations in several resting-state networks, suggesting that basic network function is altered in AD. However, the interpretation of alterations in resting-state fMRI connectivity is inherently limited since no cognitive states are explicitly expressed during fMRI. In this regard, we aimed to elucidate how resting-state fMRI connectivity relates to 1) cognition-related brain activity and 2) markers of pathologically altered brain function in AD. In order to understand at a more basic level the association between resting-state and task-related fMRI, we first examined, in a group of elderly healthy subjects, the association between functional connectivity of major networks assessed during resting-state fMRI with those acquired during memory-task related fMRI, in the same individuals. Secondly, in order to assess whether alterations in AD are associated with already well-established markers of pathological brain function in AD, we compared resting-state fMRI functional network connectivity with that in FDG-PET metabolism in AD.

Project 1: We investigated the association between functional connectivity acquired during rest and the level of activation obtained during an episodic memory task that included the encoding and forced-choice recognition of face-name pairs in elderly cognitively normal subjects. Independent component analysis (ICA) was used to identify major resting-state networks in the brain. Next, we applied ICA to the task-fMRI data to determine the components (networks) that were significantly associated with the task regressors of successful vs unsuccessful learning or recognition trials. Spatial correlation analysis between the resulting extracted resting-state and task-related fMRI components showed a spatial match in several components such as medial temporal lobe centered components and posterior components. However, apart from the spatial correspondence, the level of resting state functional connectivity did not predict the level of task-related functional connectivity in spatially matching components. Together these results suggested that particular resting-state networks are activated during a memory task, however, the level of baseline connectivity does not predict to what extent a network becomes activated during a task. Future studies may assess whether pathological resting-state connectivity predicts altered task-related connectivity in the same networks in AD.

Project 2: We examined the association between resting-state fMRI functional connectivity within major functional networks and FDG-PET metabolism in those networks, assessed in elderly healthy controls, subjects with prodromal AD (mild cognitive impairment and amyloid PET biomarker confirmed AD etiology) and AD dementia. We found that FDG-PET was generally reduced in all networks in the course of AD. The main finding was that lower network functional connectivity was associated with lower FDG-PET uptake in the Default mode network and fronto-parietal attention network across the whole group and specifically in prodromal AD, suggesting that both

modalities are associated in higher networks affected in the course of AD. These results provide insightful comprehension of the hypometabolism patterns that are typically found in AD.



CONTENT

ABSTRACT	I
CONTENT	IV
ABBREVIATIONS	VI
01 . INTRODUCTION	1
1.1. large scale networks relevance in health & disease	1
1.1.1. Brain organization in large scale intrinsic networks	1
1.1.2. Large scale networks during rest.....	2
1.1.3. Resting-state network impairments in aging and disease	4
1.1.4. Clinical relevance of rs-fMRI	5
1.1.5. Overall goal of this thesis	6
1.2. Functional Magnetic resonance imaging.....	7
1.3. Resting-State Networks in relation to TASK fMRI & episodic memory	9
1.3.1. Resting-state networks & cognition	9
1.4. Implication of large scale networks in AD.....	12
1.4.1. Alzheimer’s Disease	12
1.4.2. rsfMRI changes in AD	14
1.4.3. FDG-PET changes in AD.....	15
1.5. Open questions.....	16
02 . INTRINSIC AND EPISODIC MEMORY-TASK RELATED NETWORKS IN ELDLERY SUBJECTS	19
2.1. Summary	20

2.2. Reference	20
03 . FDG-PET METABOLISM AND RESTING-STATE NETWORK CONNECTIVITY ARE ASSOCIATED IN EARLY ALZHEIMER’S DISEASE.....	51
3.1. Summary	52
3.1. Reference	52
04 . DISCUSSION.....	90
4.1. General discussion	90
4.1.1. Functional networks engaged during successful memory and encoding	91
4.1.2. Association of FDG-PET metabolism & resting-state connectivity in AD	94
4.2. Implications across projects.....	96
4.3. Outlook.....	97
4.4. Limitations	98
05 . REFERENCES.....	99
06 . APPENDIX	110
CURRICULUM VITAE	111
LIST OF PUBLICATIONS.....	113
ACKNOWLEDGMENTS.....	114
EIDESSTATTLICHE VERICHERUNG / AFFIDAVIT	115
DECLARATION OF AUTHOR CONTRIBUTIONS	116

ABBREVIATIONS

Aβ	amyloid β peptide
AD	Alzheimer's disease
aDMN	Anterior default mode network
BOLD	Blood oxygen level dependent
DMN	Default mode network
FC	Functional connectivity
FDG	¹⁸ F-Fludeoxyglucose
fMRI	Functional magnetic resonance imaging
FPAN	Fronto-parietal attention network
ICA	Independent component analysis
MCI	Mild cognitive impairment
MRI	Magnetic resonance imaging
PET	Positron emission tomography
rsFC	Resting-state functional connectivity
rsfMRI	Resting-state functional magnetic resonance imaging
RSN	Resting-state network
TC	Time course



01.

INTRODUCTION

1.1. LARGE SCALE NETWORKS RELEVANCE IN HEALTH & DISEASE

1.1.1. Brain organization in large scale intrinsic networks

Higher cognitive abilities such as episodic memory are supported by multiple brain regions that show temporally coordinated activity (Vuilleumier & Driver, 2007). These regions form large scale functional networks (Bressler & Menon, 2010). Mesulam (Mesulam, 1990) was the first to report - based on the observation of brain lesions and neurological conditions -that cognitive functions rely on a set of large-scale networks. Since, the emergence of functional magnetic resonance imaging (fMRI), a noninvasive neuroimaging technique (for details refer to the next section on pages 7-8), has greatly contributed to the better understanding of neural functions and networks. Findings from fMRI studies during resting state (rsfMRI), when the person is not engaged in a particular task performance, suggest that the inherent neural architecture of a network doesn't

“connect” solely during a given cognitive state, but is primarily characterized by ongoing intrinsic functional connectivity. Studying the brain at rest, in absence of any input or task requirements, offers an opportunity to easily investigate the intrinsic functional connectivity within large-scale functional networks.

1.1.2. Large scale networks during rest

rsfMRI has allowed the identification of a set of resting-state networks (RSN), which are essentially defined by intrinsic resting-state functional connectivity (rsFC) i.e. synchronized time courses of spontaneous blood oxygen level dependent (BOLD) signal between distinct brain regions. It has been suggested that the slow fluctuations that are measured during resting-state reflect a network “standby” state, that serves to maintain the functional networks integrity while keeping the energy costs low (Fox & Raichle, 2007). The first RSN that was discovered, somewhat accidentally, by analyzing the slow fluctuations that occur during rest, was the default mode network (DMN). Since then a dozen of large-scale networks can consistently be identified during resting-state. These RSN share, to a large extent, the same topology as patterns of co-activation that are related to cognitive tasks (Damoiseaux et al., 2006; Daselaar, Huijbers, Eklund, Moscovitch, & Cabeza, 2013; Hedden et al., 2009; Smith et al., 2009), which include RSNs that range from those related to more basic cognitive functions such as visual, auditory or motor networks but also more complex cognitive functions such as fronto-parietal attention network (FPAN), executive network and DMN.

The DMN is a network that shows higher activity during rest compared during performance on tasks that require attention to external stimuli (Mazoyer et al., 2001; M E

Raichle et al., 2001; Shulman et al., 1997). Anatomically, the DMN comprises the medial frontal cortex, the precuneus and adjacent posterior cingulate cortex and retrosplenial cortex, the lateral parietal lobule and angular gyri and the medial temporal lobe, including the hippocampus (Buckner, Andrews-Hanna, & Schacter, 2008; Horn, Ostwald, Reiser, & Blankenburg, 2013). The DMN deactivates during externally oriented tasks, such as episodic memory encoding, working-memory or tasks that required attention to external stimuli and plays a central role in performing cognitively demanding tasks (Weissman, Roberts, Visscher, & Woldorff, 2006). The DMN can be further divided into anterior and posterior subnetworks. The anterior portion of the DMN (aDMN), comprising the medial frontal cortex is thought to be related to internally directed processes, such as autobiographical memory, thinking of the future and considering what others think or plan (Andrews-Hanna, Reidler, Sepulcre, Poulin, & Buckner, 2010). In contrast, the fronto-parietal attention network (FPAN) (also called dorsal attention network) shows the exact opposite activation pattern with decreased activation during rest and increased activation during externally oriented tasks (Carbonell et al., 2014; Chai et al., 2014; Fox et al., 2005). The FPAN comprises separate highly interconnected cortical regions in the lateral prefrontal cortex and temporo-parietal regions or hubs that regulate other functional networks such as the visual or auditory networks, motor network and salience network, depending on the type of cognitive task (Smith et al., 2009). Typically tasks that require maintaining or manipulating various sources of information while dealing with the other sources of stimuli, are memory and attention related tasks, including episodic memory recall or recollection and working memory. Such complex tasks are considerably impaired in normal aging (Anderson & Craik, 2000; Balota, Dolan, & Duchek, 2000; Grady & Craik, 2000; Kelley & Jacoby, 2000; Zacks, Hasher, & Li, 2000) and moreover in AD

(Alescio-Lautier et al., 2007; Blennow, Leon, & Zetterberg, 2006; B.C. Dickerson & Sperling, 2009; Minati, Edginton, Grazia Bruzzone, & Giaccone, 2009; Perry, Watson, & Hodges, 2000).

1.1.3. Resting-state network impairments in aging and disease

The age-related decline leads to difficulties in daily life, that are not solely due to sensory processing problems, but rather to changes in episodic memory, processing speed, working memory and executive functions (Hedden & Gabrieli, 2004). Several studies postulate that the age-related cognitive decline is not only the result of regional brain changes but also due to functional connectivity disruption with large-scale networks (Andrews-Hanna et al., 2007). Large-scale networks including the DMN and FPAN support the cognitive features that are most impaired with age. The DMN is mostly affected in its anterior to posterior components (Andrews-Hanna et al., 2007). Older adults tend to have increased levels of activation in the fronto-parietal regions, that overlap with the DMN and FPAN, and hypo-activation in the occipital regions (Li et al., 2015). The increased activation in the fronto-parietal regions is thought to compensate for the deficits in sensory processing (Reuter-Lorenz & Park, 2010, 2014). Age-related changes in the activation of the FPAN, DMN have been observed in various tasks and have been linked to worse performance in episodic memory (Grady, 2012). Because of its simplicity of application, rsfMRI provides a useful tool to investigate brain changes that are associated with normal age-related or AD-related decline. Studying the brain of elderly people during rest has shown altered iFC of major RSN in many age-related neurodegenerative diseases such as AD.

In AD, regions overlapping with the DMN, are the first to be affected in early stages, such as mild cognitive impairment (Binnewijzend et al., 2012; Chhatwal et al., 2013; Greicius, Srivastava, Reiss, & Menon, 2004; Seeley, Crawford, Zhou, Miller, & Greicius, 2009) or in healthy elderly with elevated amyloid-beta ($A\beta$) burden (Bai et al., 2008; Buckner et al., 2005; Hedden et al., 2009; Koch et al., 2015; Rombouts, Barkhof, Goekoop, Stam, & Scheltens, 2005; Sorg et al., 2007).

1.1.4. Clinical relevance of rs-fMRI

Resting-state fMRI is very attractive for clinical assessments, provided is task-free and therefore particularly easy and less stressful to implement in clinical procedures to assess brain damage or dysfunction in patients suffering from cognitive impairment or AD. The relevance of studying the brain at rest in order to gain insight in a clinical context has been shown by a couple of studies (Damoiseaux et al., 2008; Greicius, 2004). However, rsfMRI is obtained in absence of overt cognitive performance. Furthermore, the interpretability of rsFC changes that occur in age-related diseases remains poorly explained, although changes have consistently been observed. In order to better understand the clinical relevance of altered rsFC within large-scale networks, the relation with other well-established measures needs to be elucidated. Two main approaches are commonly used in clinical procedures to evaluate the degree of cognitive impairment or brain changes. The first approach is based on neuropsychological test batteries, which enable to determine the level of impairment in one or more cognitive domains. One of the first cognitive domains to be impaired in aging is episodic memory and more severe episodic memory problems may indicate an elevated risk of developing AD in the coming years (Gauthier et al., 2006; Jorm, Christensen, Korten, Jacomb, & Henderson, 2001). Moreover,

the first changes in rsFC are noticed in RSNs that overlap with brain regions involved in episodic memory (Celone et al., 2006; Chhatwal et al., 2013; M. Greicius, 2004; Hedden et al., 2009; Sorg et al., 2007; Sperling et al., 2010). Recently proposed guidelines for diagnosis of AD (Mckhann et al., 2011) recommend the use of biomarkers to aid the clinical diagnosis of AD. Among neuroimaging based biomarkers of functional brain damage, ¹⁸F-Fludeoxyglucose positron emission tomography (FDG-PET) is the best-established imaging method. FDG-PET measures glucose metabolism in the brain. In AD posterior parietal and temporal brain regions show reduced levels of FDG-PET assessed glucose metabolism already at an early stage of the disease. Glucose metabolism is particularly reduced in the temporal and posterior parietal region and frontal regions as the disease progresses, regions that overlap with the DMN (for review (Herholz, 2003)).

Even though changes in rsFC occur in regions involved with episodic memory and reduced glucose metabolism co-occurs in similar regions and at very early stages of AD, the association between rsFC changes and other well-established clinical procedures remains poorly understood.

1.1.5. Overall goal of this thesis

During the last two decades, extensive fMRI research has generated deeper understanding of the brain's intrinsic network organization and its relevance in health, aging and neurodegenerative diseases. However, the relation between altered large-scale network rsFC and other recognized measures, such as glucose metabolism and episodic memory is still lacking. Hence the aim of this thesis is to better understand how large-scale rsFC changes are associated with brain activation during an episodic memory task as a

cognitive measure. The second aim was to test whether rsfMRI assessed functional network connectivity is related to FDG-PET metabolism and shows comparable sensitivity to detect AD related functional brain impairment. To this end, two studies were conducted. In the first study, we investigated the association between functional networks related to successful episodic memory encoding and recall during a face-name association task as well as during resting-state in healthy elderly subjects. In the second study we assessed the association between FDG-PET metabolism and resting-state functional connectivity in subjects with AD dementia and controls.

1.2. FUNCTIONAL MAGNETIC RESONANCE IMAGING

Brain activity can be investigated with functional MRI, a non-invasive imaging method that measures the BOLD signal (Buxton, 2009; Logothetis & Wandell, 2004; Marcus E Raichle & Mintun, 2006). The BOLD signal captures the difference in magnetic properties of hemoglobin and deoxyhemoglobin. When hemoglobin releases its oxygen to the tissue, the amount of deoxyhemoglobin increases and disrupts the MRI magnetic field proportionally to the amount of oxygen that was used by the surrounding tissue. Neural activity increase is coupled with a high increase in cerebral blood flow and glucose consumption that surpasses the actual oxygen need. This surplus of oxygenated hemoglobin leads to a local decrease in the amount of deoxyhemoglobin in the blood and the BOLD signal is increased in the area of high neural activity. The changes in BOLD signal can be analyzed in various ways, in order determine for example which areas are activated by a given task or which areas are functionally connected during resting-state.

When fMRI is used to investigate brain activation during a cognitive task, where the BOLD signal changes in relation to stimuli (event-related design) or blocks of stimuli (i.e. block design) are tested. The BOLD signal time course of each voxel of the brain is then correlated with the task design, in order to assess whether there is a significant increase in brain activation that is associated with the task compared to baseline or a control condition. This approach enables to relate the neural activity of a given region to perceptual or cognitive processes that are thought to be triggered by the task. When investigating the brain in absence of tasks, different strategies can be used to extract the rsFC. One way to analyze FC, is to extract the BOLD signal time course (TC) from a predefined “seed region” and to correlate it with the TC of all the remaining brain voxels. Although this technique is simple and its interpretation is quite straight forward, it requires determining the seed regions based on an a priori hypothesis and is consequently limited to study system at a time. One way to circumvent these constraints is to apply techniques, such as independent component analysis (ICA). ICA is a data-driven approach to decompose the BOLD signal into a set of spatially independent components each of which is associated with a specific time course. ICA is commonly used to identify RSNs, but can also be used to extract networks related to a task. One of the still unanswered questions is: which brain networks are related to episodic memory and how are these related to know RSNs?



1.3. RESTING-STATE NETWORKS IN RELATION TO TASK FMRI & EPISODIC MEMORY

1.3.1. Resting-state networks & cognition

Studying the brain at rest has gained increasing interest in the last decades. Although a dozen of large-scale networks can consistently be identified during resting-state, it remains unclear how they are related to cognition. A major question is whether intrinsic connectivity between brain regions detected during resting-state is predictive of task-related brain activation. In a meta-analytic study that included 30'000 subjects with task-derived activation maps for different cognitive domains, Smith and colleagues were able to show that the networks extracted from task and from rest showed very close correspondence. This suggests that the brain regions that are intrinsically connected are more likely to be co-activated during a cognitive task (Smith et al., 2009). Many studies have combined task-fMRI and rsfMRI to try to better understand how the rsFC might be associated to the activation during a task. Most of the studies have used relatively simple tasks, such as motor (Arfanakis et al., 2000; Cole, Bassett, Power, Braver, & Petersen, 2014; Jiang, He, Zang, & Weng, 2004; Tavor et al., 2016), visual (Arfanakis et al., 2000; Fair et al., 2007) or language (Arfanakis et al., 2000; Cole et al., 2014; Elton & Gao, 2013; Fair et al., 2007; Tavor et al., 2016) to investigate whether rsFC and task evoked activity are independent of each other or not. Most studies report a spatial correspondence between rsFC networks and patterns of brain activation during visual, auditory or motor tasks. The use of more complex cognitive tasks, including working memory (Cole et al., 2014; Elton & Gao, 2013; Tavor et al., 2016), emotion (Cole et al., 2014; Elton & Gao, 2013; Tavor et al.,

2016) or executive functions (Cole et al., 2014; Elton & Gao, 2013) have confirmed that these findings also apply to more elaborate cognitive states. A recent study showed that rsFC alone can be used to predict the individual variability in various task activation patterns (Tavor et al., 2016). Still, remarkably few studies investigated episodic memory using rsfMRI and task-related fMRI together. In a recent study, Huijbers and colleagues, showed that activation related to episodic memory span various networks (Huijbers et al., 2013), suggesting that episodic memory relies on the interaction between multiple networks. The fact that episodic memory doesn't rely on a unique, clear-cut network, may in part explain why so few studies have investigated the relation between episodic memory task and RSNs at the network level.

Episodic memory relates to the capacity to encode and retrieve personal experiences in space and time, but also to build associations between previously unrelated items, such as names and faces. Encoding and retrieval processes rely on distinct cortical regions (Gabrieli et al., 1997 in (Chetelat et al., 2003; Sestieri et al., 2011). Various task-related fMRI studies have shown that these abilities are supported by the medial temporal lobe as well as a set of cortical areas, including the medial and lateral parietal and frontal regions, areas that overlap with the DMN (Dickerson et al., 2010, Nature Reviews). Encoding relies on a coordinated and reciprocal increase of activity in the fronto-parietal network together with the anterior part of the hippocampus, coupled with a deactivation of the posterior DMN (Daselaar, Prince, & Cabeza, 2004). In contrast, during recall, the activation patterns reverse, with an increase in activation of the DMN and the posterior portion of the hippocampus is activated (Bradford C Dickerson & Eichenbaum, 2010; Kahn, Andrews-hanna, Vincent, Snyder, & Buckner, 2008; Kim, 2015; Libby, Ekstrom, Ragland, & Ranganath, 2012; Wagner, Shannon, Kahn, & Buckner, 2005; L. Wang et al.,

2010; Ward et al., 2014). The activation of the DMN during episodic memory retrieval rather than encoding is in line with the general role of the DMN for supporting inwardly-directed, self-referential processing since recollection demands the retrieval of internal stimulus representations. It has also been shown that the magnitude of task-related deactivation in the posterior portions of the DMN are correlated with successful episodic memory and moreover that less deactivation was correlated with poor performance in elderly subjects (Miller et al., 2008). The DMN is thought to deactivate during external oriented processes, such as memory encoding and activate during internally oriented processes, such as memory retrieval. This change between deactivation and activation in the regions that are deactivated during encoding and subsequently activated during recall have been referred to as the “Encoding-retrieval flip” (Sander M. Daselaar et al., 2009; W Huijbers et al., 2012a; Kim, Daselaar, & Cabeza, 2010; Vannini et al., 2013). RsFC changes in these regions have been correlated with memory performance (Goveas et al., 2013). However, the relationship between resting-state connectivity and task-related activity still remains unclear.

Surprisingly few studies have investigated the association between episodic memory related networks and RSNs. A question that has still not been answered is which intrinsic networks are related to successful episodic memory encoding and retrieval? Moreover, understanding the link between RSNs and activation during successful episodic memory in elderly subjects, would be of importance to better understanding the memory worsening that occurs with older age and in age-related diseases such as AD.

1.4. IMPLICATION OF LARGE SCALE NETWORKS IN AD

1.4.1. Alzheimer's Disease

Alzheimer's disease is the most frequent age-associated neurodegenerative disease and the most frequent cause of dementia, accounting for 60-80% of all dementias. The prevalence of AD in 2017 in the United-States is estimated to be 5.5 million people, this includes about 5.3 million over the age of 65 (Hebert, Weuve, Scherr, & Evans, 2013). Given that the number and proportion of the population to reach 65 and older is exponentially increasing, as the baby boom generation is getting older, the amount of people who will develop AD is estimated to almost double from 48 million to 88 million by 2050 (He, Goodkind, & Kowal, 2016).

The most important risk factor for late-onset AD is age (Querfurth & LaFerla, 2010). Indeed, the proportion of elderly people with AD expands drastically with age: 3 percent of people age 65-74, 17 percent of people age 75-84 and 32 percent of people age 85 or older (*2017 Alzheimer's disease facts and figures*, 2017; Hebert et al., 2013). Generally after 60 years old, neurodegenerative processes of AD gradually lead to disturbances of cognitive, memory and behavioral functions with subsequent loss of function in performing day-to-day tasks and ultimately to death (Blennow et al., 2006).

The neurodegenerative processes of AD starts about 20-30 years before the clinical manifestations emerge (Petersen, 2004). This phase is commonly known as mild cognitive impairment (MCI), which is a syndrome of cognitive decline substantially more pronounced than expected for an individual's age and educational level, but not severe enough to constitute dementia. Usually these patients have slight cognitive impairment,

yet not enough to remarkably interfere with daily life activities. About 15 to 20 percent of people over the age of 65 years old have MCI (Roberts & Knopman, 2013). The amnesic subtype has a particularly high risk of evolving into AD and is therefore considered as a prodromal stage of AD (Gauthier et al., 2006; Petersen, 2004). In over half of the cases, MCI progresses to dementia within five years. The first symptoms insidiously appear as an amnesic syndrome, typically as difficulties in forming and retaining new episodic memories. Memory function typically degrades progressively for several years before impairments in other cognitive domains emerge, such as attention, executive functions, visuospatial functions or language (Gauthier et al., 2006; McKhann et al., 1984; Petersen, 2004).

Neuropathological features of AD

The two main neuropathological features of AD are the extracellular accumulation of amyloid-beta ($A\beta$) plaques and the intracellular accumulation of protein Tau neurofibrillary tangles, which lead to neurodegeneration and in turn to the manifestation of clinical symptoms (Querfurth & LaFerla, 2010; Scheltens et al., 2016). The loss of neuronal structures and functions is not specific to AD, however the locations where atrophy and neuronal activity may occur does allow to distinguish from other neurodegenerative diseases. Typically $A\beta$ plaques and Tau tangles tend to accumulate in brain regions involved in episodic memory and that overlap with the DMN (Buckner et al., 2005; Dickerson & Sperling, 2009; Klunk et al., 2004; Myers et al., 2014; Price & Morris, 1999; Shin, Kepe, Small, Phelps, & Barrio, 2011). Various biomarkers can be used to evaluate the level of degeneration. For example structural MRI allows to measure the medial temporal lobe atrophy, reduced hippocampal volume is present at early stage of

AD already (Karow et al., 2010). Neurodegeneration and reduced brain function is also associated with glucose consumption. Studies using FDG-PET have consistently shown that glucose metabolism is strongly reduced in temporo-parietal and posterior cingulate cortex and moreover that this pattern of hypometabolism predicts the conversion from MCI to AD with a high accuracy (de Leon et al., 2001; Mosconi, 2005). An explanation that helps understand why glucose metabolism and AD pathology spreads throughout regions that overlap with the DMN, is the cascading network failure. This theory postulates that the first AD-related impairments occur in posterior DMN and only subsequently in anterior subsystems of the DMN. These impairments result in a transient increase in connectivity in the posterior regions (consistently found in aging and MCI) that leads to a possibly detrimental increased metabolic demands (Jones et al., 2016).

1.4.2. rsfMRI changes in AD

Resting-state fMRI offers the advantageous opportunity to non-invasively investigate brain changes in AD. The results in MCI and AD patients consistently show a progressive rsFC loss in the DMN, as well as in other RSNs including the FPAN, executive network and sensory motor-network (Brier et al., 2012; Sheline & Raichle, 2013a). The most frequent and well reproduced finding is a reduction of rsFC that starts in the posterior portions of the DMN and then progresses to the anterior portion (Greicius et al., 2004; for review: Sheline & Raichle, 2013; Sorg, Riedl, Pernecky, Kurz, & Wohlschläger, 2009). RsfMRI is very sensitive to very early and subtle changes. rsFC in the DMN is reduced, before cognitive impairments occur in asymptomatic subjects with genetic risk of AD, the (Chhatwal et al., 2013) or with elevated A β (Hedden et al., 2009). One explanation of why the first rsFC changes are found in the DMN, may be that these regions are the first to

gather accumulations of A β , and reductions of glucose metabolism (Benzinger et al., 2013; Buckner et al., 2008; Drzezga et al., 2011; Förster et al., 2012; Mutlu et al., 2016).

1.4.3. FDG-PET changes in AD

FDG-PET is a well-established measure to assess brain function and level of AD related neurodegeneration. FDG-PET measures the local metabolic rate of glucose consumption and thereby a reduction of FDG-PET uptake indicates loss of neurons and synaptic activity (Herholz, Carter, & Jones, 2007; Mosconi, 2005). In AD, glucose metabolism is particularly reduced in the temporal and posterior parietal region and frontal regions as the disease progresses (for review (Herholz, 2003)), areas that overlap with the DMN and regions that have high levels of A β (Vlaskovska et al., 2010). Similarly to rsFC changes in the DMN, medial temporal and parietal FDG-PET hypometabolism predicts conversion to MCI and AD (de Leon et al., 2001; Mosconi, 2005). FDG-PET is also sensitive enough to pick up changes in subjects at risk of AD (Drzezga et al., 2011). Altogether it seems that FDG-PET hypometabolism and rsFC pick up similar aspects of AD and the spatial overlap of both modalities has been largely reported, however the question of whether and how they might be related, remains unanswered.

Few previous studies have jointly studied both modalities. A study of combined fMRI and FDG-PET has shown that in healthy elderly subjects, higher FDG-PET metabolism in visual areas was associated with higher FC in the visual and saliency regions, suggesting that FDG-PET metabolism reflects at least partially brain activity as measured by FC (Riedl et al., 2014). In subjects with early stage AD, i.e. A β positive MCI patients, reduced whole brain FC within the posterior cingulate cortex was related to hypometabolism in the same

cortical regions (Drzezga et al., 2011), suggesting a local correspondence between FDG-PET hypometabolism and FC. Both of these studies focused only on small brain regions and not on large-scale intrinsic network. Di & Biswal were the first to show that networks similar to RSNs could be identified based on FDG-PET metabolism and that the metabolic covariance in these networks was comparable to the rsfMRI FC in these networks (Di, Biswal, & Alzheimer's Disease Neuroimaging Initiative., 2012). Unfortunately, in this study FDG-PET and rsfMRI were collected in two different groups of subjects. Savio and colleagues used simultaneously acquired FDG-PET and rsfMRI in a single group of middle aged healthy subjects and could extract a set of spatially overlapping RSNs from FDG-PET images and rsfMRI images. This further supports the idea that RSNs share common underlying neural mechanisms, but does not answer the question of whether glucose metabolism and rsFC are associated at the network level in the course of AD.

1.5. OPEN QUESTIONS

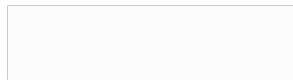
The overall aim of this thesis was to assess the association and spatial correspondence between large-scale networks rsFC and well-established clinical measures in order to better interpret the significance of RSNs and their disease-related alterations. As a measure of brain activity, we chose well-established clinical markers of aging and AD, including episodic memory task-related brain activity, as a cognitive measure and glucose metabolism, as a more basic measure of brain activity. Previous studies, mostly assumed the association between rsFC and other biomarkers based on the topographical overlap that was observed (Di et al., 2012; Di, Gohel, Thielcke, Wehrl, & Biswal, 2017; Savio et al., 2017), which gives a hint that both are related, but does not necessarily imply that they are associated. Few studies combined both rsFC and episodic memory or FDG-PET

modalities, but to our knowledge, none have until now associated both rsFC and episodic memory task activation patterns or FDG-PET patterns in the same subjects at the level of networks. To complete his gap and go one step further, we wanted to see if the rsFC in major resting-state networks can be used to predict the level episodic memory task activation of the level of FDG-PET uptake in the same networks.

Project 1: In the first project we aimed to understand the association between resting-state connectivity and task-related fMRI. We first examined in a group of elderly healthy subjects the association between functional connectivity of major networks assessed during resting-state fMRI with those acquired during a face-name association episodic memory-task related fMRI, in the same individuals. ICA was used to identify components related to successful episodic memory encoding and recognition during task-fMRI as well as during rsfMRI. Besides the assessment of spatial correspondence between components related to successful episodic memory, we aimed to test if resting-state network connectivity is predictive for the level of task-related activation.

Project 2: In the second project, we aimed to investigate whether resting-state network alterations in AD are associated with already well established markers of pathological brain function in AD, to this end we compared resting-state fMRI functional network connectivity with patterns of FDG-PET metabolism in 27 amyloid-beta negative healthy controls, 44 amyloid positive MCI patients and 25 patients with AD. ICA was used separately for both rsfMRI and FDG-PET to estimate large-scale components. First the spatial correspondence of networks issued from rsfMRI and FDG-PET was compared. Second, the association between the rsFC and mean FDG-PET signal was computed for

each major RSN component separately using linear regression. We hypothesized that higher rsFC would be associated with higher mean FDG-PET in major RSNs.



02.

INTRINSIC AND

EPISODIC MEMORY-

TASK RELATED

NETWORKS IN ELDLERY

SUBJECTS



2.1. SUMMARY

The aim of this project was to understand the association between resting-state connectivity and episodic memory task-related fMRI. To this end, we examined, in a group of elderly healthy subjects, the association between functional connectivity of major networks assessed during resting-state fMRI with those acquired during a face-name association episodic memory-task related fMRI. Independent component analysis was used to identify components related to successful episodic memory encoding and recognition during task as well as during rsfMRI. Besides the assessment of spatial correspondence between components related to successful episodic memory during task and rsfMRI, we also aimed to test if resting-state network connectivity is predictive for the level of task-related activation.

2.2. REFERENCE

The paper was published in *Frontiers in Aging Neuroscience* under the following reference:

Simon-Vermot L, Taylor ANW, Araque Caballero MÀ, Franzmeier N, Buerger K, Catak C, Janowitz D, Kambeitz-Ilankovic LM, Ertl-Wagner B, Duering M and Ewers M (2018).

Correspondence Between Resting-State and Episodic Memory-Task Related Networks in Elderly Subjects. *Frontiers in Aging Neuroscience, 10*, 362. doi: 10.3389/fnagi.2018.00362

The author of this thesis is the first author of the manuscript. ME, MD, LMKI, ANWT & LSV conceived and designed the experiment. ANWT, MÀAC, NK & LSV conducted the fMRI data acquisition. LSV and ANWT analyzed the behavioral and fMRI data. LSV and ME wrote the manuscript, which was commented on and reviewed by ANWT, MÀAC, NK, KB, LMKI & BEW.

**Correspondence between resting-state and episodic memory-task related networks
in elderly subjects**

Frontiers in Aging Neuroscience, November 2018.

doi: 10.3389/fnagi.2018.00362

Lee Simon-Vermot^a, Alexander N.W.Taylor^b, Miguel À Araque Caballero^a, Nicolai Franzmeier^a, Katharina Buerger^{a,c}, Lana M. Kambeitz-Illankovic^d, Birgit Ertl-Wagner^e, Marco Duering^a and Michael Ewers^{a,*}

^aInstitute for Stroke and Dementia Research, Klinikum der Universität München, Ludwig-Maximilians- Universität LMU, Munich, Germany

^bDepartment of Psychology, University of Southampton, Southampton, UK

^cGerman Center for Neurodegenerative Diseases (DZNE, Munich), Munich, Germany

^dDepartment of Psychiatry and Psychotherapy, Ludwig-Maximilians-Universität LMU, Munich, Germany

^eInstitute for Clinical Radiology, Klinikum der Universität München, Ludwig-Maximilian University, Munich, Germany

* Correspondence to Dr. Michael Ewers, Institute for Stroke and Dementia Research, Klinikum der Universität München, Feodor-Lynen Str. 17, 81377 Munich, Germany.

Tel: +49 89/440046221, E-mail: michael.ewers@med.uni-muenchen.de

Acknowledgement statement (including conflict of interest and funding sources):

The study was funded by ERC career integration grant (PCIG12-GA-2012-334259 to ME), LMUexcellent (to ME) and Alzheimer Forschung Initiative (to ME).

Conflicts of interest: none

ABSTRACT

Resting-state fMRI (rsfMRI) based assessment of brain activity has revealed the existence of intrinsic functional networks, which are inherent to the brain organization and function. The resting-state functional connectivity (rsFC) within intrinsic networks is thought to be a proxy of brain activity during tasks. Still, the relation between rsFC and task-related activity remains incompletely understood. Previous findings in young subjects have shown that regions that are functionally connected during rest also become activated during specific tasks. However, none of the known intrinsic networks seems to be directly related to episodic memory (EM). A rsfMRI predictor of EM would be of great interest, particularly in the case of age-related diseases. Hence, the aim of this study was first to identify networks related to successful EM and subsequently to assess whether rsFC within these networks is predictive for the level of task-related brain activity. To this end, fMRI was acquired during both rsfMRI and face-name association tasks in 38 healthy elderly subjects. ICA was used to extract networks related to successful EM encoding and recognition as well as resting-state networks (RSNs). Spatial match between networks related to successful EM and RSNs was assessed. Finally, regression was used to predict task-related network activity based on rsFC. We found that networks centered in temporal, middle temporal and frontal areas showed increased activity during successful encoding and networks situated in posterior brain regions were related to successful recognition. However, rsFC was not predictive of the task-related activity in these networks. These results suggest that particular intrinsic networks become engaged in successful episodic memory, but higher intrinsic connectivity at rest may not translate into higher network expression during episodic memory. **Keywords: Resting-state fMRI, task fMRI, episodic memory, resting-state network.**

INTRODUCTION

Functional MRI (fMRI) based assessment of brain activity during resting-state has gained a rapidly growing interest over the last couple of decades. Resting-state fMRI studies demonstrated the functional connectivity between different brain regions, suggesting the existence of intrinsic functional networks in the brain. Changes in resting-state connectivity in networks have been described in normal aging and most major psychiatric and neurodegenerative diseases (for review see Ferreira & Busatto, 2013). From a clinical point of view, resting-state fMRI is of particular interest since the task-free fMRI assessment is easier to obtain in patients and thus may provide an attractive way to assess functional brain damage. The rationale is that resting-state fMRI assessed network connectivity is a proxy for brain activity during particular cognitive processes such as episodic memory (Andrews-Hanna et al., 2010). However, since resting-state fMRI is obtained without overt cognitive performance the understanding of the relationship between intrinsic network connectivity and task-related connectivity is an open question (Elton and Gao, 2015; Shirer et al., 2012). Meta-analysis of task-based studies in more than 30,000 subjects showed task-related co-activation patterns that mapped onto major resting-state networks (Smith et al., 2009), suggesting that regions intrinsically connected during resting-state become simultaneously activated during tasks. Several studies assessing functional connectivity during both resting-state and task-related fMRI in young healthy subjects have largely confirmed such a hypothesis for a variety of cognitive tasks (Calhoun et al., 2008; Cole et al., 2014; Greicius et al., 2003). In fact, resting-state fMRI activity levels in the brain were found together with morphological brain differences to be predictive of the spatial pattern of brain activation during perception and higher cognitive abilities such as

language and working memory (Tavor et al., 2016). These studies suggest a spatial match between resting-state networks and those patterns of task related brain activation. Most previous combined resting-state and task-related fMRI studies focused on tasks based on visual or auditory perception (Arfanakis et al., 2000; Bartels and Zeki, 2005; Cole et al., 2014; Elton and Gao, 2015; Fair et al., 2007; Tavor et al., 2016), motor function (Arfanakis et al., 2000; Cole et al., 2014; Ganger et al., 2015; Jiang et al., 2004; Morgan and Price, 2004; Tavor et al., 2016), attention (Calhoun et al., 2008; Hellyer et al., 2014; Tomasi et al., 2014), language (Arfanakis et al., 2000; Cole et al., 2014; Elton and Gao, 2015; Fair et al., 2007; Hampson et al., 2010) or working memory function (Cole et al., 2014; Elton and Gao, 2015; Fransson, 2006; Tavor et al., 2016). Strikingly there is a dearth of studies testing the match between episodic memory related networks and resting-state networks. Huijbers and colleagues (2013) assessed in which resting-state networks activation peaks obtained during an episodic memory task fall, but did not attempt to test which resting-state networks showed task-related connectivity. A possible explanation for the lack of studies is the fact that none of the canonical set of large-scale resting-state networks corresponds to known patterns of episodic memory processes (Smith et al., 2009). From a clinical point of view, the establishment of a match between resting-state and episodic memory related network connectivity is of great importance to assess network failure underlying memory impairment in aging and neurodegenerative disease including Alzheimer's disease (Meskaldji et al., 2016; Zhang et al., 2016). In order to address this research gap, we assessed fMRI during both resting-state fMRI and an episodic memory task including face-name association learning in cognitive elderly subjects. Specifically, using independent-component analysis (ICA) (Calhoun et al., 2001), we assessed the

association between functional networks related to successful encoding or recognition and resting-state networks. In addition to testing the spatial match between task-related networks and resting-state networks, we assessed whether resting-state component values are predictive of the level of the task-related network expression during successful encoding or successful recognition. We hypothesized that especially medial temporal components show a match between resting-state and memory-task related networks. Secondly, we hypothesized that the level of resting-state networks is predictive of the level of task-related network connectivity in medial temporal lobe components.

MATERIALS AND METHODS

Subjects

For the current study, 38 cognitively healthy Elderly (HC) participants (age > 60) were included. All subjects were recruited at the Memory Clinic of the Institute for Stroke and Dementia Research (Klinikum der Universität Munich, Germany). In order to be classified as HC, the older adults had to perform within 1.5 SD of age and education adjusted norms on the neuropsychological tests included in the CERAD-Plus test battery. Exclusion criteria were: Presence of depressive symptoms, evidence of other acute or past neurological/psychiatric disorders, history of drug or alcohol abuse, diabetes mellitus, premorbid IQ < 85 and MRI contraindications such as presence of ferromagnetic implants, pacemakers or cochlear implants. The participants' assessment was completed in two visits: on the first day, the subjects underwent a neuropsychological and physical examination, followed by a structural MRI (T1 MPRAGE, FLAIR, DTI) and resting-state functional MRI (rsfMRI). On the second day,

the participants performed a face-name association task fMRI and subsequently rsfMRI. The study was approved by the ethics committee of the Ludwig Maximilian University, Munich. All participants provided written informed consent. The rsfMRI scan was acquired before the task fMRI ($n = 30$) or within 1 - 12 weeks after the task-fMRI ($n = 8$).

fMRI Memory task

The face-name task contained 112 encoding and 112 recognition trials, divided into 14 blocks of face-name encoding (of 8 trials), each followed by a recognition block (of 8 trials). A total of 112 different faces were used ($\frac{1}{2}$ female, $\frac{1}{2}$ male) from the Glasgow Unfamiliar Face Database (<http://www.abdnfacelab.com>). The criteria of selection for faces were direct gaze, European ethnicity, neutral expression and no face jewelry or hair accessories to standardize the facial features across different images. 168 different names ($\frac{1}{2}$ female, $\frac{1}{2}$ male) were selected from the Leipzig Corpora Collection (<http://corpora.informatik.uni-leipzig.de>) matched for character length (5 or 6 letters) and frequency of occurrences. During an encoding trial, a photo of face and a first name shown below were presented and the participant was instructed to learn the name belonging to the particular person shown. During the subsequent recognition block the faces previously seen in the encoding block were presented again, but this time together with two juxtaposed names, one correct and one distractor. The participant had to decide, via left or right button press, which of the two names had been presented previously with that face. In each recognition trial, the presented distractor could be either a new name (that had never been seen before) (56 trials) or a name that had been associated with another face in the previous encoding block (56 trials). Each

stimulus was presented for 5 seconds with a randomized inter-trial-interval (ITI) of 1500-3000 ms between trials through vision goggles attached to the head coil, which could be corrected for individual eyesight differences. Correctly recalled trials were labeled as successful recognition and incorrectly recognition trials as unsuccessful recognition. The classification of encoding trials as successful or unsuccessful was determined based on whether the corresponding face-name pair was correctly recalled. The ratio of successfully recalled trials, relative to the total amount of trials assess the subject's performance. The participants trained before the task on a laptop. The whole task took about 30 minutes to complete.

MRI parameters

A Siemens Verio 3T MRI scanner was used for all the scans. The functional task was acquired with a 12 channel head coil and a T2*-weighted echo-planar imaging (EPI) pulse sequence with 3mm x 3.4 mm x 3.4 mm slices (inter-slice gap = 1mm; echo time (TE) = 30ms, repetition time (TR) = 2000ms; flip angle = 90°; parallel acquisition (GRAPPA) with acceleration factor 2; field of view (FOV) = 220 x 220 mm; 64 x 64 data acquisition matrix). A high-resolution MPRAGE T1-weighted sequence with 1mm slices in the sagittal plain (interval time (TI) = 900 ms; TE = 2.52 ms; TR = 1750 ms; Flip angel = 90°; phasing encoding anterior to posterior; FOV = 256 x 256 mm²; matrix = 246 x 256; single acquisition) was used for the structural image. Field maps were acquired to enable the post-hoc correction of susceptibility artifacts (same parameters as the EPI, TE = 4.92/7.38 ms, TR = 488 ms and flip angle = 60°). For the resting-state fMRI acquired on the subject's first visit, a 32 channel head coil was used and an 8 minutes T2*-weighted echo-planar imaging (EPI) pulse sequence with 3.5mm voxel resolution

was acquired. The participants were instructed before the resting-state scan to keep their eyes closed and not to fall asleep.

fMRI preprocessing and Analysis

Preprocessing

The preprocessing was done using SPM12 (Wellcome Trust Centre for Neuroimaging, UCL, London, UK). All images (T1 and EPI (task and rest) and field map images) were manually reoriented to the anterior commissure and angled to the posterior commissure. The T1-weighted MPRAGE scans were segmented into grey matter (GM), white matter (WM) and cerebro-spinal fluid (CSF) maps. The diffeomorphic high dimensional transformations were estimated based on the three segments using the DARTEL tool implemented in SPM12. The resulting GM group template was co-registered to the (affine) MNI template in SPM12 and the two transformation matrices (high-dimensional and affine) were combined for spatial normalization into the MNI space.

The task and resting-state EPI images were slice-time corrected, realigned and unwrapped applying the field map to account for scanner inhomogeneity variations. None of the subjects' motion parameters were larger than 3 mm translation or 2 degrees rotation. Subsequently, for each participant, the images were co-registered to the individual's T1 image and normalized to MNI space by applying the transformation parameters estimated through DARTEL. An 8 mm Full width half maximum (FWHM) smoothing kernel was applied and the smoothed images were resampled to 1.5 mm voxel resolution. For resting-state images only, a linear trend was removed and a band

pass filter was applied to remove frequencies between 0.01 and 0.08 Hz. WM and CSF signal were regressed out of the time series voxel by voxel.

General Linear Model

A fixed-effects general linear model was used to test increased activation during correct vs incorrect trials of encoding or recognition. We created the regressors with time onsets for each stimulus presentation and convolved the time series with a canonical hemodynamic function, including six motion parameters, temporal and dispersion derivatives. Six regressors were included in the model (successful encoding, unsuccessful encoding, successful recognition, unsuccessful recognition, encoding instructions and recognition instructions). The regression models were computed at subject level for subsequent group analyses (see Statistics below).

Independent Component Analysis

We applied group independent component analysis (ICA) to decompose the fMRI data into a set of components, where spatial independence between components is defined based on maximizing the independence of the voxel-based BOLD time series between sets of voxels. The GIFT toolbox (GroupICAT v4.0a, <http://mialab.mrn.org/software/gift/>) was used to perform such a group spatial ICA using the Infomax algorithm (Bell and Sejnowski, 1995), separately for task fMRI and resting-state fMRI. For the task fMRI, we used the minimum description length algorithm (MDL) to estimate the ideal number of spatially independent components (IC) (Li et al., 2007), which resulted in 24 ICs. Prior to the estimation the image time courses were intensity normalized to a mean of 100. The ICA was repeated 20 times using ICASSO (Himberg et al., 2004), to verify that the component estimates were stable. The subject-specific spatial maps and associated time courses were generated

via back-reconstruction using the GICA3 method (Himberg et al., 2004). For rsfMRI, we applied the ICA with a fixed number of ICs ($n=24$). This number was chosen in order to have a comparable number of ICs for both tasks and rsfMR. The data was first preprocessed across subjects so that the image time courses are scaled to the same global mean, this was done by extracting the mean per time point from each volume.

For the ICA on task fMRI, the association between a components time course and the task-design matrix was assessed via temporal sorting. To this end, regressors including the temporal onset and duration of each stimulus were constructed for each of the four trial types: “successful_encoding”, “unsuccessful_encoding”, “successful_recognition” and “unsuccessful_recognition”. This resulted for each participant into 4 beta-coefficients for each component. In order to test which component’s time course was significantly associated with correct encoding or correct recognition, we applied a one-sample t-test to the beta-weights across subjects. For those components that showed a significant association of the BOLD signal with stimulus presentation during either correct encoding or correct recognition we subsequently tested via two-sample t-test if the association was higher for successful vs unsuccessful condition. In order to spatially match the thus determined task-related components of either successful encoding or recognition against the rsfMRI components, we conducted spatial regression analyses between each pair of any of those task-related and any resting-state IC maps, i.e. Pearson product-moment correlations across z-score transformed voxel values of any given pair of IC maps. In addition, to test whether any matching components corresponded to previously established resting-state networks, we computed spatial regression between those ICs and template sets of 10 and 70 ICA components that were previously established based on resting-state fMRI scans (Smith et al., 2009). The

spatial overlap was further quantified with the Dice similarity coefficient. Specifically, both the Smith maps and task ICA components were thresholded at 3 and were binarized, using the threshold $z > 1$ and the Dice coefficient of the overlap between the binarized resting-state and task-associated IC maps were computed. The Dice coefficient were computed as the ratio of the number of voxels within overlapping regions of a given pair of binarized ICs and the total number of voxels of the two ICs. and is interpreted as following: <0.2 poor, $0.2-0.4$ fair, $0.4-0.6$ moderate, $0.6-0.8$ good and >0.8 excellent correspondence. Bonferroni correction was applied to correct for multiple testing.

Statistical Analysis

For the memory task-related fMRI brain activation, the contrasts “successful_encoding > unsuccessful_encoding” and “successful_recognition > unsuccessful_recognition” were modeled for each individual, while correcting for age and gender. At the group level, the assessment of increased activation for successful encoding and successful recognition was computed using a full factorial model in which these contrasts were specified: “successful_encoding > unsuccessful_encoding” and “successful_recognition > unsuccessful_recognition”. The significance threshold was set at $p=0.001$ at the voxel level and FWE-corrected at $p=0.05$ at the cluster level.

To assess whether higher network activation was present for successful encoding and successful recognition we computed paired t-tests on the beta-values comparing “successful_encoding > unsuccessful_encoding” and “successful_recognition > unsuccessful_recognition”. Before computing the paired t-test, all the data was checked for outliers and removed if the standard deviation was larger than 3. The normal distribution of the data was tested with the Shapiro test. The Shapiro test was

significant for recognition_correct for network 8 (posterior parietal network), networks 9 (frontal) and 21 (auditory) for incorrect recognition. For these networks, a Wilcoxon signed rank test was used.

Next we aim to examine - beyond the spatial correspondence between group-level resting-state and task-related ICs - the predictive value of the expression of resting-state IC for predicting the degree of task-related activity of the spatially corresponding IC. To this end, we conducted a linear regression analyses according to: $Y_i \approx X_i + \text{Age}_i + \text{Gender}_i + \varepsilon$. Where Y_i is the predicted subject's beta-value of given task-related IC and X_i is a subject's beta value of the spatially matching resting-state IC. The beta-coefficient Y to be predicted was derived in the previous regression analysis regression an IC time course onto the task-design matrix of either successful encoding or recall trials. The beta-coefficient X of the corresponding resting state IC was computed by regressing the subject-specific resting-state IC time-course onto the group-level IC time course, i.e. the beta-coefficient X indicates to what extent a group IC was expressed in a given subject. We corrected for type-1 error due to multiple comparison by applying Bonferroni correction.

RESULTS

Demographics details are displayed in table 1.

Brain activation during successful memory

Voxel-based GLM analysis of face-name task fMRI showed significant activation for successful encoding > unsuccessful encoding in fronto-temporal and parietal region of the left hemisphere (voxel-level threshold $\alpha=0.001$ and FWE corrected cluster level at $\alpha=0.05$, see Figure 1, left panel and table 2 for cluster statistics and peak locations). For

successful recognition > unsuccessful recognition we found bilateral clusters of activation mainly in the medio-frontal, posterior-cingulate, occipital and inferior temporal as well as in the hippocampus (voxel-level threshold $\alpha=0.001$ and FWE corrected cluster level at $\alpha=0.05$, see Figure 1, right panel and table 3 for cluster statistics and peak locations).

ICA-based Network activity during successful encoding and recognition

Paired t-tests were computed in order to find the networks that show higher task-related activity during successful encoding compared to unsuccessful encoding. The same comparison was done between for successful vs unsuccessful recognition. For encoding, time courses of four ICs showed higher task-related variation during correct vs incorrect trials a) medial orbito-frontal network ($t(37)=2.0$, $p=0.026$), b) lateral temporal-frontal network ($t(37)=2.74$, $p=0.0047$) c) occipital network ($t(37)=7.91$, $p<0.0001$) and d) hippocampal network ($t(37)=3.85$, $p<0.001$) (Figure 2, left panel). For recognition, three ICs showed higher task-related BOLD signal variation during correct vs incorrect trials for: a) posterior parietal network ($t(37)=1.84$, $p=0.037$), b) occipital network ($t(36)=1.98$, $p=0.025$) and c) posterior cingulate-occipital network ($V(36) = 561$, $p = 0.0006$, Figure 3).

Spatial correspondence between task-related and resting-state networks

For each of the four task-related components associated with successful encoding, spatial regression analysis showed a unique match to a particular rsfMRI component, including a medial-orbito-frontal component ($r=0.68$, $p <0.0001$, Figure 2A), lateral fronto-temporal component ($r=0.39$, $p <0.0001$, Figure 2B), visual component ($r=0.61$, $p <0.0001$, Figure 2C) and the hippocampal component ($r=0.74$, $p <0.0001$, Figure 2D).

For each of the 3 task-related components associated with successful recognition, spatial regression analysis showed a unique match to rsfMRI components for the posterior parietal network ($r=0.64$, $p < 0.00001$, Figure 3A), the posterior-cingulate-occipital network ($r=0.57$, $p < 0.0001$, Figure 2B) and the occipital network ($r=0.45$, $p < 0.0001$, Figure 2C). All presented p -values are Bonferroni corrected for multiple testing.

To ensure that the spatial correlation found between task-associated networks and rest is not solely present within our sample, we computed the spatial correlation between the seven task activated network and the intrinsic resting-state networks reported previously in an independent sample (Smith et al., 2009). Spatial regression of these components (based on task for group rsfMRI) with *a priori* derived rsfMRI components based on a 10 component ICA rsfMRI analysis (Smith et al., 2009) yielded no significant spatial overlap ($p > 0.05$). When applying the spatial regression based on the 70 component ICA analysis (Smith et al., 2009), we found significant spatial overlap for all seven task-fMRI components associated with either successful encoding or successful recognition ($p < 0.0001$, details are listed in Table 4 and Figure 4).

Prediction of network activity during successful encoding and recognition based on rsfMRI network expression

As a last step, we aimed to see whether a subject's network activity during successful performance on the episodic memory task could be predicted at subject's level of expression of the spatially corresponding resting-state network. No association was found ($p > 0.05$).

DISCUSSION

The major findings of the current study were that task-related activity of 1) networks within the medial temporal lobe and temporal and medial frontal cortex were associated with successful memory encoding and 2) networks primarily within the posterior parietal and occipital brain regions were associated with successful memory recognition. Each of these networks showed a spatial match to resting-state components. However, higher resting-state connectivity did not predict higher task-related network activity for these networks. Together these results suggest that particular intrinsic networks become engaged successful episodic memory, but higher intrinsic connectivity at rest may not translate into higher network expression during episodic memory.

Our first findings showed that medial temporal and frontal networks were engaged during successful encoding but posterior parietal and occipital networks were engaged during successful recognition. These results are largely consistent with those of a recent meta-analysis of brain activation during episodic-memory task, demonstrating increased activation of the hippocampus, lateral prefrontal cortex, and lateral temporal brain areas during encoding, hippocampal and posterior parietal activation during recognition memory (Kim, 2015). Our findings are also consistent with previous findings of successful encoding-related hippocampus activity during face-name association learning in young subjects (Sperling et al., 2003; Zeineh et al., 2003) and cognitively healthy older subjects (Pariente et al., 2005). In contrast, our task-related activity in the posterior parietal brain regions during successful recognition but not encoding is consistent with the previous proposed encoding/retrieval flip hypothesis of stronger engagement of the posterior parietal brain regions during retrieval compared

to encoding (Daselaar et al., 2009). Activity in the occipital brain areas were associated with both successful encoding and recognition owing to the visual presentation of the stimuli on both conditions. Together, the current findings of the ICA based analysis of task-related brain activity recapitulates largely previous fMRI activation studies on episodic memory.

For our second finding, we identified for each task-related network a unique match of a resting-state network. Importantly, in the current study those networks obtained during both task and rest corresponded to resting-state network components previously reported in an independent study using high dimensional ICA (i.e. $N = 70$ estimated ICs). In contrast, no significant overlap was found with large-scale networks, although a partial overlap with the DMN was evident for the medial temporal network during encoding and the posterior cingulate-occipital network during recognition. These findings suggest that smaller functional clusters rather than the entire large-scale networks are recruited during successful episodic memory. Our findings of such a spatially circumscribed successful memory related functional connectivity, also explains why the matching of large-scale resting state networks to episodic memory related patterns of brain activity among the canonical set of resting-state networks has been difficult so far (Smith et al., 2009). Large-scale networks such as the DMN and fronto-parietal controls networks are not singular networks but heterogeneous in nature (Cole and Schneider, 2007; Power et al., 2011), containing several distinct subcomponents where each supports different cognitive functions (Cole and Schneider, 2007; Cole et al., 2013). Subcomponents may be selectively activated during memory (Shirer et al., 2012) and couple across different large-scale networks in a task-dependent manner (Bassett et al., 2011). For the DMN regions, we found that task-

related network activity during successful retrieval overlapped with DMN selectively in posterior parietal regions. This is consistent with previous findings of the posterior parietal brain regions to be selective for successful retrieval of more “objective” facts (for meta-analysis see Spaniol et al., 2009), such as those tapped by the current recognition task of face-name pairs. In contrast, previous findings on autobiographical memory, i.e. memory of more personal events, have been found in both anterior and posterior regions of the DMN (Elton and Gao, 2015; Spreng and Grady, 2010). The selective involvement of the anterior medial frontal DMN may be specifically required for supporting self-referential processes during autobiographic memory (Andrews-Hanna et al., 2010; Sestieri et al., 2011). Together the current findings suggest the involvement of intrinsically wired networks that depart from large-scale canonical networks and match smaller clusters that are selectively recruited during successful episodic memory encoding and retrieval.

For our third result, we did not find the level of connectivity during resting-state to be predictive of the level of task-related connectivity. Note that this approach is fundamentally different from identifying intrinsic networks that may be recruited during a task (i.e. finding a spatial match), where in this case the strength of resting-state connectivity is probed as a predictor of task-related network “activation”. Results from a seminal previous study suggested that the task-induced activation is the additive combination of ongoing resting-state network connectivity and task-specific recruitment of neural activity (Fox et al., 2006). In fact, during a finger-tapping task that led to unilateral motor cortex activation, functional connectivity of the non-activated contra-lateral motor cortex explained over 85% of the task-related activity in the activated side of the motor cortex (Fox et al., 2006). The current results are not in

conflict with previous results; rather they suggest that a higher resting-state connectivity per se does not translate into higher task-related synchronization of brain activity in that network. A recent study reported resting-state network connectivity to be predictive of task-related activity (Tavor et al., 2016). However, it is important to note that only the spatial extent and distribution of task-related brain activity was assessed and not the level of task-related connectivity or activation was predicted. Thus, that predictive power derives mostly from the spatial match between resting-state and task-related networks.

For the interpretation of the current results, some caveats must be taken into consideration. It is possible that task-related network activation couldn't be predicted based on resting-state network connectivity, due to the measures we used as proxies of network "expression". For resting-state we used values (time course) that express the strength of connectivity within a given network for given subject, in relation to group mean. For task-related activation we used the beta-values for each subject, as used in (Vannini et al., 2013). Concerned by the fact that, both might measure different processes and therefore fail to yield to significant results, we computed the regressions again; this time using network connectivity, in the same way as calculated for rest. The findings were comparable. Signaling that the first findings were most probably not due to the measures we used. There are many ways to analyze functional connectivity during resting-state and during task, all of which have their strengths, weaknesses, and vary in their interpretation. Although different methods merit to be investigated, this is not the focus of the current study. Another possibility could be that the successful episodic memory task-specific activation that is thought to be an additive effect on the ongoing resting-state activity is a too small difference in HC. This difference could be

changed in psychiatric diseases, such as Alzheimer's disease. The association between episodic memory task activated networks and their equivalents in rest should be investigated in the future.

In conclusion, we could show that specific networks are specifically activated during successful episodic memory and are also present during resting-state. The level of connectivity within these networks during resting-state was however not predictive of the level of task-related activation.

REFERENCE

- Andrews-Hanna, J.R., et al., 2010. Functional-anatomic fractionation of the brain's default network. *Neuron*. 65, 550-62.
- Arfanakis, K., et al., 2000. Combining independent component analysis and correlation analysis to probe interregional connectivity in fMRI task activation datasets. *Magn Reson Imaging*. 18, 921-30.
- Bartels, A., Zeki, S., 2005. Brain dynamics during natural viewing conditions--a new guide for mapping connectivity in vivo. *Neuroimage*. 24, 339-49.
- Bassett, D.S., et al., 2011. Dynamic reconfiguration of human brain networks during learning. *Proc Natl Acad Sci U S A*. 108, 7641-6.
- Bell, A.J., Sejnowski, T.J., 1995. An information-maximization approach to blind separation and blind deconvolution. *Neural Comput*. 7, 1129-59.
- Calhoun, V.D., et al., 2001. fMRI activation in a visual-perception task: network of areas detected using the general linear model and independent components analysis. *NeuroImage*. 14, 1080-8.
- Calhoun, V.D., Kiehl, K.A., Pearlson, G.D., 2008. Modulation of temporally coherent brain networks estimated using ICA at rest and during cognitive tasks. *Hum Brain Mapp*. 29, 828-38.
- Cole, M.W., Schneider, W., 2007. The cognitive control network: Integrated cortical regions with dissociable functions. *Neuroimage*. 37, 343-60.
- Cole, M.W., et al., 2013. Multi-task connectivity reveals flexible hubs for adaptive task control. *Nat Neurosci*. 16, 1348-55.
- Cole, M.W., et al., 2014. Intrinsic and task-evoked network architectures of the human brain. *Neuron*. 83, 238-51.
- Daselaar, S.M., et al., 2009. Posterior midline and ventral parietal activity is associated with retrieval success and encoding failure. *Front Hum Neurosci*. 3, 13.
- Elton, A., Gao, W., 2015. Task-positive Functional Connectivity of the Default Mode Network Transcends Task Domain. *J Cogn Neurosci*. 27, 2369-81.
- Fair, D.A., et al., 2007. A method for using blocked and event-related fMRI data to study "resting state" functional connectivity. *Neuroimage*. 35, 396-405.
- Ferreira, L. K., & Busatto, G. F. (2013). Resting-state functional connectivity in normal brain aging. *Neuroscience and Biobehavioral Reviews*.
<https://doi.org/10.1016/j.neubiorev.2013.01.017>
- Fox, M.D., et al., 2006. Coherent spontaneous activity accounts for trial-to-trial variability in human evoked brain responses. *Nature neuroscience*. 9, 23-5.
- Fransson, P., 2006. How default is the default mode of brain function? Further evidence from intrinsic BOLD signal fluctuations. *Neuropsychologia*. 44, 2836-45.
- Ganger, S., et al., 2015. Comparison of continuously acquired resting state and extracted analogues from active tasks. *Hum Brain Mapp*. 36, 4053-63.
- Greicius, M.D., et al., 2003. Functional connectivity in the resting brain: a network analysis of the default mode hypothesis. *Proc Natl Acad Sci U S A*. 100, 253-8.
- Hampson, M., et al., 2010. Functional connectivity between task-positive and task-negative brain areas and its relation to working memory performance. *Magn Reson Imaging*. 28, 1051-7.
- Hellyer, P.J., et al., 2014. The control of global brain dynamics: opposing actions of frontoparietal control and default mode networks on attention. *J Neurosci*. 34, 451-61.
- Himberg, J., Hyvarinen, A., Esposito, F., 2004. Validating the independent components of neuroimaging time series via clustering and visualization. *Neuroimage*. 22, 1214-22.

- Huijbers, W., Schultz, A. P., Vannini, P., McLaren, D. G., Wigman, S. E., & Ward, A. M. (2013). The Encoding / Retrieval Flip: Interactions between Memory Performance and Memory Stage and Relationship to Intrinsic Cortical Networks, 1163-1179. <https://doi.org/10.1162/jocn>
- Jiang, T., et al., 2004. Modulation of functional connectivity during the resting state and the motor task. *Hum Brain Mapp.* 22, 63-71.
- Kim, H. (2015). Encoding and retrieval along the long axis of the hippocampus and their relationships with dorsal attention and default mode networks: The HERNET model. *Hippocampus*, 25(4), 500-510. <https://doi.org/10.1002/hipo.22387>
- Meskaldji, D.E., et al., 2016. Prediction of long-term memory scores in MCI based on resting-state fMRI. *Neuroimage Clin.* 12, 785-795.
- Morgan, V.L., Price, R.R., 2004. The effect of sensorimotor activation on functional connectivity mapping with MRI. *Magn Reson Imaging.* 22, 1069-75.
- Pariante, J., et al., 2005. Alzheimer's patients engage an alternative network during a memory task. *Ann Neurol.* 58, 870-9.
- Power, J.D., et al., 2011. Functional network organization of the human brain. *Neuron.* 72, 665-78.
- Salami, A., Eriksson, J., Nyberg, L., 2012. Opposing effects of aging on large-scale brain systems for memory encoding and cognitive control. *J Neurosci.* 32, 10749-57.
- Sestieri, C., et al., 2011. Episodic memory retrieval, parietal cortex, and the default mode network: functional and topographic analyses. *J Neurosci.* 31, 4407-20.
- Shirer, W.R., et al., 2012. Decoding subject-driven cognitive states with whole-brain connectivity patterns. *Cereb Cortex.* 22, 158-65.
- Smith, S.M., et al., 2009. Correspondence of the brain's functional architecture during activation and rest. *Proc Natl Acad Sci U S A.* 106, 13040-5.
- Spaniol, J., et al., 2009. Event-related fMRI studies of episodic encoding and retrieval: meta-analyses using activation likelihood estimation. *Neuropsychologia.* 47, 1765-79.
- Sperling, R., et al., 2003. Putting names to faces: successful encoding of associative memories activates the anterior hippocampal formation. *Neuroimage.* 20, 1400-10.
- Spreng, R.N., Grady, C.L., 2010. Patterns of brain activity supporting autobiographical memory, prospection, and theory of mind, and their relationship to the default mode network. *J Cogn Neurosci.* 22, 1112-23.
- Tavor, I., et al., 2016. Task-free MRI predicts individual differences in brain activity during task performance. *Science.* 352, 216-20.
- Tomasi, D., et al., 2014. Functional connectivity and brain activation: a synergistic approach. *Cereb Cortex.* 24, 2619-29.
- Vannini, P., Hedden, T., Huijbers, W., Ward, A., Johnson, K. A., & Sperling, R. A. (2013). The Ups and Downs of the Posteromedial Cortex: Age- and Amyloid-Related Functional Alterations of the Encoding/Retrieval Flip in Cognitively Normal Older Adults. *Cerebral Cortex*, 23, 1317-1328. <https://doi.org/10.1093/cercor/bhs108>
- Zeineh, M.M., et al., 2003. Dynamics of the hippocampus during encoding and retrieval of face-name pairs. *Science.* 299, 577-80.
- Zhang, Y., et al., 2016. Enhanced resting-state functional connectivity between core memory-task activation peaks is associated with memory impairment in MCI. *Neurobiol Aging.* 45, 43-9.

TABLES

Table 1

N	Age	Education	MMSE ^a (z-score)	CDR
38	72.5 (5.78)	13.61 (3.04)	0.39 (0.99)	0.01 (0.08)

^a Z-scores are corrected for standard population ages and education based on CERAD population norm values.

Table 2: Local maxima of significant clusters associated with successful encoding

Region Label	Extent	t-value	MNI Coordinates		
			x	y	z
R Calcarine Gyrus	2589	6.844	13.5	-91.5	15.0
L Lingual Gyrus	2589	5.581	-12.0	-90.0	-6.0
L Inferior Occipital Gyrus	2589	4.434	-37.5	-81.0	-4.5
L IFG (p. Triangularis)	1867	6.200	-45.0	15.0	24.0
L Middle Frontal Gyrus	1867	3.989	-40.5	7.5	46.5
R Caudate Nucleus	302	5.287	21.0	1.5	21.0
L Middle Occipital Gyrus	797	5.103	-27.0	-70.5	33.0
L Precentral Gyrus	820	5.097	-39.0	-12.0	42.0
L Postcentral Gyrus	820	4.967	-55.5	-10.5	28.5
L Middle Frontal Gyrus	390	4.922	-24.0	18.0	43.5
L Superior Frontal Gyrus	710	4.840	-13.5	34.5	49.5
L Superior Frontal Gyrus	710	4.495	-18.0	57.0	24.0
L Middle Temporal Gyrus	318	4.726	-58.5	-36.0	12.0
L Precentral Gyrus	315	4.676	-34.5	-6.0	49.5
R Linual Gyrus	266	4.570	10.5	-66.0	1.5
R Fusiform Gyrus	297	4.496	33.0	-72.0	-13.5
L IFG (p. Triangularis)	328	4.254	-34.5	39.0	9.0

Table 3: Local maxima of significant clusters associated with successful recognition

Region Label	Extent	t-value	MNI Coordinates		
			x	y	z
L Mid Orbital Gyrus	2464	6.568	-9.0	48.0	-1.5
R Mid Orbital Gyrus	2464	5.095	13.5	49.5	-1.5
R Middle Temporal Gyrus	657	5.703	43.5	-72.0	3.0
R Cerebelum (VI)	1680	5.386	21.0	-82.5	-13.5
L Cerebelum (Crus 1)	1680	5.150	-7.5	-85.5	-15.0
R Fusiform Gyrus	1680	3.687	31.5	-64.5	-13.5

Table 4: Spatial correlation and overlap between networks activated during successful episodic memory encoding or recognition and 70 resting-state maps from Smith et al. 2009

Task networks	Dice Coefficient	Dice coefficient. rating	Spatial Correlation coefficient	p-value
SUCCESSFUL ENCODING				
Med-orbito-frontal	0.29588	fair	0.299	<0.001
Lateral fronto-temporal	0.39746	fair	0.365	<0.001
Visual	0.68855	moderate	0.472	<0.001
Hippocampal	1.0913	excellent	0.538	<0.001
SUCCESSFUL RECOGNITION				
Posterior parietal	0.52081	moderate	0.398	<0.001
Posterior cingulate- occipital	0.82164	excellent	0.541	<0.001
Occipital	0.44051	moderate	0.348	<0.001

Figure 1: fMRI brain activation during successful memory task

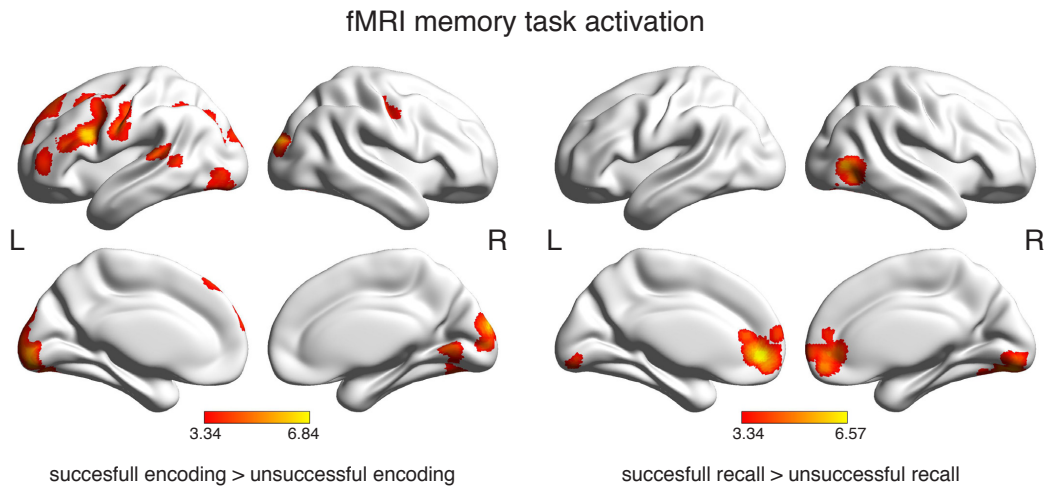


Figure 2: Network activation during successful encoding memory task and corresponding networks during rest.

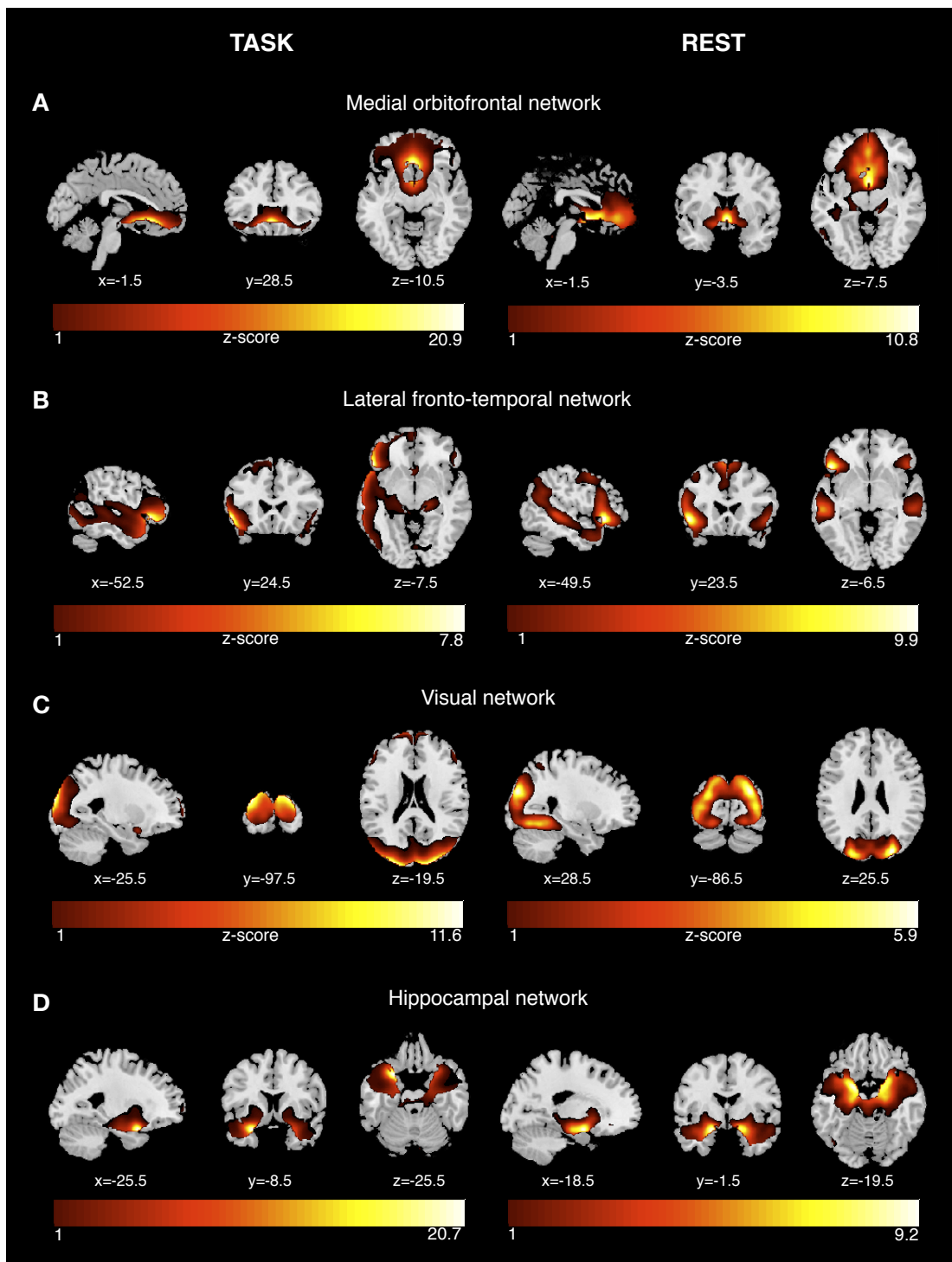


Figure 3: Network activation during successful recognition memory task and corresponding networks during rest.

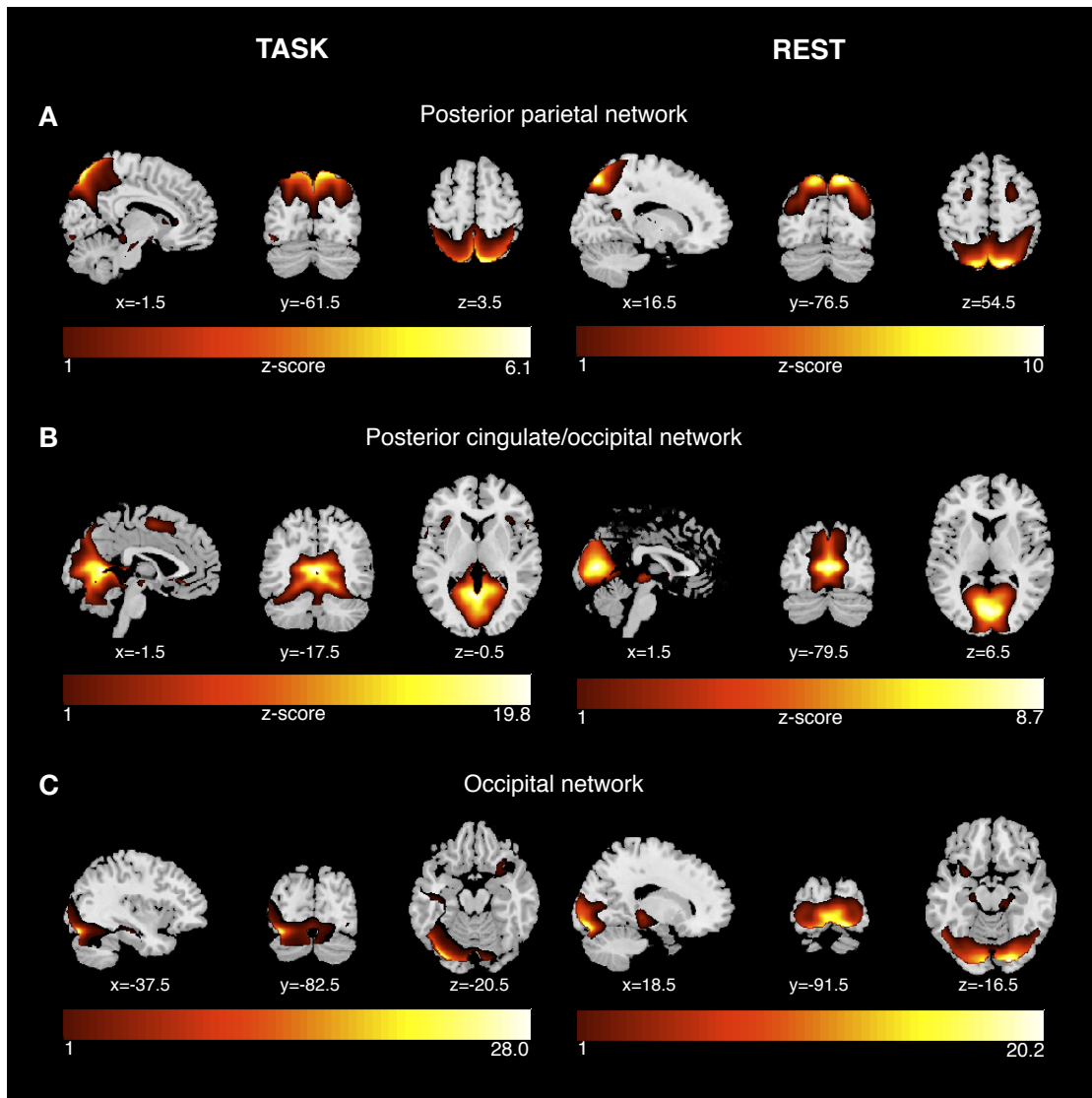
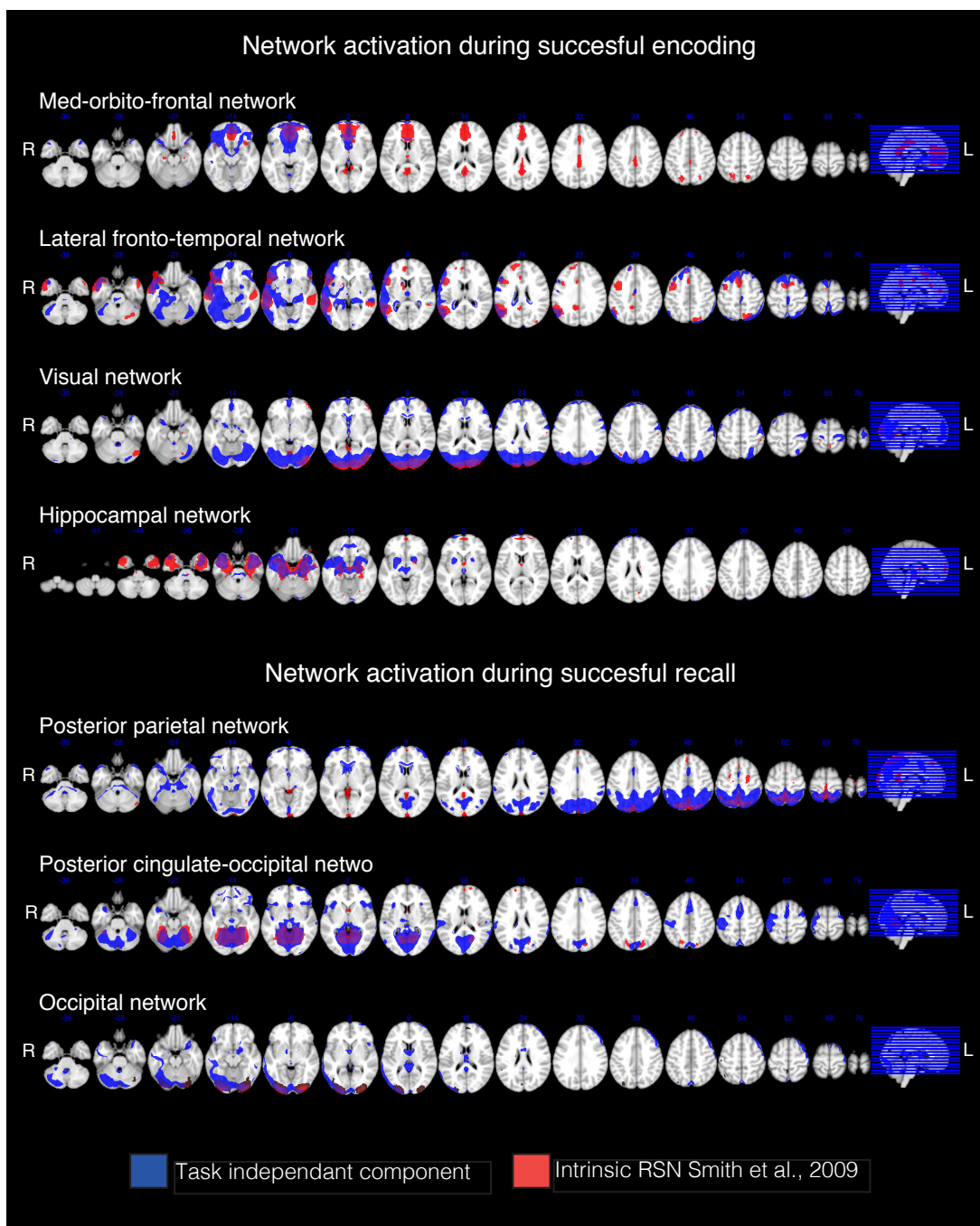


Figure 4: Spatial correspondence between 7 successful memory task networks and 70 RSN (Smith et al. 2009).



03.

FDG-PET METABOLISM

AND RESTING-STATE

NETWORK

CONNECTIVITY ARE

ASSOCIATED IN EARLY

ALZHEIMER'S DISEASE

3.1 SUMMARY

The goal of the second project was to assess whether resting-state network alterations in AD are associated with already well-established markers of pathological brain function in AD. To this end, we compared resting-state fMRI functional network connectivity with patterns of FDG-PET metabolism in 27 amyloid-beta negative healthy controls, 44 amyloid positive MCI patients and 25 patients with AD. ICA was used separately for both rsfMRI and FDG-PET to estimate large-scale components. First the spatial correspondence of networks issued from rsfMRI and FDG-PET was compared. Second, the association between the rsFC and mean FDG-PET signal was computed for each major RSN component separately using linear regression. We hypothesized that higher rsFC would be associated with higher mean FDG-PET in major RSNs.

3.2 REFERENCE

Lee Simon-Vermot, Nicolai Franzmeier, Yifei Zhang, Jinyi Ren, Miguel Á. Araque Caballero, and Michael Ewers, for the Alzheimer's Disease Neuroimaging Initiative (ADNI). (2017). Under review.

The author of this thesis is the first author of the manuscript. ME & LSV designed the research experiment. LSV analyzed fMRI. LSV & MÀAC analyzed the FDG-PET data. LSV conducted the statistical analysis with the help of YZ & JR. LSV, NF & ME wrote the manuscript, which was commented on and reviewed by MÀAC, NK, YZ & JR.

FDG-PET Metabolism and Resting-State Network Connectivity Are Associated In Early Alzheimer's Disease

Lee Simon-Vermot^a, Nicolai Franzmeier^a, Yifei Zhang^b, Jinyi Ren^a, Miguel Á. Araque Caballero^a, and Michael Ewers^a, for the Alzheimer's Disease Neuroimaging Initiative* (ADNI)

^a Institute for Stroke and Dementia Research, Klinikum der Universität München, Ludwig-Maximilians-Universität LMU, Feodor-Lynen Straße 17, 81377 Munich, Germany.

^b College of Information Engineering, Shanghai Maritime University, 1550 Haigang Avenue, 201306 Shanghai, China.

*Data used in preparation of this article were obtained from the Alzheimer's Disease Neuroimaging Initiative (ADNI) database (adni.loni.usc.edu). As such, the investigators within the ADNI contributed to the design and implementation of ADNI and/or provided data but did not participate in analysis or writing of this report. A complete listing of ADNI investigators can be found at: http://adni.loni.usc.edu/wp-content/uploads/how_to_apply/ADNI_Acknowledgement_List.pdf

Correspondence to Dr. Michael Ewers, Institute for Stroke and Dementia Research, Klinikum der Universität München, Feodor-Lynen Str. 17, 81377 Munich, Germany.

Tel: +49 89/440046221, E-mail: michael.ewers@med.uni-muenchen.de

Supplemental Data:

supplementary figure 1, supplementary figure 2, supplementary figure 3

Acknowledgement statement (including conflict of interest and funding sources):

The study was funded by ERC career integration grant (PCIG12-GA-2012-334259 to ME), LMUexcellent (to ME) and Alzheimer Forschung Initiative (to ME).

Conflicts of interest: none

ABSTRACT

In Alzheimer's disease (AD), FDG-PET hypometabolism is a key pathological brain alteration that occurs particularly in temporo-parietal brain areas. This typical FDG-PET hypometabolism pattern shows a large spatial overlap with particular resting-state networks such as the default-mode network (DMN). The intrinsic functional connectivity assessable via resting-state functional MRI is a defining feature of such networks, where functional connectivity of major networks spanning higher cortical brain areas, such as the DMN and fronto-parietal attention network, have been found altered in AD. However, the association between metabolic and functional connectivity network changes in AD remains poorly understood. In this study, we investigated the association between FDG-PET metabolism and functional connectivity in the major resting-state networks in elderly amyloid-beta negative healthy controls (HC, n=27), amyloid-beta positive subjects with mild cognitive impairment (MCI-A β +, n=44) and AD dementia (AD, n=25). We found that FDG-PET metabolism in the DMN and occipital brain areas was reduced in MCI-A β +, and globally in AD. For resting state fMRI networks extracted via independent component analysis, functional connectivity was increased in the anterior DMN and fronto-parietal control networks in MCI-A β + and AD compared to HC. Lower FDG-PET was associated with lower functional connectivity exclusively in the DMN and fronto-parietal attention networks in the whole sample and in particular in MCI-A β +. These results suggest that lower FDG-PET metabolism is associated with lower functional connectivity in major cortical resting-state networks in subjects with high A β load.

Keywords: Alzheimer's disease, Mild Cognitive Impairment, Functional Connectivity, resting-state fMRI, FDG PET, resting-state network

INTRODUCTION

Reduced glucose metabolism as detected by FDG-PET is a major pathological brain change in Alzheimer's disease (AD). Particularly, temporo-parietal brain areas exhibit reduced FDG-PET, which becomes detectable years before the onset of dementia symptoms [1-3]. FDG-PET is typically obtained during rest and thought to act as a marker of steady-state glucose metabolism of spontaneous brain activity, hence FDG-PET hypometabolism may reflect impaired neural signaling in AD. Results from resting-state functional MRI (rsfMRI) studies suggest that spontaneous neural activity is not random but shows synchronicity between brain regions comprising functional networks [4,5]. The rsfMRI assessed functional connectivity (FC), i.e. correlation of rsfMRI BOLD signal changes between different brain regions, is a measure of network integrity. In AD, FC particularly in the posterior parietal default-mode network (DMN) is reduced [6], while more frontal networks such as the anterior DMN (aDMN) showed an increase in FC [7-9]. The regional distribution of FDG-PET hypometabolism largely overlaps with the DMN in subjects at genetic risk of AD [10] and predementia stages of AD [1], suggesting network-specific alterations of FDG-PET early in the course of AD [11,12]. However, the association between FDG-PET metabolism and rsfMRI FC in resting-state networks in AD is poorly understood. A common approach to assess the relation between FDG-PET and rsfMRI is to examine the spatial overlap between the covariance patterns in FDG-PET with those of rsfMRI networks [13]. Studies using such an approach have revealed significant spatial overlap in connectivity patterns between FDG-PET and rsfMRI in young and older healthy adults, although only inconsistently for the DMN [14,15]. A limitation of this approach is that the FDG-PET covariance patterns were estimated across subjects since only one average FDG-PET image per

subjects was available, preventing to assess directly FC between brain regions. An alternative is to test the association between rsfMRI connectivity and FDG-PET uptake across subjects [16]. So far, no study has tested at subject-level the association between FC within each of the major resting-state networks (RSN) and FDG-PET uptake in AD. In order to address this research gap, we investigated the association between FDG-PET uptake and rsfMRI connectivity in major RSNs, where both modalities were assessed in amyloid negative healthy controls (HC), prodromal AD (i.e. amyloid-beta ($A\beta$) positive subjects with mild cognitive impairment (MCI- $A\beta$ +) and AD dementia.

MATERIALS AND METHODS

Participants

For the current study, data were obtained from the Alzheimer's Disease Neuroimaging Initiative (ADNI, phases GO and II) database (adni.loni.usc.edu). ADNI is a longitudinal study started in 2003 as a public-private partnership, which was set up with the goal to investigate neuroimaging (MRI, PET) features, neuropsychological characteristics as well as other biomarkers in order to predict and monitor AD-related neurodegenerative and cognitive changes [17]. For up-to-date information, see www.adni-info.org. Ethical approval was obtained by the ADNI investigators.

Apart from the inclusion criteria defined by ADNI, the following inclusion criteria were implemented: availability of rsfMRI, T1-weighted MRI, FDG-PET and AV45-PET. In addition, subjects had to fulfill diagnostic criteria including classification as normal controls with normal low amyloid deposition measured by global AV45 PET (HC $A\beta$ -), mild cognitive impairment with abnormally high AV45 PET (MCI $A\beta$ +) or AD dementia. In order to determine each subjects $A\beta$ -status, we applied pre-established cut-off

values [18] to the global AV45-PET standardized uptake value ratio (SUVR), with abnormal amyloid uptake (i.e. A β +) defined as an AV45-PET SUVR \geq 1.11. To be defined as HC, subjects had to show normal cognitive performance in standardized neuropsychological testing. Amnesic MCI was diagnosed following the Mayo clinic criteria [19], and AD dementia was diagnosed following the National Institute of Neurological and Communicative Disorders and Stroke-Alzheimer's Disease and Related Disorders Association (NINCDS-ADRDA) criteria. A total of N = 145 subjects met these criteria. Twenty seven subjects had to be excluded due to failed MRI processing, either due to an incomplete MRI scan (n = 1), signal loss or gross atrophy including large ventricles that did not allow for sufficient spatial normalization (n = 18), motion larger than 2mm (in any of the 3 translation directions) or 2° (in any of the 3 rotation axes) visible in the functional MRI scans (n = 6). The final sample size (N=96) encompassed 27 HC, 44 MCI-A β + and 25 AD.

MRI acquisition

Resting state-fMRI images were acquired using a single shot T2*-weighted echo planar imaging with a TR of 3000 ms, a flip angle of 80° and 3.3 mm isotropic voxel size, collecting a total of 140 volumes. Prior to the resting-state scan, all subjects were instructed to keep their eyes open. All MRI scans were collected on Philips 3T MRI scanners, using an 8-channel head matrix coil. High-resolution T1-weighted images were collected using a 3D MP-RAGE sequence, with whole-brain coverage at a voxel resolution of 1 × 1 × 1.2 mm.

AV45-PET

AV45- PET scans were assessed during four time frames 300 seconds each measured 50 minutes after intravenous tracer injection (http://adni.loni.usc.edu/wp-content/uploads/2010/05/ADNI2_PET_Tech_Manual_0142011.pdf). Global AV45-PET uptake was assessed as a summary measure of the SUVR in a set of predefined cortical ROIs that have been described previously [20]. Details on the preprocessing of the AV45-PET images are available online (<http://adni.loni.usc.edu/data-samples/pet/>).

FDG-PET acquisition

FDG-PET scans were acquired on PET scanners from different manufacturers (Siemens, GE and Philips). Dynamic 3D scans were recorded in six 300 seconds time frames measured 30 minutes after an intravenous tracer injection. Each frame was registered to the first time frame of the raw image. Each subject's co-registered, averaged images were subsequently reoriented to a standard grid parallel to the anterior commissure - posterior commissure (AC-PC) line. An averaged image was generated from these AC-PC co-registered frames and then intensity normalized facilitating comparability of PET images from different scanner types. Details on the FDG-PET acquisition protocol are available online at http://adni.loni.usc.edu/wp-content/uploads/2010/05/ADNI2_PET_Tech_Manual_0142011.pdf.

FDG-PET preprocessing

All preprocessing steps were performed with SPM 8 (Wellcome Trust Centre for Neuroimaging, University College London). Initially, all FDG-PET images were registered to the T1-weighted anatomic images. To spatially normalize the FDG-PET images, each subjects' T1-weighted MRI scans were segmented in gray matter (GM),

white matter (WM), and cerebrospinal fluid (CSF) maps [21]. Spatial normalization parameters were estimated based on a high-dimensional non-linear registration algorithm included in SPM's DARTEL toolbox to warp all GM maps to an average group specific GM template [22], which was subsequently registered to a T1 template in MNI standard space to estimate affine transformation parameters. Next, the normalization matrices including the non-linear and the affine normalization parameters were combined and applied to the segmented GM images as well as the co-registered FDG-PET images. During normalization, all FDG-PET images were smoothed using an 8mm full width half at half maximum (FWHM) Gaussian kernel. To address inter-subject differences in the global FDG-PET signal, each spatially normalized FDG-PET images was individually adjusted to the mean FDG-PET signal of the pons and cerebellar vermis.

MRI preprocessing

In an initial step, we discarded the first 10 volumes of the rsfMRI images due to known signal instabilities at the beginning of an fMRI session. All remaining 130 volumes were realigned to the first volume to correct for motion, and co-registered to the T1-weighted anatomical images. Equivalent to the normalization of FDG-PET data, the non-linear and affine normalization parameters were combined and applied to the registered fMRI volumes for spatial normalization to MNI standard space. The images were smoothed using a 6 mm FWHM Gaussian kernel to increase signal-to-noise ratio and reduce inter subject differences. We further applied detrending to remove low frequency signal intensity drift and subjected the scans to a band-pass filter retaining a frequency band of 0.01-0.08 Hz. Lastly, we regressed out the 6 motion parameters,

which were derived during the motion correction procedure, and the BOLD signal averaged separately across the WM and CSF voxels. Global signal removal is an inherent part of the independent component analysis (ICA, see below) and was not conducted at this stage.

Spatially normalized GM maps, smoothed with an 8mm FWHM Gaussian kernel (in line with the approach described in [23]) were created for each subject in order to extract the GM volume. Modulation was applied during the normalization step, in order to maintain local GM concentrations after warping the images to the template.

Independent component analysis of rsfMRI

To extract functional networks from resting-state fMRI data, we conducted a group ICA analysis (Calhoun et al., 2001) on the whole sample, using the algorithms of the GIFT toolbox (<http://mialab.mrn.org/software/gift/>). The ICA was run on preprocessed rsfMRI data with the number of components to extract set a priori to 20, in line with various previous studies that this number of ICs yields a robust identification of core resting-state networks [24–26]. The ICA analysis was repeated 20 times using ICASSO to assess the stability of the resulting estimation and stability indices were above 0.95 for all components. Based on the group-level network estimation, subject-specific network maps were back-reconstructed using the GICA3 algorithm a subsequently transformed to z-scores.

Extraction of mean FC and FDG-PET per network

Based on previously established rsfMRI network templates [25,27], major intrinsic networks (n = 10) were readily identifiable by visual inspection of the rsfMRI ICA maps

in the current study. The rsfMRI ICA maps were thresholded at $z > 1$. As a measure of mean FC per network, the voxel-wise IC values were averaged within the thresholded, binarized and GM masked IC maps for each of the 10 resting-state networks, consistent with previous studies to derive average FC index based on ICA [28–30]. The mean signal-to-noise ratio (SNR) was extracted from each network, in order to control for the fMRI BOLD signal variability caused by field homogeneities. SNR is defined as signal intensity average across the entire time series, divided by the standard deviation of the signal within the time series [27]. In order to compute the average FDG-PET values within the resting-state networks, the binarized ($z > 1$) and GM-masked rsfMRI IC maps were superimposed onto the spatially normalized FDG-PET image in MNI space. The FDG-PET were averaged across the voxels covered by an IC mask was computed for each resting-state network. Similarly, thresholded rsfMRI IC maps were superimposed onto the spatially normalized and modulated GM maps in order to extract the mean GM volume per resting-state network.

Source based morphometry of FDG-PET

In order to test the covariance pattern of FDG-PET across subjects, we used source-based morphometry (SBM), an ICA based algorithm implemented in the GIFT Toolbox that allows extracting covariance patterns (i.e. functional networks) based on single time point measurements per subjects. Prior to running SBM, we estimated the optimal number of components encompassed in the FDG-PET data by applying the minimum description length algorithm, resulting in a total of 22 components. Subsequently, SBM was run on normalized FDG-PET images using the ICA infomax algorithm with the number of components set to 22. This analysis was repeated 20 times using ICASSO to

assess the stability of network estimation. The stability indices were above 0.9 for all components. Note that such IC maps of FDG-PET represent the covariance of FDG-PET images across subjects and, in contrast to the ICA based on rsfMRI, no subject-specific IC maps can be reconstructed. In order to assess whether the IC maps of FDG-PET correspond to rsfMRI IC maps, we assessed the spatial similarity of the IC from the FDG-PET SBM analysis and rsfMRI derived networks. To this end, we computed the pair-wise spatial correlation between the 10 rsfMRI networks and each of the 22 FDG-PET SBM components. The spatial overlap was further quantified with the Dice similarity coefficient. Specifically, the IC components from the rsfMRI were binarized, using the threshold $z > 1$ and GM and for FDG-PET the SBM components were binarized, using the threshold $z > 1$, and the Dice coefficient was computed for the overlap between the binarized component maps. The Dice coefficient measures the overlap between two images divided by their mean volume and is interpreted as following: <0.2 poor, $0.2-0.4$ fair, $0.4-0.6$ moderate, $0.6-0.8$ good and >0.8 excellent correspondence.

Statistical analysis

Sample demographics and cognitive scores were compared between diagnostic groups using ANCOVAs for continuous measures and Chi-squared tests for categorical measures.

First we assessed group differences in the mean FDG-PET and mean FC for each network. For each resting-state network ($n = 10$), we ran an ANCOVA, with mean FC (or mean FDG-PET) as the dependent variable, and group (i.e. HC vs. MCI-Ab+ vs. AD),

age, gender, years of education and SNR as predictors. In case of significant main effect of group, Tukey's HSD post-hoc tests were applied for pair-wise group comparisons.

Next, we tested for each resting-state network the association between FC and FDG-PET within the whole sample. We applied linear regression analysis for each resting-state network, with mean FDG-PET as dependent variable and mean FC as the independent variable, while correcting for network's mean SNR, network's mean GM volume, diagnosis, age, gender and education. All presented p-values are controlled for multiple testing using the Bonferroni method (for 10 tests). In addition, for exploratory reasons, we ran these regression analyses separately for each diagnostic group.

RESULTS

Sample demographics are shown in table 1.

Group differences in FDG-PET and rsfMRI connectivity in resting-state networks

Based on ICA applied to rsfMRI, we identified 10 major resting state networks that matched the canonical networks (supplementary figure 1). The other 10 components included mostly noise (supplementary figure 2). For each resting-state network, we used an ANOVA to compare the subject-specific average FDG-PET and rsfMRI FC values between the diagnostic groups. For FDG-PET, the MCI A β + group showed reduced values selectively in the DMN and auditory network (auditory 2) compared to HC (table 2 & figure 1). AD subjects showed within each network decreased FDG-PET compared to MCI A β + and HC, suggesting a global decrease in FDG-PET (table 2 & figure 1). For rsfMRI FC, we observed an increase in FC values within the aDMN from HC to AD, where the group difference became significant for AD > HC (table 3 & figure 1). For the right fronto-parietal attention network (right FPAN), rsfMRI FC was

increased in MCI-A β + compared to HC and AD. No decreases in rsfMRI FC values in MCI-A β + or AD compared to HC were observed for any of the networks.

Association between functional network FC values and FDG-PET

Across all groups, there was a positive association between mean FDG-PET and mean rsfMRI FC within the DMN and bilateral FPAN components. Specifically, the linear regressions revealed a positive association for the aDMN ($t(88) = 3.33$, Slope Estimate (Beta) /Standard Error (B/SE) = $0.94/0.28$, $p = 0.012$), the DMN ($t(88) = 3.28$, B/SE = $1.14/0.35$, $p = 0.015$), the left FPAN ($t(88) = 3.34$, B/SE = $1.07/0.32$, $p = 0.012$) and the right FPAN ($t(88) = 3.21$, B/SE = $0.89/0.28$, $p = 0.018$, figure 2). When the association between FDG-PET and rsfMRI FC was tested separately for each diagnostic group, associations were found only for MCI-A β + subjects: there was a positive association between mean FDG-PET and mean rsfMRI FC for the DMN ($t(38) = 3.02$, B/SE = $1.8/0.59$, $p = 0.044$), the left FPAN ($t(38) = 3.03$, B/SE = $1.79/0.59$, $p = 0.043$), and right FPAN ($t(38) = 3.17$, B/SE = $1.25/0.39$, $p = 0.03$). Although HC and AD groups showed associations in the same direction as in the MCI-A β +, the results were not significant.

Network detection in FDG-PET across subjects

In order to identify covariance patterns of FDG-PET across subjects, we ran an ICA across subjects, called SBM. In order to identify which FDG-PET components matched the rsfMRI derived resting state networks, we computed the spatial correlation and Dice coefficient of the overlap between the FDG-PET components and the 10 rsfMRI components. The Dice coefficient revealed a good overlap (Dice coefficient = 0.6-0.8) for the DMN, left FPAN and the first auditory network (Figure 3, table 4). A moderate overlap (Dice coefficient = 0.4-0.6) was found for the aDMN and the medial occipital

visual network. The spatial overlap was fair (Dice coefficient = 0.2-0.4) for the motor network, DAN and second auditory network. The right FPAN and lateral visual network (VISUAL 2) only had poor (Dice coefficient < 0.2) spatial correspondence in FDG-PET derived networks. Similarly, the spatial correlation between rsfMRI FC and FDG-PET was highest for those with good and moderate DICE coefficient, including the DMN, aDMN, left FPAN and an auditory network (table 4). The components that didn't correspond to resting-state networks included mostly noise (Supplementary Figure 3).

DISCUSSION

The major finding of the current study was that higher functional connectivity within the resting-state networks, including the DMN and FPAN was associated with higher FDG-PET metabolism across elderly HC, MCI-A β + and AD dementia subjects. These results suggest higher rsfMRI connectivity is associated with higher FDG-PET metabolism in major cortical networks that are affected in AD.

Our first finding of the association between higher FDG-PET and higher rsfMRI FC in the DMN and FPAN across HC, MCI-A β + and AD is in general agreement with results from previous findings in HC subjects, assessing rsfMRI connectivity, and in addition FDG-PET uptake [16] or arterial spin labelling assessed cerebral blood flow, a proxy of glucose metabolism [31,32]. Similar to the current results, the associations between the modalities were highest in the DMN and FPAN [33-35]. Together these results suggest a network-specific correlation between modalities during rest. The question arises why the rsfMRI vs FDG-PET correlations were the strongest in the DMN and FPAN. One possibility is that the resting-state network specificity of findings was disease dependent. In the current study the cross-modal association between rsfMRI and FDG-

PET was significant only in the MCI-A β + when analyzed group-wise, however, the smaller group sample size may have led to insignificant results in HC and AD. Given that the same resting-state network specificity of the FDG-PET vs rsfMRI association was observed also in previous studies in young healthy adults [33,35,36], it is thus unlikely that the regional heterogeneity in the FDG-PET vs. rsfMRI correlation was due to network-specific AD pathology. An alternative explanation is that the DMN, which shows high anti-correlated connectivity to the FPAN [4], is most active during rest, and thus the predominant fluctuations of activity in the DMN and FPAN during resting-state may have contributed to the network-specific covariation of rsfMRI and FDG-PET. An activity-dependent association between FDG-PET and rsfMRI connectivity during resting-state was shown in an eyes-closed vs. eyes-open comparison, where the association between both modalities was stronger in the activated visual and salience networks during the eyes-open “task” [37]. From this perspective, the resting-state can be considered a condition where certain networks such as the DMN vs. FPAN show higher FC and thus higher glucose metabolism.

For our second finding, FDG-PET and rsfMRI were differentially changed in prodromal AD, with FDG-PET being decreased, primarily in the DMN, but rsfMRI being increased in the right FPAN. The results are consistent with previous findings on lower FDG-PET metabolism [38] but increased FC in more frontal brain areas in AD [8,39–42]. One possible explanation for the differences in the AD-related change in FDG-PET compared to rsfMRI connectivity could be that fact that FDG-PET signal may be not only be driven by neural activity. It has previously been shown that glucose consumption by astrocytes significantly affects the FDG-PET signal [43]. Results from pharmacological stimulation of astrocytes in vivo have shown increased FDG-PET

signal [44], suggesting that FDG-PET levels are partially driven by astroglia activity independent from neural signaling. Amyloid-pathology may lead to impaired astrocyte activation and thus reduced FDG-PET signal. In fact, brain areas with highest aerobic glycolysis are preferentially distributed in regions of the DMN [45], which match the distribution of amyloid pathology [46]. The astrocyte induced FDG-PET signal changes may not impart on rsfMRI assessed neural activity, thus leading to a mismatch in the FDG-PET and rsfMRI signal changes in AD [47]. Other possible explanations are that rsfMRI exhibits a lower signal to noise ratio than FDG-PET, and thus the reduced brain activity may have been detected by FDG-PET in networks such as the DMN, but not by rsfMRI connectivity.

For our third finding, a subset of rsfMRI networks showed a spatial match to the patterns of FDG-PET connectivity, suggesting presence of metabolic networks that correspond to rsfMRI detected functional networks [13,14]. Consistent with previous reports [15], FDG-PET covariance patterns corresponded to DMN and FPANs along with primary sensory networks. These results suggest that FDG-PET itself may show functional connectivity that matched that of neural activity as assessed by fMRI. However, since the assessment of FDG-PET covariant networks is derived from static FDG-PET acquisition, as done in these previous studies, it does not allow for the assessment of individual connectivity. Future studies with dynamic FDG-PET are needed in order to fully establish to what degree metabolic networks correspond to rsfMRI assessed networks. Altered FDG-PET connectivity assessed across subjects has been reported in groups of AD patients [48-50], thus FDG-PET connectivity assessed based on dynamic FDG-PET at the subject-level may prove a clinically useful marker of functional network damage in patients with AD.

For the interpretation of the current study, some caveats need to be taken into account. First of all, it is possible that the network-specific association between FDG-PET and rsfMRI connectivity might be due to regional variations in SNR in rsfMRI. For example, SNR is typically higher in frontal regions [51]. In order to guard against the influence of signal precision for the assessment of the FDG-PET vs. rsfMRI association, we have computed voxel-wise the SNR and controlled the regression analysis for SNR. Still, we cannot exclude that the absence of a cross-modal association may be partially due to such method dependent discrepancies in measurement precision rather than in true differences of underlying biological processes.

Secondly, we used rsfMRI IC values as a measure of network connectivity as previously established [28,52] and applied in several previous studies as measures of resting state connectivity [53–55]. It needs to be acknowledged that resting-state networks can be characterized by a plethora of other measures such as seed-based functional connectivity [56], regional homogeneity [57], global connectivity [35], amplitude of low frequency fluctuations (ALFF) [58]. These measures have each a different interpretation and merit further investigation. Still, the systematic investigation of commonalities and differences in the result patterns is beyond the scope of the current study. Differences are likely to be small for the assessment between rsfMRI and FDG-PET associations [35], and thus a large scale study would be needed to detect meaningful and reliable differences with sufficient statistical validity.

Lastly, although the association between FC and FDG-PET was significant, the effect size was moderate, with only about maximally 25% of the variance of one modality explained by the other. Thus, a large extent of variability between both modalities remains unexplained. The relationship between neurovascular coupling and energy

metabolism is complex. Combinations of FDG-PET with additional measures including MR spectroscopy of glutamate [16], high-resolution EEG or molecular PET to test astrocyte activity [59] may be a promising to understand the association between metabolic and neural activity. Advanced methods of simultaneous acquisition of (dynamic) FDG-PET and fMRI provide powerful tools [15] to unravel the different sources that contribute to functional network connectivity.

REFERENCES:

- [1] Benzinger TLS, Blazey T, Jack CR, Koeppe RA, Su Y, Xiong C, et al. Regional variability of imaging biomarkers in autosomal dominant Alzheimer's disease. *Proc Natl Acad Sci* 2013;110:E4502–9. doi:10.1073/pnas.1317918110.
- [2] Drzezga A, Lautenschlager N, Siebner H, Riemenschneider M, Willoch F, Minoshima S, et al. Cerebral metabolic changes accompanying conversion of mild cognitive impairment into alzheimer's disease: A PET follow-up study. *Eur J Nucl Med Mol Imaging* 2003;30. doi:10.1007/s00259-003-1194-1.
- [3] Förster S, Grimmer T, Miederer I, Henriksen G, Yousefi BH, Graner P, et al. Regional Expansion of Hypometabolism in Alzheimer's Disease Follows Amyloid Deposition with Temporal Delay. *Biol Psychiatry* 2012;71:792–7. doi:10.1016/j.biopsych.2011.04.023.
- [4] Fox MD, Snyder AZ, Vincent JL, Corbetta M, Van Essen DC, Raichle ME. The human brain is intrinsically organized into dynamic, anticorrelated functional networks. *Proc Natl Acad Sci U S A* 2005;102:9673–8. doi:10.1073/pnas.0504136102.
- [5] Power JD, Cohen AL, Nelson SM, Wig GS, Barnes KA, Church JA, et al. Functional Network Organization of the Human Brain. *Neuron* 2011;72:665–78. doi:10.1016/j.neuron.2011.09.006.
- [6] Sorg C, Riedl V, Mühlau M, Calhoun VD, Eichele T, Läer L, et al. Selective changes of resting-state networks in individuals at risk for Alzheimer ' s disease. *PNAS* 2007;104.
- [7] Jones DT, Knopman DS, Gunter JL, Graff-Radford J, Vemuri P, Boeve BF, et al. Cascading network failure across the Alzheimer's disease spectrum. *Brain* 2016;139:547–62. doi:10.1093/brain/awv338.
- [8] Sala-Llonch R, Fortea J, Bartrés-Faz D, Bosch B, Lladó A, Peña-Gómez C, et al. Evolving brain functional abnormalities in psen1 mutation carriers: A resting and visual encoding fMRI study. *J Alzheimer's Dis* 2013;36:165–75. doi:10.3233/JAD-130062.

- [9] Franzmeier N, Buerger K, Teipel S, Stern Y, Dichgans M, Ewers M. Cognitive reserve moderates the association between functional network anti-correlations and memory in MCI. *Neurobiol Aging* 2017;50:152–62. doi:10.1016/j.neurobiolaging.2016.11.013.
- [10] Reiman EM, Caselli RJ, Yun LS, Chen K, Bandy D, Minoshima S, et al. Preclinical Evidence of Alzheimer's Disease in Persons Homozygous for the $\epsilon 4$ Allele for Apolipoprotein E. *N Engl J Med* 1996;334:752–8. doi:10.1056/NEJM199603213341202.
- [11] Drzezga A, Becker JA, Van Dijk KR a, Sreenivasan A, Talukdar T, Sullivan C, et al. Neuronal dysfunction and disconnection of cortical hubs in non-demented subjects with elevated amyloid burden. *Brain* 2011;134:1635–46. doi:10.1093/brain/awr066.
- [12] Mutlu J, Landeau B, Tomadesso C, de Flores R, Mézenge F, de La Sayette V, et al. Connectivity disruption, atrophy, and hypometabolism within posterior cingulate networks in Alzheimer's disease. *Front Neurosci* 2016;10:1–10. doi:10.3389/fnins.2016.00582.
- [13] Di X, Biswal BB, Alzheimer's Disease Neuroimaging Initiative. Metabolic Brain Covariant Networks as Revealed by FDG-PET with Reference to Resting-State fMRI Networks. *Brain Connect* 2012;2:275–83. doi:10.1089/brain.2012.0086.
- [14] Di X, Gohel S, Thielcke A, Wehrl HF, Biswal BB. Do all roads lead to Rome? A comparison of brain networks derived from inter-subject volumetric and metabolic covariance and moment-to-moment hemodynamic correlations in old individuals. *Brain Struct Funct* 2017. doi:10.1007/s00429-017-1438-7.
- [15] Savio A, Fänger S, Tahmasian M, Rachakonda S, Manoliu A, Sorg C, et al. Resting state networks as simultaneously measured with fMRI and PET. *J Nucl Med* 2017. doi:10.2967/jnumed.116.185835.
- [16] Passow S, Specht K, Adamsen TC, Biermann M, Brekke N, Craven AR, et al. Default-mode network functional connectivity is closely related to metabolic activity. *Hum Brain Mapp* 2015. doi:10.1002/hbm.22753.
- [17] Mueller S, Weiner M, Thal L, Petersen R, Jack C, Jagust W, et al. Ways toward an

- early diagnosis in Alzheimer's disease: The Alzheimer's Disease Neuroimaging Initiative (ADNI). *Alzheimers Dement* 2005;1:55-66. doi:10.1016/j.jalz.2005.06.003.
- [18] Landau SM, Breault C, Joshi AD, Pontecorvo M, Mathis CA, Jagust WJ, et al. Amyloid- β Imaging with Pittsburgh Compound B and Florbetapir: Comparing Radiotracers and Quantification Methods and Initiative for the Alzheimer's Disease Neuroimaging. *Soc Nucl Med* 2013;54:70-7. doi:10.2967/jnumed.112.109009.
- [19] Petersen RC. Mild cognitive impairment as a diagnostic entity. *J Intern Med* 2004;256:183-94. doi:10.1111/j.1365-2796.2004.01388.x.
- [20] Landau SM, Breault C, Joshi AD, Pontecorvo M, Mathis CA, Jagust WJ, et al. Amyloid- β Imaging with Pittsburgh Compound B and Florbetapir: Comparing Radiotracers and Quantification Methods and Initiative for the Alzheimer's Disease Neuroimaging. *Soc Nucl Med* 2013;54:70-7. doi:10.2967/jnumed.112.109009.
- [21] Ashburner J, Friston KJ. Unified segmentation. *Neuroimage* 2005;26:839-51. doi:10.1016/j.neuroimage.2005.02.018.
- [22] Ashburner J. A fast diffeomorphic image registration algorithm. *Neuroimage* 2007;38:95-113. doi:10.1016/j.neuroimage.2007.07.007.
- [23] Mak HK-F, Zhang Z, Yau KK-W, Zhang L, Chan Q, Chu L-W. Efficacy of voxel-based morphometry with DARTEL and standard registration as imaging biomarkers in Alzheimer's disease patients and cognitively normal older adults at 3.0 Tesla MR imaging. *J Alzheimers Dis* 2011;23:655-64. doi:10.3233/JAD-2010-101659.
- [24] Abou-Elseoud A, Starck T, Remes J, Nikkinen J, Tervonen O, Kiviniemi V. The effect of model order selection in group PICA. *Hum Brain Mapp* 2010;31:1207-16. doi:10.1002/hbm.20929.
- [25] Smith SM, Fox PT, Miller KL, Glahn DC, Fox PM, Mackay CE, et al. Correspondence of the brain's functional architecture during activation and rest. *Proc Natl Acad Sci* 2009;106:13040-5. doi:10.1073/pnas.0905267106.

- [26] Di X, Biswal BB. Identifying the default mode network structure using dynamic causal modeling on resting-state functional magnetic resonance imaging. *Neuroimage* 2014;86:53–9. doi:10.1016/j.neuroimage.2013.07.071.
- [27] Yeo BTT, Krienen FM, Sepulcre J, Sabuncu MR, Lashkari D, Hollinshead M, et al. The organization of the human cerebral cortex estimated by intrinsic functional connectivity. *J Neurophysiol* 2011;106:1125–65. doi:10.1152/jn.00338.2011.
- [28] Calhoun VD, Liu J, Adali T. A review of group ICA for fMRI data and ICA for joint inference of imaging, genetic, and ERP data. *Neuroimage* 2009;45:163–72. doi:10.1016/j.neuroimage.2008.10.057.
- [29] Pasquini L, Scherr M, Tahmasian M, Meng C, Myers NE, Ortner M, et al. Link between hippocampus' raised local and eased global intrinsic connectivity in AD. *Alzheimer's Dement* 2015;11:475–84. doi:10.1016/j.jalz.2014.02.007.
- [30] Taylor ANW, Kambeitz-Illankovic L, Gesierich B, Simon-Vermot L, Franzmeier N, Araque Caballero MÁ, et al. Tract-specific white matter hyperintensities disrupt neural network function in Alzheimer's disease. *Alzheimer's Dement* 2017;13:225–35. doi:10.1016/j.jalz.2016.06.2358.
- [31] Li Z, Zhu Y, Childress AR, Detre JA, Wang Z. Relations between BOLD fMRI-Derived Resting Brain Activity and Cerebral Blood Flow. *PLoS One* 2012;7:1–11. doi:10.1371/journal.pone.0044556.
- [32] Liang X, Zou Q, He Y, Yang Y. Coupling of functional connectivity and regional cerebral blood flow reveals a physiological basis for network hubs of the human brain. *Proc Natl Acad Sci* 2013;110:1929–34. doi:10.1073/pnas.1214900110.
- [33] Aiello M, Salvatore E, Cachia A, Pappatà S, Cavaliere C, Prinster A, et al. Relationship between simultaneously acquired resting-state regional cerebral glucose metabolism and functional MRI: A PET/MR hybrid scanner study. *Neuroimage* 2015. doi:10.1016/j.neuroimage.2015.03.017.
- [34] Tomasi D, Wang G, Volkow N. Energetic cost of brain functional connectivity. *Proc Natl Acad Sci* 2013;110:13642–7. doi:10.1073/pnas.1303346110/-/DCSupplemental.www.pnas.org/cgi/doi/10.1073/pnas.1303346110.
- [35] Liang X, Zou Q, He Y, Yang Y. Coupling of functional connectivity and regional

- cerebral blood flow reveals a physiological basis for network hubs of the human brain. *Proc Natl Acad Sci* 2013;110:1929–34. doi:10.1073/pnas.1214900110.
- [36] Tomasi D, Wang G, Volkow N. Energetic cost of brain functional connectivity. *Proc Natl Acad Sci* 2013;110:13642–7. doi:10.1073/pnas.1303346110/-/DCSupplemental.www.pnas.org/cgi/doi/10.1073/pnas.1303346110.
- [37] Riedl V, Bienkowska K, Strobel C, Tahmasian M, Grimmer T, Forster S, et al. Local Activity Determines Functional Connectivity in the Resting Human Brain: A Simultaneous FDG-PET/fMRI Study. *J Neurosci* 2014. doi:10.1523/JNEUROSCI.0492-14.2014.
- [38] Mosconi L. Brain glucose metabolism in the early and specific diagnosis of Alzheimer’s disease. FDG-PET studies in MCI and AD. *Eur J Nucl Med Mol Imaging* 2005;32:486–510. doi:10.1007/s00259-005-1762-7.
- [39] Damoiseaux JS, Prater KE, Miller BL, Greicius MD. Functional connectivity tracks clinical deterioration in Alzheimer’s disease. *Neurobiol Aging* 2012;33:828.e19-828.e30. doi:10.1016/j.neurobiolaging.2011.06.024.
- [40] Jones DT, Machulda MM, Vemuri P, McDade EM, Zeng G, Senjem ML, et al. Age-related changes in the default mode network are more advanced in Alzheimer disease. *Neurology* 2011;77:1524–31. doi:10.1212/WNL.0b013e318233b33d.
- [41] Wang P, Zhou B, Yao H, Zhan Y, Zhang Z, Cui Y, et al. Aberrant intra- and inter-network connectivity architectures in Alzheimer’s disease and mild cognitive impairment. vol. 148. 2015. doi:10.1038/srep14824.
- [42] Zhang Y, Simon-Vermot L, Araque Caballero MÁ, Gesierich B, Taylor ANW, Duering M, et al. Enhanced resting-state functional connectivity between core memory-task activation peaks is associated with memory impairment in MCI. *Neurobiol Aging* 2016;45:43–9. doi:10.1016/j.neurobiolaging.2016.04.018.
- [43] Pellerin L, Magistretti PJ. Glutamate uptake into astrocytes stimulates aerobic glycolysis: a mechanism coupling neuronal activity to glucose utilization. *Proc Natl Acad Sci* 1994;91:10625–9. doi:10.1073/pnas.91.22.10625.
- [44] Zimmer ER, Parent MJ, Souza DG, Leuzy A, Lecrux C, Kim H-I, et al. [18F]FDG PET signal is driven by astroglial glutamate transport. *Nat Neurosci* 2017;20.

- doi:10.1038/nn.4492.
- [45] Vaishnavi SN, Vlassenko AG, Rundle MM, Snyder AZ, Mintun MA, Raichle ME. Regional aerobic glycolysis in the human brain. *PNAS* 2010;107:17757–62. doi:10.1073/pnas.1010459107.
- [46] Vlassenko AG, Vaishnavi SN, Couture L, Sacco D, Shannon BJ, Mach RH, et al. Spatial correlation between brain aerobic glycolysis and amyloid- β (A β) deposition. *PNAS* 2010;107:17763–7. doi:10.1073/pnas.1010461107.
- [47] Zimmer ER, Parent MJ, Souza DG, Leuzy A, Lecrux C, Kim H-I, et al. [18F]FDG PET signal is driven by astroglial glutamate transport. *Nat Neurosci* 2017;20. doi:10.1038/nn.4492.
- [48] Morbelli S, Perneckzy R, Drzezga A, Frisoni GB, Caroli A, van Berckel BNM, et al. Metabolic Networks Underlying Cognitive Reserve in Prodromal Alzheimer Disease: A European Alzheimer Disease Consortium Project. *J Nucl Med* 2013;54:894–902. doi:10.2967/jnumed.112.113928.
- [49] Sanabria-Diaz G, Martínez-Montes E, Melie-Garcia L, Initiative N. Glucose Metabolism during Resting State Reveals Abnormal Brain Networks Organization in the Alzheimer's Disease and Mild Cognitive Impairment for the Alzheimer's Disease. *PLoS One* 2013;8. doi:10.1371/.
- [50] Seo EH, Lee DY, Lee J-M, Park J-S, Sohn BK, Lee DS, et al. Whole-brain Functional Networks in Cognitively Normal, Mild Cognitive Impairment, and Alzheimer's Disease. *PLoS One* 2013;8:e53922. doi:10.1371/journal.pone.0053922.
- [51] Krüger G, Glover GH. Physiological noise in oxygenation-sensitive magnetic resonance imaging. *Magn Reson Med* 2001;46:631–7. doi:10.1002/mrm.1240.
- [52] Calhoun VD, Adali T, Pearlson GD, Pekar JJ. A Method for Making Group Inferences from Functional MRI Data Using Independent Component Analysis. *Hum Brain Mapp* 2001;14:140–51. doi:10.1002/hbm.
- [53] Chhatwal JP, Schultz AP, Johnson KA, Benzinger TLS, Jack CR, Salloway S, et al. Impaired Default Network Functional Connectivity in Autosomal Dominant Alzheimer's Disease: Findings from the DIAN Study. *Neurology* 2013;81:S40–S40.

- [54] Pasquini L, Scherr M, Tahmasian M, Meng C, Myers NE, Ortner M, et al. Link between hippocampus' raised local and eased global intrinsic connectivity in AD. *Alzheimer's Dement* 2015;11:475–84. doi:10.1016/j.jalz.2014.02.007.
- [55] Taylor ANW, Kambeitz-Ilankovic L, Gesierich B, Simon-Vermot L, Franzmeier N, Araque Caballero MÁ, et al. Tract-specific white matter hyperintensities disrupt neural network function in Alzheimer's disease. *Alzheimer's Dement* 2017;13:225–35. doi:10.1016/j.jalz.2016.06.2358.
- [56] Suresh E joel A. On the relationship between seed based and ICA-based measures of functional connectivity. *Magn Reson* 2011;66:644–57. doi:10.1002/mrm.22818.On.
- [57] Zuo X-N, Ehmke R, Mennes M, Imperati D, Castellanos FX, Sporns O, et al. Network Centrality in the Human Functional Connectome. *Cereb Cortex* 2012;22:1862– 1875. doi:10.1093/cercor/bhr269.
- [58] Zou Q-H, Zhu C-Z, Yang Y, Zuo X-N, Long X-Y, Cao Q-J, et al. An improved approach to detection of amplitude of low-frequency fluctuation (ALFF) for resting-state fMRI: Fractional ALFF. vol. 172. 2008. doi:10.1016/j.jneumeth.2008.04.012.
- [59] Rodriguez-Vieitez E, Saint-Aubert L, Carter SF, Almkvist O, Farid K, Schöll M, et al. Diverging longitudinal changes in astrogliosis and amyloid PET in autosomal dominant Alzheimer's disease. *Brain* 2016;139:922–36. doi:10.1093/brain/awv404.

TABLES:**Table 1: Demographic data and neuropsychological characteristics**

	HC A β - (n=27)	MCI-A β + (n=44)	AD- A β + (n=25)	ANOVA	
	Mean(SD/Range)	Mean(SD/Range)	Mean(SD/Range)	F(df)	p-value
Gender (f/m)	18/9	18/26	13/12	$\chi^2=4.45(2)$	0.1077
Age (years)	74.6 (6.33/24.5)	72.4 (6.52/28.2)	72.23 (7.18/30.6)	1.131	0.327
Years of education	16.11(2.17/8)	16.14 (2.57/8)	15.68 (2.34/8)	0.32	0.727
MMSE score	28.88(1.31/5)	27.41(1.69/6)	23.00(2.53/8)	70.34	<0.001

f = female, m = male, HC: healthy controls; MCI: mild cognitive impairment; AD: Alzheimer's dementia; MMSE: Mini-Mental-State -Examination. For the MMSE, one subject (HC) had no MMSE score and was hence excluded from this ANOVA.

Table 2: Group differences in FDG-PET for each resting-state network

Network	Mean FDG-PET (SD)			ANCOVA (DX)		Tukey HSD		
	HC	MCI-A β +	AD	F(df _M , df _R)	p-value	p (HC vs MCI-A β +	p (MCI-A β + vs AD)	p (HC vs AD)
AUDITORY 1	1.23 (0.08)	1.19 (0.1)	1.13 (0.08)	(2, 90)= 10.47	<0.0001	n.s	0.0036	0.0005
AUDITORY 2	1.25 (0.08)	1.19 (0.09)	1.08 (0.12)	(2, 90)= 22.94	<0.0001	0.013	<0.0001	<0.0001
DAN	1.3 (0.1)	1.26 (0.09)	1.13 (0.13)	(2, 90)= 20.33	<0.0001	n.s	<0.0001	<0.0001
aDMN	1.29 (0.09)	1.26 (0.11)	1.16 (0.11)	(2, 90)= 12.38	<0.0001	n.s	0.0003	<0.0001
DMN	1.4 (0.09)	1.33 (0.12)	1.18 (0.12)	(2, 90)= 28.42	<0.0001	0.016	<0.0001	<0.0001
LFPAN	1.3 (0.09)	1.25 (0.11)	1.14 (0.13)	(2, 90)= 15.12	<0.0001	n.s	0.0002	<0.0001
MOTOR	1.24 (0.1)	1.23 (0.09)	1.17 (0.09)	(2, 90)= 4.40	0.013	n.s	0.045	0.015
RFPAN	1.35 (0.1)	1.29 (0.12)	1.17 (0.13)	(2, 90)= 15.70	<0.0001	n.s	0.0002	<0.0001
VISUAL 1	1.41(0.11)	1.38 (0.09)	1.29 (0.11)	(2, 90)= 10.16	0.0001	n.s	0.0018	0.0001
VISUAL 2	1.34 (0.)	1.3 (0.08)	1.22 (0.13)	(2, 90)= 10.10	0.0001	n.s	0.0018	0.0001

ANCOVA on network mean FDG-PET signal between the diagnostic groups (p-values are Bonferroni corrected for 10 tests).

DX: Diagnostic group; aDMN: anterior default mode network; AUDITORY 1: first auditory network, AUDITORY 2: second auditory network; DAN: dorsal attention network; DMN: default mode network; LFPAN: left fronto-parietal attention network; Motor: motor network; RFPAN: right fronto-parietal attention network; VISUAL 1: medial occipital visual network; VISUAL 2: lateral occipital visual network.

Table 3 Group differences in rsfMRI FC for each resting-state network

Network	Mean FDG-PET (SD)			ANCOVA (DX)		Tukey HSD		
	HC	MCI-A β +	AD	F(df _M , df _R)	p-value	p (HC vs MCI-A β +	p (MCI-A β + vs AD)	p (HC vs AD)
AUDITORY 1	1.05 (0.35)	1.1 (0.3)	1.05 (0.33)	(2, 90)= 0.33	0.71	n.s	n.s	n.s
AUDITORY 2	0.8 (0.68)	0.81 (0.27)	0.86 (0.27)	(2, 90)= 0.31	0.74	n.s	n.s	n.s
DAN	1.04 (0.3)	1.07 (0.33)	1.07 (0.33)	(2, 90)= 0.07	0.93	n.s	n.s	n.s
aDMN	0.82 (0.28)	0.96 (0.26)	1.01 (0.3)	(2, 90)= 3.51	0.035	n.s	n.s	0.038
DMN	1.25 (1.24)	1.22 (1.23)	1.2 (1.15)	(2, 90)= 0.1	0.91	n.s	n.s	n.s
LFPAN	0.97 (0.33)	1.06 (0.38)	1.0 (0.29)	(2, 90)= 0.63	0.54	n.s	n.s	n.s
MOTOR	1.05 (0.39)	1.16 (0.31)	1.1 (0.35)	(2, 90)= 0.91	0.41	n.s	n.s	n.s
RFPAN	0.91 (0.31)	1.21 (0.30)	0.98 (0.36)	(2, 90)= 8.42	0.0003	0.0006	0.013	n.s
VISUAL 1	1.14 (0.44)	1.22 (0.46)	1.34 (0.55)	(2, 90)= 1.31	0.28	n.s	n.s	n.s
VISUAL 2	0.94 (0.35)	1.03 (0.38)	0.98 (0.32)	(2, 90)= 0.73	0.49	n.s	n.s	n.s

ANCOVA on network mean FC between the diagnostic groups (p-values are Bonferroni corrected for 10 tests).

DX: Diagnostic group; aDMN: anterior default mode network; AUDITORY 1: first auditory network, AUDITORY 2: second auditory network; DAN: dorsal attention network; DMN: default mode network; LFPAN: left fronto-parietal attention network; Motor: motor network; RFPAN: right fronto-parietal attention network; VISUAL 1: medial occipital visual network; VISUAL 2: lateral occipital visual network.

Table 4: Spatial correlation and overlap between independent components from rsfMRI and FDG-PET

ICA components	Dice Coefficient	Dice coefficient. rating	Spatial Correlation coefficient	p-value
AUDITORY 1	0.66598	Good	0.54964	<0.001
LFPAN	0.64737	Good	0.47187	<0.001
DMN	0.62042	Good	0.57363	<0.001
VISUAL 1	0.5918	Moderate	0.31522	<0.001
aDMN	0.58993	Moderate	0.52805	<0.001
MOTOR	0.35554	Fair	0.41055	<0.001
DAN	0.34917	Fair	0.2863	<0.001
AUDITORY 2	0.31822	Fair	0.31152	<0.001
RFPAN	0.19931	Poor	0.15476	<0.001
VISUAL 2	0.18863	Poor	0.09189	<0.001

IC: independent component; DMN: default mode network; AUDITORY 1: first auditory network, aDMN: anterior default mode network; LFPAN: left fronto-parietal attention network; Motor: motor network; VISUAL 1: medial occipital visual network; AUDITORY 2: second auditory network; DAN: dorsal attention network; RFPAN: right fronto-parietal attention network; VISUAL 2: lateral occipital visual network.

FIGURES

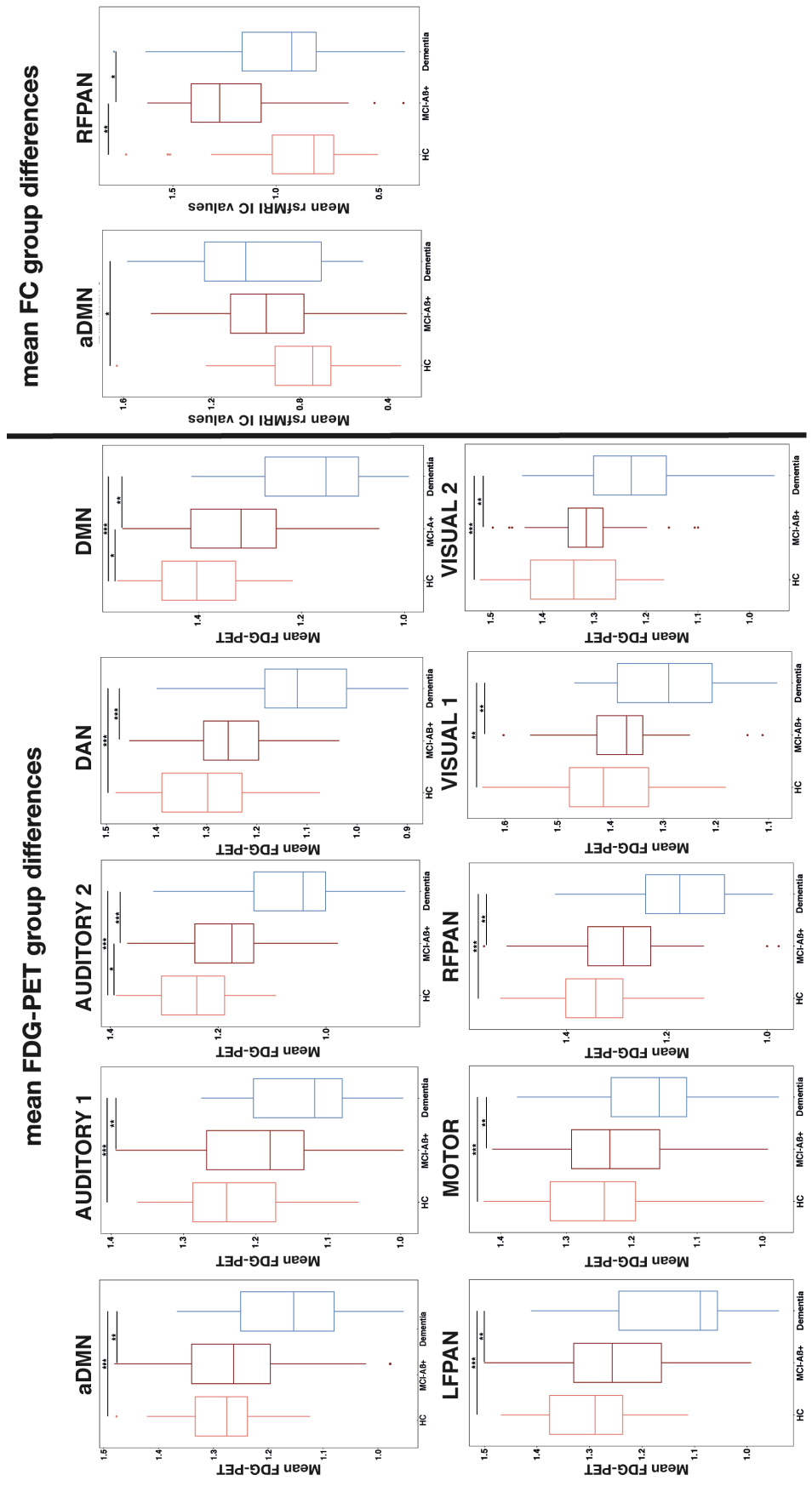


Figure 1: Boxplots of group differences for mean FDG-PET signal for each network (right) and mean FC (left). aDMN: anterior default mode network; AUDITORY 1: first auditory network, AUDITORY 2: second auditory network; DAN: dorsal attention network; DMN: default mode network; LFPAN: left fronto-parietal attention network; MOTPR: motor network; RFPAN: right fronto-parietal attention network; VISUAL 1: lateral occipital visual network; VISUAL 2: medial occipital visual network.

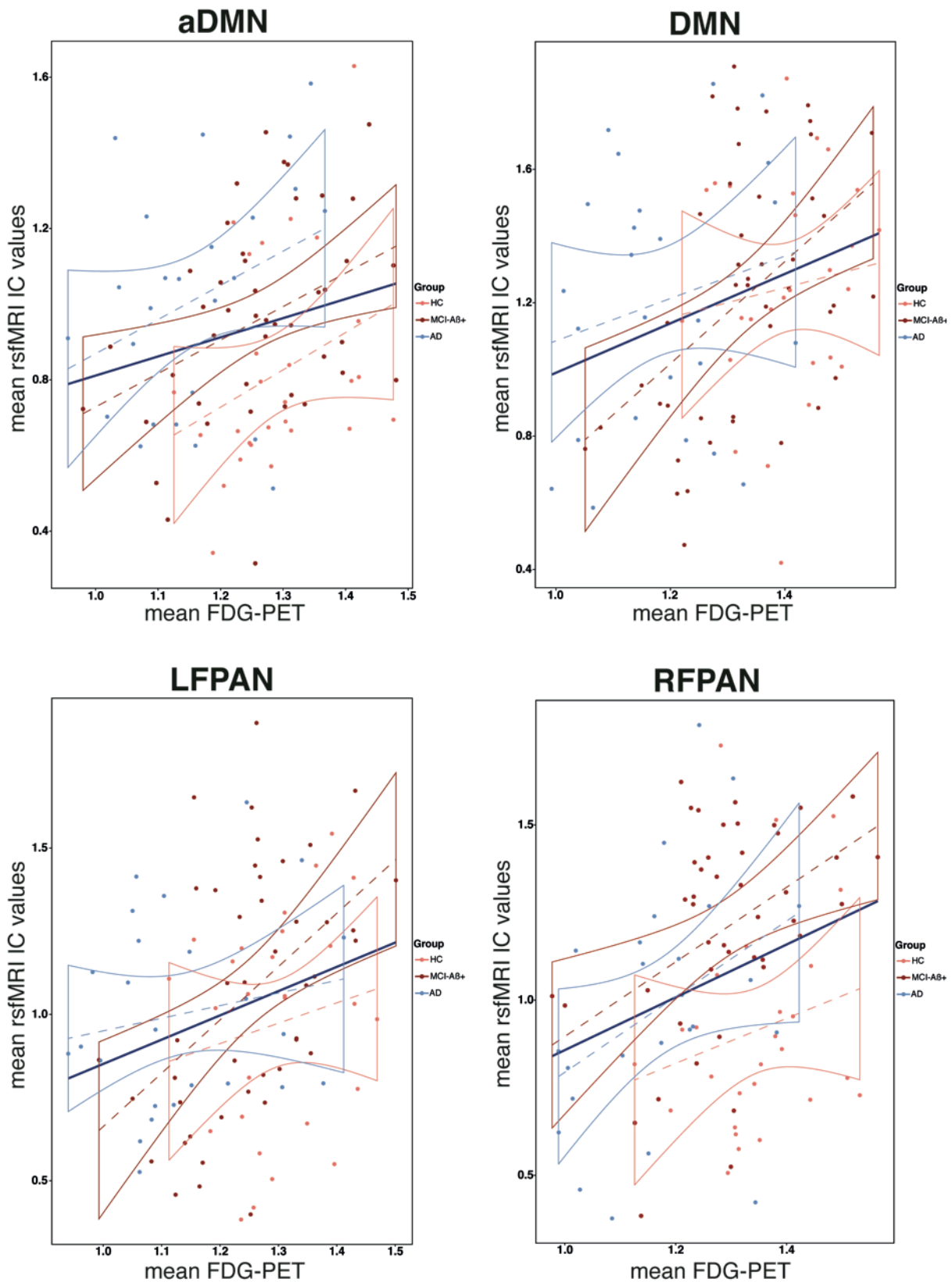


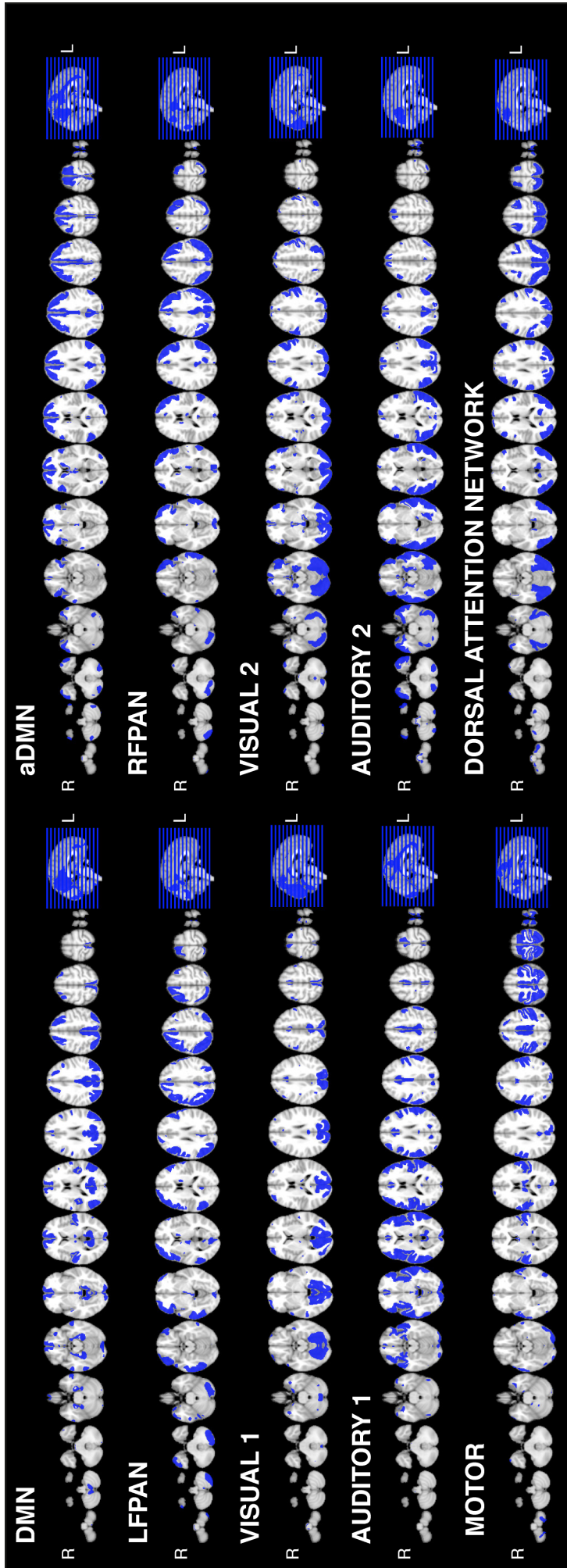
Figure 2: Scatterplots of the association between the mean level of glucose metabolism and the degree of resting-state functional connectivity (FC) in the whole pooled sample (dark blue line) for intrinsic networks derived from the ICA analysis.

aDMN: anterior default mode network; DMN: default mode network; LFPAN: left fronto-parietal attention network; RFPAN: right fronto-parietal attention network.

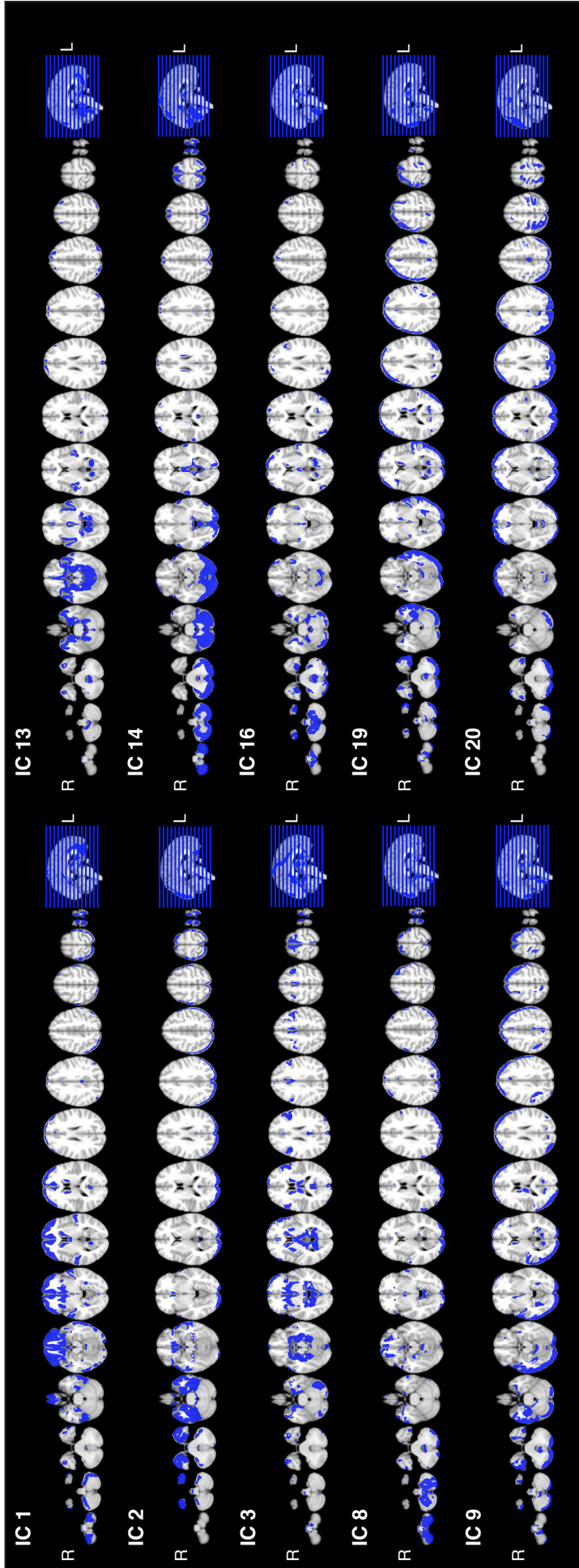


Figure 3: Superimposition of axial slices for each of the 10 ICA derived resting-state network maps and the SBM derived maps of FDG-PET. Each component map was thresholded at $z > 1$ and masked by a binary GM template.

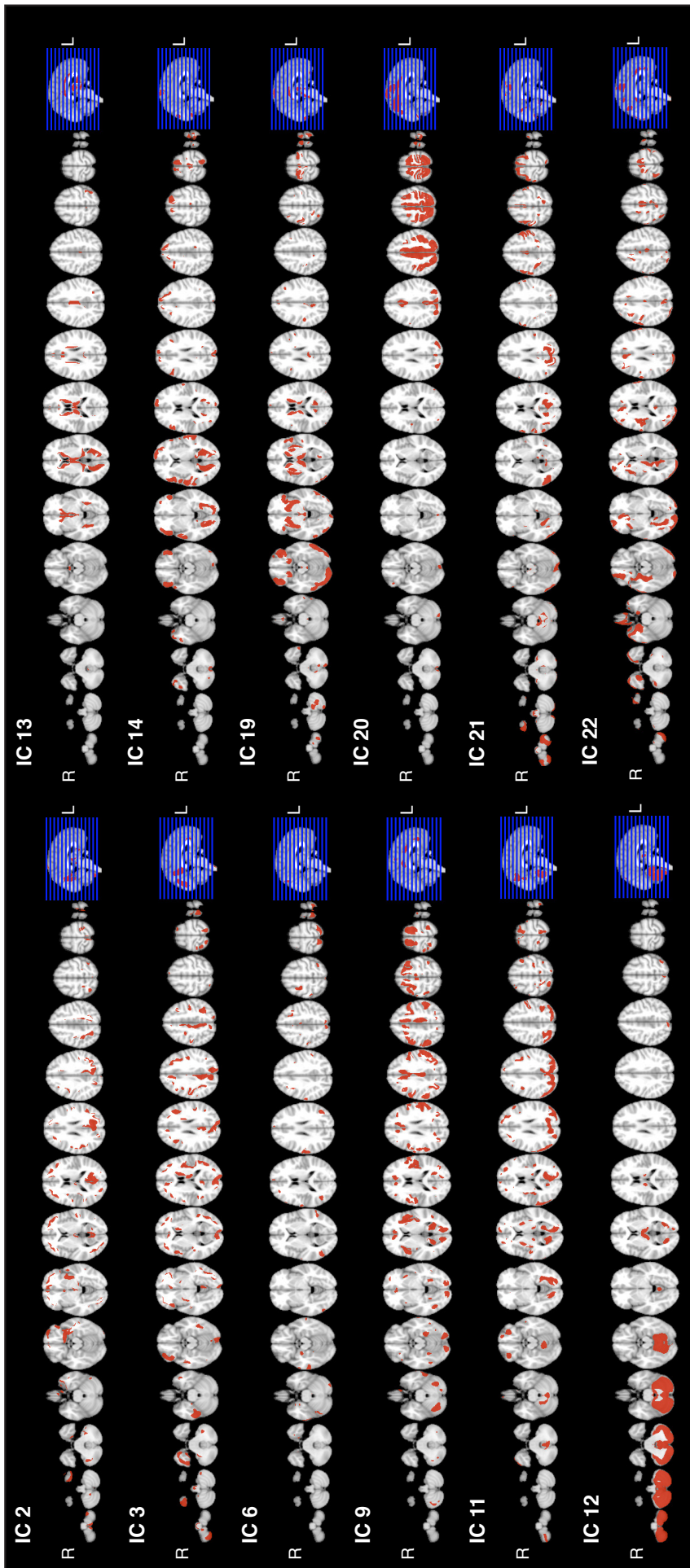
SUPPLEMENTARY MATERIAL



Supplementary figure 1: Axial slices of the rsfMRI ICA maps representing canonical resting-state networks. Component maps were thresholded at $z > 1$ and masked with the binary GM template.



Supplementary figure 2: Axial slices of excluded rsfMRI ICA maps representing noise. Component maps were thresholded at $z > 1$ and masked with the binary GM template.



Supplementary figure 3: Axial slices of excluded SBM derived FDG-PET maps representing noise. Component maps are thresholded at $z > 1$ and masked with the binary GM template.

04.

DISCUSSION

1.1. GENERAL DISCUSSION

Resting-state fMRI is a widely used method to investigate the brain's organization and function in health, aging as well as in various psychiatric diseases, such as AD. Changes in rsFC within large-scale networks have been extensively reported in aging and in AD (for review Andrews-Hanna et al., 2007; Damoiseaux et al., 2008; Sheline & Raichle, 2013). RsFC is an attractive alternative to task-fMRI in order to assess brain activity, mostly because it is easier to obtain in patients who are cognitive impaired and have difficulties in following task instructions. However, the relationship between rsfMRI-assessed functional network connectivity and task-related functional network connectivity is not well understood and remains a largely under-investigated assumption of the rationale of rsfMRI studies on human brain function. In order to elucidate the relationship between rsfMRI and neural processes that underlie episodic memory, we examined the correspondence of functional networks related to successful episodic memory with those obtained during resting-state in healthy subjects. In a second step, we aimed to test

whether rsfMRI can be used to detect disease-related functional network abnormalities that may underlie cognitive impairment, such as those occurring in AD. To this end, a second study was conducted, where the aim was to test whether rsfMRI networks that are altered in AD are associated to FDG-PET hypometabolism, which is considered to be one of the most reliable biomarkers of functional impairment in AD. In the following sections, the main findings of both projects are detailed and discussed.

4.1.1 Functional networks engaged during successful memory and encoding

The major aim of this study was to investigate the association between rsfMRI assessed functional networks and the functional networks active during successful episodic memory encoding and recall during a face-name association task. The first finding was that successful encoding was associated with task-related functional networks that covered the medial temporal lobe and medial frontal areas. While the posterior parietal and occipital regions were activated during successful recognition of face-name pairs. These findings are consistent with previously reported functional networks underlying successful encoding and retrieval of episodic memory (Huijbers et al., 2012). A meta-analysis showed that the hippocampus and regions that overlap with the fronto-parietal attention network are associated with episodic memory encoding, whereas regions associated with recognition span rather in posterior regions that associated with the DMN (Kim, 2015). The second finding was the unique spatial match between the task-related functional networks and the rsfMRI components obtained within the same subjects. In addition, those functional networks that showed intra-subject correspondence also showed a spatial match to previously reported resting-state subnetworks from the meta-

analysis of 3,000 subjects, using a 70 component ICA (Smith et al., 2009). These smaller networks that well matched the task-related networks were subcomponents of large-scale RSNs including the DMN and FPAN. Together these results suggest that subcomponents of RSNs are recruited during episodic memory encoding and recognition. The fact that episodic memory processes seem to be supported by smaller fractions of multiple large-scale RSNs may also explain why it has been previously difficult to identify a single network among the set of canonical large-scale networks that supports episodic memory. That is, large-scale networks underlying visual, motor, saliency detection or executive functions have been described, but no specific large-scale network has been assigned to episodic memory (Damoiseaux et al., 2006). Rather our results are consistent with previous attempts to map cognitive functions to subcomponents of larger RSNs (Shirer, Ryali, Rykhlevskaia, Menon, & Greicius, 2012), including, in particular, subcomponents of the DMN during memory retrieval (Andrews-Hanna et al., 2010). The activation of the posterior medial parietal cortex during retrieval but not encoding has been previously found to be predictive of successful memory performance (Daselaar et al., 2009; Huijbers et al., 2012; Huijbers et al., 2013; Vannini et al., 2013). Wang and colleagues showed that increased region-of-interest based rsFC between the posterior cingulate and the hippocampus predicted subsequent recall of a face-name association task in older adults (Wang et al., 2010). Together, these results suggest that the hippocampus network and the FPAN underlie successful encoding and subcomponents of the DMN support successful memory retrieval.

Finally, we wanted to go one step further to better understand the relevance of resting-state networks in the context of episodic memory. We assessed whether the level of task-related activation within the network subcomponents could be predicted based on the

level of functional connectivity during resting-state. We found that the level of resting-state connectivity wasn't predictive of the level of task-related network expression. This approach is different to the methods generally used to assess how resting-state networks relate to task, which relies on the spatial match. In this case, the goal was to predict task-related activation based on the connectivity strength during rest. In 2006, Fox and colleagues (Fox, Snyder, Zacks, & Raichle, 2006) suggested that task-related activation is the result of the additive combination between the resting-state connectivity and task-specific neural activation. Our results do not contradict this postulate, but rather indicate that stronger rsFC does not translate into stronger task-related connectivity.

Taken together, the results of the study indicate that rsfMRI can't be used as a substitute for episodic memory task-related connectivity. However, the current findings suggest that a subset of regions that are part of intrinsic networks are selectively recruited during successful episodic memory encoding and retrieval. These results support the cognitive relevance of resting-state networks. Furthermore, they indicate that rsFC within these subnetworks could indeed be useful to investigate the changes in episodic memory that occur in the course of AD.

Relevance of resting-state networks to predict cognitive performance and outlook to application in disease



Multiple rsfMRI studies in AD demonstrated that rsfMRI assessed functional connectivity, particularly in the DMN, is reduced in MCI and AD dementia. Furthermore, that rsfMRI is a potential alternative to FDG-PET to detect disease specific functional brain changes that may underlie cognitive impairment. FDG-PET hypometabolism is considered as a core feasible biomarker of functional impairment in AD, but, is an invasive costly imaging

technique to detect altered brain function in MCI and AD. Typically, regions of FDG-PET hypometabolism in AD overlap with DMN regions. Still, the relationship between rsfMRI differences in DMN and FDG-PET hypometabolism remains poorly understood.

4.1.2 Association of FDG-PET metabolism & resting-state connectivity in Alzheimer's disease

The main finding was that higher functional connectivity was associated with higher FDG-PET metabolism specifically in the DMN and FPAN in the pooled group of healthy elderly subjects, MCI with high A β and patients with AD. When analyzed for each diagnostic group separately, a positive association between FDG-PET glucose metabolism and rsfMRI functional connectivity in the DMN and in the left and right FPAN was observed in MCI. The associations between rsfMRI connectivity and FDG-PET were also positive in the HC and AD groups but did not reach statistical significance probably due to the lower sample size when compared to MCI. These results suggest that both modalities are positively associated within major cortical functional networks. These results are consistent with findings from previous studies reporting associations between resting-state connectivity and FDG-PET in the DMN (Passow et al., 2015) or cerebral blood flow, measured by arterial spin-labeling (Li, Zhu, Childress, Detre, & Wang, 2012; Liang, Zou, He, & Yang, 2013) in healthy subjects. The question arises why were the strongest associations observed specifically in the DMN and FPAN? One likely possibility is that the DMN shows the highest connectivity during resting state. The activity is typically anticorrelated with the FPAN during rest. Thus, in the current resting-state study, inter-individual differences in network activity may be most sensitively measured by rsfMRI and FDG-PET in the DMN and FPAN, which may have facilitated the detection of the

intermodal correlations within these networks. Another possibility could be that the both networks are made of highly connected hubs, that also contain a higher proportion of long distance connections (Liang et al., 2013). This could require higher energy needs and therefore trigger the strongest association between both in the DMN and FPAN.

For the group differences in rsFC and FDG-PET, we found that FDG-PET but not rsfMRI was decreased in the DMN of MCI and AD subjects compared to HC. In contrast, rsFC but not FDG-PET was increased in the right FPAN in the MCI and AD groups compared to HC. The change of direction in each modality is consistent with previous findings. Resting-state FC increase in frontal areas has also been reported in people with a genetic risk factor for AD (Sala-Llonch et al., 2013) and in early AD (Damoiseaux, Prater, Miller, & Greicius, 2012; Jones et al., 2011; Wang et al., 2015; Zhang et al., 2016). For FDG-PET, hypometabolism in the posterior parietal lobe in MCI and AD has been reported in multiple studies (Teipel et al., 2015).

Thus it is likely that although FDG-PET and rsfMRI are overall positively associated, disease related processes might alter glucose consumption and neural connectivity in partially different ways. Previous studies have shown that astrocyte glucose consumption significantly increases the FDG-PET signal (Pellerin & Magistretti, 1994; Zimmer et al., 2017). Amyloid-pathology, which is strongest in the regions overlapping with the DMN (Vlassenko et al., 2010) could impact on the astrocytes activity and thereby lead to a reduction of the FDG-PET signal in the DMN. The astrocyte activity possibly impairs the FDG-PET signal, while not affecting rsfMRI derived neural activity and thereby lead to the different patterns found in FDG-PET and rsfMRI in AD.

It remains surprising that FDG-PET and rsfMRI were still positively associated despite the inconsistent direction of change in MCI and AD. One explanation is that the group differences within large-scale networks may not be homogeneous within the whole network but show local differences that were not accounted for in this case by averaging the connectivity of the entire network. Hence, an ICA with a higher number of estimated rsfMRI components may have revealed regional subcomponents (e.g. of the DMN) that show a similar direction of AD related change as was observed for FDG-PET. Due to the relatively small sample size in the current study, we did not conduct ICA with a higher number of components, which may be done however in future larger studies.

4.2 IMPLICATIONS ACROSS PROJECTS

The main question of this thesis was to investigate whether large-scale network rsFC is a valid proxy to assess the network activity that underlies brain function. With both studies we could demonstrate that resting-state networks, in particular the DMN and FPAN, are engaged in episodic memory processes. However, the level of rsfMRI connectivity was not predictive of the level of brain activation during successful memory task performance. Although resting-state FC was related to FDG-PET in MCI, disease specific changes in posterior parietal brain areas were detectable via FDG-PET but not in rsfMRI. Thus, the diagnostic reliability of rsfMRI to specifically detect early changes in AD is still open to debate. One of main difficulties of finding a good diagnostic measure is that AD is a very complex neurodegenerative disease that starts with insidious changes decades before the clinical manifestation episodic memory impairments. This implies the necessity of using methods that can pick up very subtle changes, which occur in distributed brain regions, i.e. neural networks. Previous studies have tried to establish rsfMRI as a feasible

biomarker of AD, but until now the diagnostic level is still not sufficient from a clinical point of view for the individual diagnosis. In 2004, Greicius et al. looked at how well the individual goodness-of-fit scores matched a DMN template and could correctly categorize 11 of 13 AD subjects and 10 of 13 HC, which resulted in a sensitivity of 85% and specificity of 77% (Greicius et al., 2004). However, the study samples contained two extreme groups, namely healthy controls and AD patients and were very small; such a small group size isn't optimal for extracting networks using ICA. A more recent study used the individual DMN connectivity of early AD patients and HC and compared them to an average DMN connectivity score to separate both groups, which yield to a sensitivity of 77.3% and a specificity of 70% (Balthazar, de Campos, Franco, Damasceno, & Cendes, 2014). A major concern about this study is that they calculated the reference DMN based on the HC in that sample, which could lead to over fitting the data. Taken together, it seems that rsfMRI lacks a satisfactory level of sensitivity and specificity (>80%) for the diagnosis of AD at an early stage. This may be due to the fact that the DMN as a whole isn't specific enough and perhaps that looking at the subcomponents, which are specifically related to successful episodic memory, could be more accurate. However, before making any claim about the usability of these episodic memory-related subnetworks, future studies must be conducted.



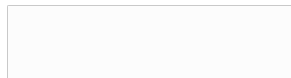
4.3 OUTLOOK

Future studies should investigate whether and how the subnetworks related to episodic memory are impaired at various stages of AD. These should include combined dynamic FDG-PET and fMRI in healthy elderly, MCI and AD subjects in order to assess how these subnetworks are changed and impaired in the course of AD. Another possibility could be

to use dynamic rsfMRI analysis to gain more insight into how the networks activate vs deactivate during encoding and recall and how the coordination of these subnetworks is impaired by AD could be more informative, than just looking at one state.

4.4 LIMITATIONS

For the interpretation of the current project, some limitations must be taken into consideration. First, two different groups of subjects were used in both projects. In the first project, we only looked at HC. Having MCI and AD patients might have enabled us to generalize the findings in a more straightforward way. For the second project, the data was provided by the Alzheimer's Disease Neuroimaging Initiative (ADNI), where multicenter variability may reduce the statistical power to detect disease related group difference in rsfMRI or FDG-PET.



05.

REFERENCES

- 2017 Alzheimer's disease facts and figures. (2017). *Alzheimer's & Dementia* 13. <https://doi.org/http://dx.doi.org/10.1016/j.jalz.2017.02.001>
- Alescio-Lautier, B., Michel, B. F., Herrera, C., Elahmadi, A., Chambon, C., Touzet, C., & Paban, V. (2007). Visual and visuospatial short-term memory in mild cognitive impairment and Alzheimer disease: Role of attention. *Neuropsychologia*, 45(8), 1948–1960. <https://doi.org/10.1016/j.neuropsychologia.2006.04.033>
- Anderson, N. D., & Craik, F. I. M. (2000). Memory in the aging brain. In *The Oxford handbook of memory* (pp. 411–425). Retrieved from [http://chomsky.hum.uct.ac.za/Refs/Anderson_&_Craik_\(2000\)_Memory_in_the_Aging_Brain.pdf](http://chomsky.hum.uct.ac.za/Refs/Anderson_&_Craik_(2000)_Memory_in_the_Aging_Brain.pdf)
- Andrews-Hanna, J. R., Reidler, J. S., Sepulcre, J., Poulin, R., & Buckner, R. L. (2010). Functional-Anatomic Fractionation of the Brain's Default Network. *Neuron*, 65(4), 550–562. <https://doi.org/10.1016/j.neuron.2010.02.005>
- Andrews-Hanna, J. R., Snyder, A. Z., Vincent, J. L., Lustig, C., Head, D., Raichle, M. E., & Buckner, R. L. (2007). Disruption of Large-Scale Brain Systems in Advanced Aging. *Neuron*, 56(5), 924–935. <https://doi.org/10.1016/j.neuron.2007.10.038>
- Arfanakis, K., Cordes, D., Haughton, V. M., Moritz, C. H., Quigley, M. A., & Meyerand, M. E. (2000). Combining independent component analysis and correlation analysis to probe interregional connectivity in fMRI task activation datasets. *Magnetic Resonance Imaging*, 18(8), 921–930. [https://doi.org/10.1016/S0730-725X\(00\)00190-9](https://doi.org/10.1016/S0730-725X(00)00190-9)
- Bai, F., Zhang, Z., Yu, H., Shi, Y., Yuan, Y., Zhu, W., ... Qian, Y. (2008). Default-mode network activity distinguishes amnesic type mild cognitive impairment from healthy aging: A combined structural and resting-state functional MRI study. *Neuroscience Letters*, 438, 111–115. <https://doi.org/10.1016/j.neulet.2008.04.021>

- Balota, D. a, Dolan, P. O., & Duchek, J. M. (2000). Memory changes in healthy older adults. *The Oxford Handbook of Memory, The Oxford*, 395–409. Retrieved from <http://www.psych.wustl.edu/coglab/publications/BalotaDolanDuchekMemchapter2000.pdf>
- Balthazar, M. L. F., de Campos, B. M., Franco, A. R., Damasceno, B. P., & Cendes, F. (2014). Whole cortical and default mode network mean functional connectivity as potential biomarkers for mild Alzheimer's disease. *Psychiatry Research - Neuroimaging*, 221(1), 37–42. <https://doi.org/10.1016/j.psychresns.2013.10.010>
- Benzinger, T. L. S., Blazey, T., Jack, C. R., Koeppe, R. A., Su, Y., Xiong, C., ... Morris, J. C. (2013). Regional variability of imaging biomarkers in autosomal dominant Alzheimer's disease. *Proceedings of the National Academy of Sciences of the United States of America*, 110(47), E4502-9. <https://doi.org/10.1073/pnas.1317918110>
- Binnewijzend, M. a a, Schoonheim, M. M., Sanz-Arigita, E., Wink, A. M., van der Flier, W. M., Tolboom, N., ... Barkhof, F. (2012). Resting-state fMRI changes in Alzheimer's disease and mild cognitive impairment. *Neurobiology of Aging*, 33(9), 2018–28. <https://doi.org/10.1016/j.neurobiolaging.2011.07.003>
- Blennow, K., Leon, M. J. De, & Zetterberg, H. (2006). Alzheimer ' s disease. *Lancet*, 368, 387–403.
- Bressler, S. L., & Menon, V. (2010). Large-scale brain networks in cognition: emerging methods and principles. *Trends in Cognitive Sciences*, 14(6), 277–90. <https://doi.org/10.1016/j.tics.2010.04.004>
- Brier, M. R., Thomas, J. B., Snyder, A. Z., Benzinger, T. L., Zhang, D., Raichle, M. E., ... Ances, B. M. (2012). Loss of Intranetwork and Internetwork Resting State Functional Connections with Alzheimer's Disease Progression. *Journal of Neuroscience*. <https://doi.org/10.1523/JNEUROSCI.5698-11.2012>
- Buckner, R. L., Andrews-Hanna, J. R., & Schacter, D. L. (2008). The brain's default network: anatomy, function, and relevance to disease. *Annals of the New York Academy of Sciences*, 1124, 1–38. <https://doi.org/10.1196/annals.1440.011>
- Buckner, R. L., Snyder, A. Z., Shannon, B. J., LaRossa, G., Sachs, R., Fotenos, A. F., ... Mintun, M. a. (2005). Molecular, structural, and functional characterization of Alzheimer's disease: evidence for a relationship between default activity, amyloid, and memory. *The Journal of Neuroscience: The Official Journal of the Society for Neuroscience*, 25(34), 7709–17. <https://doi.org/10.1523/JNEUROSCI.2177-05.2005>
- Buxton, R. B. (2009). *An Introduction to Functional Magnetic Resonance Imaging: Principles and Techniques*.
- Celone, K. a, Calhoun, V. D., Dickerson, B. C., Atri, A., Chua, E. F., Miller, S. L., ... Sperling, R. a. (2006). Alterations in memory networks in mild cognitive impairment and Alzheimer's disease: an independent component analysis. *The Journal of Neuroscience: The Official Journal of the Society for Neuroscience*, 26(40), 10222–31. <https://doi.org/10.1523/JNEUROSCI.2250-06.2006>

- Chhatwal, J. P., Schultz, A. P., Johnson, K. A., Benzinger, T. L. S., Jack, C. R., Salloway, S., ... Sperling, R. A. (2013). Impaired Default Network Functional Connectivity in Autosomal Dominant Alzheimer's Disease: Findings from the DIAN Study. *Neurology*, *81*(8), S40-S40.
- Cole, M. W., Bassett, D. S., Power, J. D., Braver, T. S., & Petersen, S. E. (2014). Intrinsic and task-evoked network architectures of the human brain. *Neuron*, *83*(1), 238-251. <https://doi.org/10.1016/j.neuron.2014.05.014>
- Damoiseaux, J. S., Beckmann, C. F., Arigita, E. J. S., Barkhof, F., Scheltens, P., Stam, C. J., ... Rombouts, S. A. R. B. (2008). Reduced resting-state brain activity in the "default network" in normal aging. *Cerebral Cortex*, *18*(8), 1856-1864. <https://doi.org/10.1093/cercor/bhm207>
- Damoiseaux, J. S., Prater, K. E., Miller, B. L., & Greicius, M. D. (2012). Functional connectivity tracks clinical deterioration in Alzheimer's disease. *Neurobiology of Aging*, *33*(4), 828.e19-828.e30. <https://doi.org/10.1016/j.neurobiolaging.2011.06.024>
- Damoiseaux, J. S., Rombouts, S. A. R. B., Barkhof, F., Scheltens, P., Stam, C. J., Smith, S. M., & Beckmann, C. F. (2006). Consistent resting-state networks. *PNAS*, *103*(2), 13848-13853.
- Daselaar, S. M., Huijbers, W., Eklund, K., Moscovitch, M., & Cabeza, R. (2013). Resting-state functional connectivity of ventral parietal regions associated with attention reorienting and episodic recollection. *Frontiers in Human Neuroscience*, *7*(February), 38. <https://doi.org/10.3389/fnhum.2013.00038>
- Daselaar, S. M., Prince, S. E., & Cabeza, R. (2004). When less means more: deactivations during encoding that predict subsequent memory. *NeuroImage*, *23*(3), 921-7. <https://doi.org/10.1016/j.neuroimage.2004.07.031>
- Daselaar, S. M., Prince, S. E., Dennis, N. A., Hayes, S. M., Kim, H., & Cabeza, R. (2009). Posterior midline and ventral parietal activity is associated with retrieval success and encoding failure. *Frontiers in Human Neuroscience*, *3*, 13. <https://doi.org/10.3389/neuro.09.013.2009>
- de Leon, M. J., Convit, A., Wolf, O. T., Tarshish, C. Y., DeSanti, S., Rusinek, H., ... Fowler, J. (2001). Prediction of cognitive decline in normal elderly subjects with 2-[(18)F]fluoro-2-deoxy-D-glucose/positron-emission tomography (FDG/PET). *Proceedings of the National Academy of Sciences of the United States of America*, *98*(19), 10966-71. <https://doi.org/10.1073/pnas.191044198>
- Di, X., Biswal, B. B., & Alzheimer's Disease Neuroimaging Initiative. (2012). Metabolic Brain Covariant Networks as Revealed by FDG-PET with Reference to Resting-State fMRI Networks. *Brain Connectivity*, *2*(5), 275-283. <https://doi.org/10.1089/brain.2012.0086>
- Di, X., Gohel, S., Thielcke, A., Wehrl, H. F., & Biswal, B. B. (2017). Do all roads lead to Rome? A comparison of brain networks derived from inter-subject volumetric and metabolic covariance and moment-to-moment hemodynamic correlations in old individuals. *Brain Structure and Function*. <https://doi.org/10.1007/s00429-017-1438-7>

- Dickerson, B. C., & Eichenbaum, H. (2010). The episodic memory system: neurocircuitry and disorders. *Neuropsychopharmacology: Official Publication of the American College of Neuropsychopharmacology*, 35(1), 86–104. <https://doi.org/10.1038/npp.2009.126>
- Dickerson, B. C., & Sperling, R. a. (2009). Large-scale functional brain network abnormalities in Alzheimer's disease: insights from functional neuroimaging. *Behavioural Neurology*, 21(1), 63–75. <https://doi.org/10.3233/BEN-2009-0227>. Large-scale
- Drzezga, A., Becker, J. A., Van Dijk, K. R. A., Sreenivasan, A., Talukdar, T., Sullivan, C., ... Sperling, R. A. (2011). Neuronal dysfunction and disconnection of cortical hubs in non-demented subjects with elevated amyloid burden. *Brain*. <https://doi.org/10.1093/brain/awr066>
- Elton, A., & Gao, W. (2013). Task-positive Functional Connectivity of the Default Mode Network Network Transcends Task Domain. *Journal of Cognitive Neuroscience*, 27(12), 2369–2381. https://doi.org/10.1162/jocn_a_00859
- Fair, D. A., Schlaggar, B. L., Cohen, A. L., Miezin, F. M., Dosenbach, N. U. F., Wenger, K. K., ... Petersen, S. E. (2007). A method for using blocked and event-related fMRI data to study “resting state” functional connectivity. *NeuroImage*, 35(1), 396–405. <https://doi.org/10.1016/j.neuroimage.2006.11.051>
- Förster, S., Grimmer, T., Miederer, I., Henriksen, G., Yousefi, B. H., Graner, P., ... Drzezga, A. (2012). Regional Expansion of Hypometabolism in Alzheimer's Disease Follows Amyloid Deposition with Temporal Delay. *Biological Psychiatry*, 71(9), 792–797. <https://doi.org/10.1016/j.biopsych.2011.04.023>
- Fox, M. D., & Raichle, M. E. (2007). Spontaneous fluctuations in brain activity observed with functional magnetic resonance imaging. *Nature Reviews. Neuroscience*, 8(9), 700–11. <https://doi.org/10.1038/nrn2201>
- Fox, M. D., Snyder, A. Z., Zacks, J. M., & Raichle, M. E. (2006). Coherent spontaneous activity accounts for trial-to-trial variability in human evoked brain responses. *Nature Neuroscience*, 9(1), 23–25. <https://doi.org/10.1038/nn1616>
- Gauthier, S., Reisberg, B., Zaudig, M., Petersen, R. C., Ritchie, K., Broich, K., ... Winblad, B. (2006). Seminar Mild cognitive impairment.
- Goveas, J. S., Xie, C., Chen, G., Li, W., Ward, B. D., Franczak, M. B., ... Li, S.-J. (2013). Functional network endophenotypes unravel the effects of apolipoprotein E epsilon 4 in middle-aged adults. *PLoS One*, 8(2), e55902. <https://doi.org/10.1371/journal.pone.0055902>
- Grady, C. (2012). The cognitive neuroscience of ageing. *Nature Reviews. Neuroscience*, 13(7), 491–505. <https://doi.org/10.1038/nrn3256>
- Grady, C. L., & Craik, F. I. (2000). Changes in memory processing with age. *Current Opinion in Neurobiology*, 10(2), 224–231. [https://doi.org/10.1016/S0959-4388\(00\)00073-8](https://doi.org/10.1016/S0959-4388(00)00073-8)
- Greicius, M. (2004). Default-mode network activity distinguishes Alzheimer's disease from healthy aging: evidence from functional MRI. *Proceedings of the ...* Retrieved from <http://www.pnas.org/content/101/13/4637.short>

- Greicius, M. D., Srivastava, G., Reiss, A. L., & Menon, V. (2004). Default-mode network activity distinguishes Alzheimer's disease from healthy aging: evidence from functional MRI. *Proceedings of the National Academy of Sciences of the United States of America*, *101*(13), 4637–42. <https://doi.org/10.1073/pnas.0308627101>
- He, W., Goodkind, D., & Kowal, P. (2016). U.S. Census Bureau, International Population Reports, P95/16–1, An Aging World: 2015. *U.S. Government Publishing Office, Washington, DC, 2016.*
- Hebert, L. E., Weuve, J., Scherr, P. A., & Evans, D. A. (2013). Alzheimer disease in the United States (2010–2050) estimated using the 2010 census. *Neurology*, *80*(19), 1778–1783. <https://doi.org/10.1212/WNL.0b013e31828726f5>
- Hedden, T., & Gabrieli, J. D. E. (2004). Insights into the ageing mind: a view from cognitive neuroscience. *Nature Reviews Neuroscience*, *5*(2), 87–96. <https://doi.org/10.1038/nrn1323>
- Hedden, T., Van Dijk, K. R. A., Becker, J. A., Mehta, A., Sperling, R. A., Johnson, K. A., & Buckner, R. L. (2009). Disruption of functional connectivity in clinically normal older adults harboring amyloid burden. *The Journal of Neuroscience : The Official Journal of the Society for Neuroscience*, *29*, 12686–12694. <https://doi.org/10.1523/JNEUROSCI.3189-09.2009>
- Herholz, K. (2003). PET studies in dementia. *Annals of Nuclear Medicine*, *17*(2), 79–89.
- Herholz, K., Carter, S. F., & Jones, M. (2007). Positron emission tomography imaging in dementia. *The British Journal of Radiology*, *80*(special_issue_2), S160–S167. <https://doi.org/10.1259/bjr/97295129>
- Horn, A., Ostwald, D., Reisert, M., & Blankenburg, F. (2013). The structural-functional connectome and the default mode network of the human brain. *NeuroImage*. <https://doi.org/10.1016/j.neuroimage.2013.09.069>
- Huijbers, W., Schultz, A. P., Vannini, P., McLaren, D. G., Wigman, S. E., & Ward, A. M. (2013). The Encoding / Retrieval Flip : Interactions between Memory Performance and Memory Stage and Relationship to Intrinsic Cortical Networks, 1163–1179. <https://doi.org/10.1162/jocn>
- Huijbers, W., Vannini, P., Sperling, R. A., Pennartz, C., Cabeza, R., & Daselaar, S. M. (2012a). Explaining the encoding/retrieval flip: memory-related deactivations and activations in the posteromedial cortex. *Neuropsychologia*, *50*(14). <https://doi.org/10.1016/j.neuropsychologia.2012.08.021>
- Jiang, T., He, Y., Zang, Y., & Weng, X. (2004). Modulation of Functional Connectivity during the Resting State and the Motor Task. *Human Brain Mapping*, *22*(1), 63–71. <https://doi.org/10.1002/hbm.20012>
- Jones, D. T., Knopman, D. S., Gunter, J. L., Graff-Radford, J., Vemuri, P., Boeve, B. F., ... Jack, C. R. (2016). Cascading network failure across the Alzheimer's disease spectrum. *BRAIN*, *139*, 547–562. <https://doi.org/10.1093/brain/awv338>
- Jones, D. T., Machulda, M. M., Vemuri, P., McDade, E. M., Zeng, G., Senjem, M. L., ... Jack, C. R. J. (2011). Age-related changes in the default mode network are more advanced in Alzheimer disease. *Neurology*, *77*(16), 1524–1531. <https://doi.org/10.1212/WNL.0b013e318233b33d>

- Jorm, A. F., Christensen, H., Korten, A. E., Jacomb, P. A., & Henderson, A. S. (2001). Memory complaints as a precursor of memory impairment in older people: a longitudinal analysis over 7-8 years. *Psychological Medicine*, *31*(3), 441-9. Retrieved from <http://www.ncbi.nlm.nih.gov/pubmed/11305852>
- Kahn, I., Andrews-hanna, J. R., Vincent, J. L., Snyder, A. Z., & Buckner, R. L. (2008). Distinct Cortical Anatomy Linked to Subregions of the Medial Temporal Lobe Revealed by Intrinsic Functional Connectivity, 129-139. <https://doi.org/10.1152/jn.00077.2008>.
- Karow, D. S., Mcevoy, L. K., Fennema-Notestine, C., Hagler, D. J., Jennings, R. G., Brewer, J. B., ... Dale, A. M. (2010). Relative Capability of MR Imaging and FDG PET to Depict Changes Associated with Prodromal and Early Alzheimer Disease 1. *Radiology.rsna.org N Radiology*, *256*(3—September). <https://doi.org/10.1148/radiol.10091402/-/DC1>
- Kelley, C., & Jacoby, L. L. L. (2000). Recollection and familiarity: Process-dissociation. *The Oxford Handbook of Memory*, 215-228. Retrieved from <http://psiexp.ss.uci.edu/research/papers/memory/KelleyJacoby.pdf>
- Kim, H. (2015). Encoding and retrieval along the long axis of the hippocampus and their relationships with dorsal attention and default mode networks: The HERNET model. *Hippocampus*, *25*(4), 500-510. <https://doi.org/10.1002/hipo.22387>
- Kim, H., Daselaar, S. M., & Cabeza, R. (2010). Overlapping brain activity between episodic memory encoding and retrieval: Roles of the task-positive and task-negative networks, *49*(1), 1045-1054. <https://doi.org/10.1016/j.neuroimage.2009.07.058>.Overlapping
- Klunk, W. E., Engler, H., Nordberg, A., Wang, Y., Blomqvist, G., Holt, D. P., ... Långstro, B. (2004). Imaging Brain Amyloid in Alzheimer ' s Disease with Pittsburgh Compound-B.
- Koch, K., Myers, N. E., Göttler, J., Pasquini, L., Grimmer, T., Förster, S., ... Sorg, C. (2015). Disrupted intrinsic networks link amyloid- β pathology and impaired cognition in prodromal Alzheimer's disease. *Cerebral Cortex*, *25*(12), 4678-4688. <https://doi.org/10.1093/cercor/bhu151>
- Li, H. J., Hou, X. H., Liu, H. H., Yue, C. L., Lu, G. M., & Zuo, X. N. (2015). Putting age-related task activation into large-scale brain networks: A meta-analysis of 114 fMRI studies on healthy aging. *Neuroscience and Biobehavioral Reviews*, *57*(16), 156-174. <https://doi.org/10.1016/j.neubiorev.2015.08.013>
- Li, Z., Zhu, Y., Childress, A. R., Detre, J. A., & Wang, Z. (2012). Relations between BOLD fMRI-Derived Resting Brain Activity and Cerebral Blood Flow. *PLoS ONE*, *7*(9), 1-11. <https://doi.org/10.1371/journal.pone.0044556>
- Liang, X., Zou, Q., He, Y., & Yang, Y. (2013). Coupling of functional connectivity and regional cerebral blood flow reveals a physiological basis for network hubs of the human brain. *Proceedings of the National Academy of Sciences*, *110*(5), 1929-1934. <https://doi.org/10.1073/pnas.1214900110>

- Libby, L. a, Ekstrom, A. D., Ragland, J. D., & Ranganath, C. (2012). Differential connectivity of perirhinal and parahippocampal cortices within human hippocampal subregions revealed by high-resolution functional imaging. *The Journal of Neuroscience: The Official Journal of the Society for Neuroscience*, 32(19), 6550–60. <https://doi.org/10.1523/JNEUROSCI.3711-11.2012>
- Logothetis, N. K., & Wandell, B. A. (2004). Interpreting the BOLD Signal. *Annual Review of Physiology*, 66(1), 735–769. <https://doi.org/10.1146/annurev.physiol.66.082602.092845>
- Mazoyer, B., Zago, L., Mellet, E., Bricogne, S., Etard, O., Houdé, O., ... Tzourio-Mazoyer, N. (2001). Cortical networks for working memory and executive functions sustain the conscious resting state in man. *Brain Research Bulletin*, 54(3), 287–298. [https://doi.org/10.1016/S0361-9230\(00\)00437-8](https://doi.org/10.1016/S0361-9230(00)00437-8)
- McKhann, G., Drachman, D., Folstein, M., Katzman, R., Price, D., & Stadlan, E. M. (1984). Clinical diagnosis of Alzheimer's disease: report of the NINCDS-ADRDA Work Group under the auspices of Department of Health and Human Services Task Force on Alzheimer's Disease. *Neurology*, 34(7), 939–44. <https://doi.org/10.1212/WNL.34.7.939>
- Mckhann, G. M., Knopman, D. S., Chertkow, H., Hyman, B. T., Jack, C. R., Kawas, C. H., ... Phelps, C. H. (2011). The diagnosis of dementia due to Alzheimer's disease: Recommendations from the National Institute on Aging-Alzheimer's Association workgroups on diagnostic guidelines for Alzheimer's disease. *Alzheimer's & Dementia*, 7, 263–269. <https://doi.org/10.1016/j.jalz.2011.03.005>
- Mesulam, M.-M. (1990). Large-scale neurocognitive networks and distributed processing for attention, language, and memory. *Annals of Neurology*. <https://doi.org/10.1002/ana.410280502>
- Miller, S. L., Celone, K., DePeau, K., Diamond, E., Dickerson, B. C., Rentz, D., ... Sperling, R. A. (2008). Age-related memory impairment associated with loss of parietal deactivation but preserved hippocampal activation. *Proceedings of the National Academy of Sciences of the United States of America*, 105, 2181–2186. <https://doi.org/10.1073/pnas.0706818105>
- Minati, L., Edginton, T., Grazia Bruzzone, M., & Giaccone, G. (2009). Reviews: Current concepts in alzheimer's disease: A multidisciplinary review. *American Journal of Alzheimer's Disease and Other Dementias*, 24(2), 95–121. <https://doi.org/10.1177/1533317508328602>
- Mosconi, L. (2005). Brain glucose metabolism in the early and specific diagnosis of Alzheimer's disease: FDG-PET studies in MCI and AD. *European Journal of Nuclear Medicine and Molecular Imaging*. <https://doi.org/10.1007/s00259-005-1762-7>
- Mutlu, J., Landeau, B., Tomadesso, C., de Flores, R., Mézenge, F., de La Sayette, V., ... Chételat, G. (2016). Connectivity disruption, atrophy, and hypometabolism within posterior cingulate networks in Alzheimer's disease. *Frontiers in Neuroscience*, 10(DEC), 1–10. <https://doi.org/10.3389/fnins.2016.00582>
- Myers, N., Pasquini, L., Göttler, J., Grimmer, T., Koch, K., Ortner, M., ... Sorg, C. (2014). Within-patient correspondence of amyloid- β and intrinsic network connectivity in Alzheimer's disease. *Brain: A Journal of Neurology*, 137(Pt 7), 2052–64. <https://doi.org/10.1093/brain/awu103>

- Passow, S., Specht, K., Adamsen, T. C., Biermann, M., Brekke, N., Craven, A. R., ... Hugdahl, K. (2015). Default-mode network functional connectivity is closely related to metabolic activity. *Human Brain Mapping*. <https://doi.org/10.1002/hbm.22753>
- Pellerin, L., & Magistretti, P. J. (1994). Glutamate uptake into astrocytes stimulates aerobic glycolysis: a mechanism coupling neuronal activity to glucose utilization. *Proceedings of the National Academy of Sciences*, *91*(22), 10625–10629. <https://doi.org/10.1073/pnas.91.22.10625>
- Perry, R. J., Watson, P., & Hodges, J. R. (2000). The nature and staging of attention dysfunction in early (minimal and mild) Alzheimer's disease: relationship to episodic and semantic memory impairment. *Neuropsychologia*, *38*(3), 252–71. Retrieved from <http://www.ncbi.nlm.nih.gov/pubmed/10678692>
- Petersen, R. C. (2004). Mild cognitive impairment as a diagnostic entity. *Journal of Internal Medicine*, *256*(3), 183–94. <https://doi.org/10.1111/j.1365-2796.2004.01388.x>
- Price, J. L., & Morris, J. C. (1999). Tangles and plaques in nondemented aging and "preclinical" Alzheimer's disease. *Annals of Neurology*, *45*(3), 358–68. Retrieved from <http://www.ncbi.nlm.nih.gov/pubmed/10072051>
- Querfurth, H. W., & LaFerla, F. M. (2010). Alzheimer's disease. *The New England Journal of Medicine*, *362*(4), 329–44. <https://doi.org/10.1056/NEJMra0909142>
- Raichle, M. E., MacLeod, a M., Snyder, a Z., Powers, W. J., Gusnard, D. a, & Shulman, G. L. (2001). A default mode of brain function. *Proceedings of the National Academy of Sciences of the United States of America*, *98*(2), 676–82. <https://doi.org/10.1073/pnas.98.2.676>
- Raichle, M. E., & Mintun, M. A. (2006). Brain work and brain imaging. *Annual Review of Neuroscience*, *29*, 449–76. <https://doi.org/10.1146/annurev.neuro.29.051605.112819>
- Reuter-Lorenz, P. A., & Park, D. C. (2010). Human Neuroscience and the Aging Mind: A New Look at Old Problems. *Journal of Gerontology: Psychological Sciences*, *65*(410), 405–415. <https://doi.org/10.1093/geronb/gbq035>
- Reuter-Lorenz, P. A., & Park, D. C. (2014). How does it STAC up? Revisiting the scaffolding theory of aging and cognition. *Neuropsychology Review*, *24*(3), 355–70. <https://doi.org/10.1007/s11065-014-9270-9>
- Riedl, V., Bienkowska, K., Strobel, C., Tahmasian, M., Grimmer, T., Förster, S., ... Drzezga, A. (2014). Local activity determines functional connectivity in the resting human brain: a simultaneous FDG-PET/fMRI study. *The Journal of Neuroscience: The Official Journal of the Society for Neuroscience*, *34*(18), 6260–6. <https://doi.org/10.1523/JNEUROSCI.0492-14.2014>
- Roberts, R., & Knopman, D. S. (2013). Classification and Epidemiology of MCI. *Clinics in Geriatric Medicine*, *29*(4), 753–772. <https://doi.org/10.1016/j.cger.2013.07.003>
- Rombouts, S. A. R. B., Barkhof, F., Goekoop, R., Stam, C. J., & Scheltens, P. (2005). Altered resting state networks in mild cognitive impairment and mild Alzheimer's disease: An fMRI study. *Human Brain Mapping*, *26*(4), 231–239. <https://doi.org/10.1002/hbm.20160>

- Sala-Llonch, R., Fortea, J., Bartrés-Faz, D., Bosch, B., Lladó, A., Peña-Gómez, C., ... Sánchez-Valle, R. (2013). Evolving brain functional abnormalities in psen1 mutation carriers: A resting and visual encoding fMRI study. *Journal of Alzheimer's Disease*, 36(1), 165–175. <https://doi.org/10.3233/JAD-130062>
- Savio, A., Fünker, S., Tahmasian, M., Rachakonda, S., Manoliu, A., Sorg, C., ... Yakushev, I. (2017). Resting state networks as simultaneously measured with fMRI and PET. *Journal of Nuclear Medicine*. <https://doi.org/10.2967/jnumed.116.185835>
- Scheltens, P., Blennow, K., Breteler, M. M. B., de Strooper, B., Frisoni, G. B., Salloway, S., & Van der Flier, W. M. aria. (2016). Alzheimer's disease. *Lancet (London, England)*, 388(10043), 505–517. [https://doi.org/10.1016/S0140-6736\(15\)01124-1](https://doi.org/10.1016/S0140-6736(15)01124-1)
- Seeley, W. W., Crawford, R. K., Zhou, J., Miller, B. L., & Greicius, M. D. (2009). Neurodegenerative diseases target large-scale human brain networks. *Neuron*, 62(1), 42–52. <https://doi.org/10.1016/j.neuron.2009.03.024>
- Sheline, Y. I., & Raichle, M. E. (2013a). Resting state functional connectivity in preclinical Alzheimer's disease. *Biological Psychiatry*, 74(5), 340–7. <https://doi.org/10.1016/j.biopsych.2012.11.028>
- Sheline, Y. I., & Raichle, M. E. (2013b). Resting State Functional Connectivity in Preclinical Alzheimer's Disease. *Biological Psychiatry*, 1–8. <https://doi.org/10.1016/j.biopsych.2012.11.028>
- Shin, J., Kepe, V., Small, G. W., Phelps, M. E., & Barrio, J. R. (2011). Multimodal Imaging of Alzheimer Pathophysiology in the Brain's Default Mode Network. *International Journal of Alzheimer's Disease*, 2011, 1–8. <https://doi.org/10.4061/2011/687945>
- Shirer, W. R., Ryali, S., Rykhlevskaia, E., Menon, V., & Greicius, M. D. (2012). Decoding subject-driven cognitive states with whole-brain connectivity patterns. *Cerebral Cortex (New York, N.Y. : 1991)*, 22(1), 158–65. <https://doi.org/10.1093/cercor/bhr099>
- Shulman, G. L., Fiez, J. A., Corbetta, M., Buckner, R. L., Miezin, F. M., Raichle, M., & Petersen, S. E. (1997). Common Blood Flow Changes across Visual Tasks: 11. Decreases in Cerebral Cortex. *J Cogn Neurosci*, 9(5), 648–663. <https://doi.org/10.1162/jocn.1997.9.5.624>
- Smith, S. M., Fox, P. T., Miller, K. L., Glahn, D. C., Fox, P. M., Mackay, C. E., ... Beckmann, C. F. (2009). Correspondence of the brain's functional architecture during activation and rest. *Proceedings of the National Academy of Sciences*, 106(31), 13040–13045. <https://doi.org/10.1073/pnas.0905267106>
- Sorg, C., Riedl, V., Mühlau, M., Calhoun, V. D., Eichele, T., Läer, L., ... Wohlschläger, A. M. (2007). Selective changes of resting-state networks in individuals at risk for Alzheimer's disease. *PNAS*, 104(47). Retrieved from <http://www.pnas.org/content/suppl/2007/11/02/0708803104.DC1>
- Sorg, C., Riedl, V., Pernecky, R., Kurz, A., & Wohlschläger, A. M. (2009). Impact of Alzheimer's disease on the functional connectivity of spontaneous brain activity. *Current Alzheimer Research*, 6(6), 541–553. <https://doi.org/10.2174/156720509790147106>

- Sperling, R. a, Dickerson, B. C., Pihlajamaki, M., Vannini, P., LaViolette, P. S., Vitolo, O. V, ... Johnson, K. a. (2010). Functional alterations in memory networks in early Alzheimer's disease. *Neuromolecular Medicine*, 12(1), 27-43. <https://doi.org/10.1007/s12017-009-8109-7>
- Tavor, I., Jones, O. P., Mars, R. B., Smith, S. M., Behrens, T. E. J., Jbabdi, S., & Parker Jones, O. (2016). Task-free MRI predicts individual differences in brain activity during task performance. *Science*, 352(6282), 216-220. <https://doi.org/10.1126/science.aad8127>
- Teipel, S., Drzezga, A., Grothe, M. J., Barthel, H., Chételat, G., Schuff, N., ... Fellgiebel, A. (2015). Multimodal imaging in Alzheimer's disease: Validity and usefulness for early detection. *The Lancet Neurology*. [https://doi.org/10.1016/S1474-4422\(15\)00093-9](https://doi.org/10.1016/S1474-4422(15)00093-9)
- Vannini, P., Hedden, T., Huijbers, W., Ward, A., Johnson, K. A., & Sperling, R. A. (2013). The Ups and Downs of the Posteromedial Cortex: Age-and Amyloid-Related Functional Alterations of the Encoding/Retrieval Flip in Cognitively Normal Older Adults. *Cerebral Cortex*, 23, 1317-1328. <https://doi.org/10.1093/cercor/bhs108>
- Vlassenko, A. G., Vaishnavi, S. N., Couture, L., Sacco, D., Shannon, B. J., Mach, R. H., ... Mintun, M. A. (2010). Spatial correlation between brain aerobic glycolysis and amyloid- β (A β) deposition. *PNAS*, 107(41), 17763-17767. <https://doi.org/10.1073/pnas.1010461107>
- Vuilleumier, P., & Driver, J. (2007). Modulation of visual processing by attention and emotion: windows on causal interactions between human brain regions. *Philosophical Transactions of the Royal Society of London. Series B, Biological Sciences*, 362(1481), 837-55. <https://doi.org/10.1098/rstb.2007.2092>
- Wagner, A. D., Shannon, B. J., Kahn, I., & Buckner, R. L. (2005). Parietal lobe contributions to episodic memory retrieval. *Trends in Cognitive Sciences*, 9(9), 445-453. <https://doi.org/10.1016/j.tics.2005.07.001>
- Wang, L., Laviolette, P., O'Keefe, K., Putcha, D., Bakkour, A., Van Dijk, K. R. a, ... Sperling, R. a. (2010). Intrinsic connectivity between the hippocampus and posteromedial cortex predicts memory performance in cognitively intact older individuals. *NeuroImage*, 51(2), 910-7. <https://doi.org/10.1016/j.neuroimage.2010.02.046>
- Wang, P., Zhou, B., Yao, H., Zhan, Y., Zhang, Z., Cui, Y., ... Jiang, T. (2015). *Aberrant intra- and inter-network connectivity architectures in Alzheimer's disease and mild cognitive impairment*. *Nature Scientific Reports* (Vol. 148). <https://doi.org/10.1038/srep14824>
- Ward, A. M., Schultz, A. P., Huijbers, W., Van Dijk, K. R. A., Hedden, T., & Sperling, R. A. (2014). The parahippocampal gyrus links the default-mode cortical network with the medial temporal lobe memory system. *Human Brain Mapping*, 35(3), 1061-1073.
- Weissman, D. H., Roberts, K. C., Visscher, K. M., & Woldorff, M. G. (2006). The neural bases of momentary lapses in attention. *Nature Neuroscience*, 9(7), 971-978. <https://doi.org/10.1038/nn1727>
- Zacks, R. T., Hasher, L., & Li, K. Z. H. (2000). Human Memory. *The Handbook of Aging and Cognition*, 293-357. <https://doi.org/10.3758/s13423-011-0086-9>

- Zhang, Y., Simon-Vermot, L., Araque Caballero, M. Á., Gesierich, B., Taylor, A. N. W., Duering, M., ... Ewers, M. (2016). Enhanced resting-state functional connectivity between core memory-task activation peaks is associated with memory impairment in MCI. *Neurobiology of Aging*, *45*, 43–49. <https://doi.org/10.1016/j.neurobiolaging.2016.04.018>
- Zimmer, E. R., Parent, M. J., Souza, D. G., Leuzy, A., Lecrux, C., Kim, H.-I., ... Rosa-Neto, P. (2017). [18F]FDG PET signal is driven by astroglial glutamate transport. *Nature Neuroscience*, *20*(3). <https://doi.org/10.1038/nn.4492>



06.

APPENDIX



LEE SIMON-VERMOT

NATIONALITIES: Swiss & American

EDUCATION

PHD IN SYSTEMIC NEUROSCIENCES

02/2013 - present | Graduate School of Systemic Neurosciences |

Ludwig Maximilian University | Munich

PhD student at the research group „Brain Imaging and Biomarker Research“ at the Institute for Stroke & Dementia research, Klinikum der Universität München, in Munich, under the supervision of Prof. Michael Ewers.

Thesis title: „Association between Resting-State Functional Connectivity, Glucose Metabolism and Task-Activation of Neural Networks“

MASTER IN NEURO-COGNITIVE PSYCHOLOGY

10/2010 - 08/2012 | Ludwig Maximilian University | Munich

Master thesis: conducted at “Neuro-Kopf-Zentrum”, Klinikum rechts der Isar, Munich, under the supervision of Prof. Christian Sorg. Title: “Aberrant fronto-striatal intrinsic functional connectivity in mild cognitive impairment and Alzheimer’s disease” (grade: 1.0)

Diploma: Master of Science

BACHELOR IN PSYCHOLOGY

09/2007 - 07/2010 | Université de Genève | Geneva, Switzerland

Erasmus Program:

09/2008 - 07/2009 | Institut für Psychologie | Humboldt Universität | Berlin

Diploma: Bachelor in Psychology

MEDICINE

09/2005 - 09/2007 | Université de Genève | Geneva, Switzerland

First year of medical school

CONFERENCES

ORAL PRESENTATIONS

Kongress der Deutschen Gesellschaft für Neurologie, Munich, Germany, Sep. 15th – 19th, 2014.

Advisory board, Munich, Germany, Aug., 2013

The International conference on Basic and Clinical multimodal Imaging (BaCI), University of Geneva, Switzerland, September 4 – 8th, 2013.

POSTER PRESENTATIONS

The Alzheimer's Association International Conference, Washington DC, USA, July 18th – 23th, 2015.

The Alzheimer's Association International Conference, Copenhagen, Denmark, July 12th – 17th, 2014.

LANGUAGES

ENGLISH

Mother tongue

FRENCH

Mother tongue

GERMAN

Fluent speaking
Very good writing



LIST OF PUBLICATIONS

Simon-Vermot L, Taylor ANW, Araque Caballero MÀ, Franzmeier N, Buerger K, Catak C, Janowitz D, Kambeitz-Ilankovic LM, Ertl-Wagner B, Duering M and Ewers M (2018).

Correspondence Between Resting-State and Episodic Memory-Task Related Networks in Elderly Subjects. *Front Aging Neurosci.*, 10, 362. doi: 10.3389/fnagi.2018.00362

Franzmeier N, Göttler J, Grimmer T, Drzezga A, Áraque-Caballero MA, **Simon-Vermot L**, Taylor ANW, Bürger K, Catak C, Janowitz D, Müller C, Duering M, Sorg C, Ewers M. (2017). Resting-State Connectivity of the Left Frontal Cortex to the Default Mode and Dorsal Attention Network Supports Reserve in Mild Cognitive Impairment. *Front Aging Neurosci.*, 9, 264. doi: 10.3389/fnagi.2017.00264.

Franzmeier N, Hartmann JC, Taylor ANW, Araque Caballero MÁ, **Simon-Vermot L**, Buerger K, Kambeitz-Ilankovic LM, Ertl-Wagner B, Mueller C, Catak C, Janowitz D, Stahl R, Dichgans M, Duering M, Ewers M. (2017). Left Frontal Hub Connectivity during Memory Performance Supports Reserve in Aging and Mild Cognitive Impairment. *J Alzheimers Dis.*, 59(4). 1381-1392. doi: 10.3233/JAD-170360.

Franzmeier N, Caballero MÁA, Taylor ANW, **Simon-Vermot L**, Buerger K, Ertl-Wagner B, Mueller C, Catak C, Janowitz D, Baykara E, Gesierich B, Duering M, Ewers M; Alzheimer's Disease Neuroimaging Initiative. (2017). Resting-state global functional connectivity as a biomarker of cognitive reserve in mild cognitive impairment. *Brain Imaging Behav.* 11(2), 368-382. doi: 10.1007/s11682-016-9599-1.

Zhang Y, **Simon-Vermot L**, Araque Caballero MÁ, Gesierich B, Taylor ANW, Duering M, Dichgans M, Ewers M; Alzheimer's Disease Neuroimaging Initiative. (2016). Enhanced resting-state functional connectivity between core memory-task activation peaks is associated with memory impairment in MCI. *Neurobiol Aging*, 45, 43-49. doi: 10.1016/j.neurobiolaging.2016.04.018

Taylor ANW, Kambeitz-Ilankovic L, Gesierich B, **Simon-Vermot L**, Franzmeier N, Araque Caballero MÁ, Müller S, Hesheng L, Ertl-Wagner B, Bürger K, Weiner MW, Dichgans M, Duering M, Ewers M; Alzheimer's Disease Neuroimaging Initiative (ADNI). (2017). Tract-specific white matter hyperintensities disrupt neural network function in Alzheimer's disease. *Alzheimers Dement.* 13(3), 225-235. doi: 10.1016/j.jalz.2016.06.2358

ACKNOWLEDGMENTS

First and foremost, I would like to thank my supervisor Professor Dr. Michael Ewers for giving me the opportunity to complete my PhD. I am very grateful for his guidance, advice and patience.

I am very grateful to my thesis advisory committee. I enjoyed and profited a lot from the fruitful discussions with Professor Dr. Axel Rominger, Professor Dr. Stefan Glasauer and Dr. Christian Vollmar. I thank them for the time they spent to guide me and discuss my project.

Many thanks to the Graduate School of Systemic Neurosciences for their constant support and the wonderful, welcoming and motivating environment they created for their students. I would especially like to thank Lena Bittl for her listening and support during my PhD, she always found solutions to enable me to finalize this thesis.

Finally, my deepest gratitude belongs to my Mother, my Brother, my partner Peter and my friends Myriam and Chloé for their unconditional love and for the many ways they supported me during the last years.

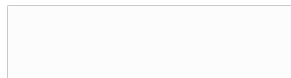


EIDESSTATTLICHE VERICHERUNG / AFFIDAVIT

Hiermit versichere ich an Eides statt, dass ich die vorliegende Dissertation “Association between Resting-State Functional Connectivity, Glucose Metabolism and Task-Activation of Neural Networks” selbstständig angefertigt habe, mich außer der angegebenen keiner weiteren Hilfsmittel bedient und alle Erkenntnisse, die aus dem Schrifttum ganz oder annähernd übernommen sind, als solche kenntlich gemacht und nach ihrer Herkunft unter Bezeichnung der Fundstelle einzeln nachgewiesen habe.

I hereby confirm that the dissertation “Association between Resting-State Functional Connectivity, Glucose Metabolism and Task-Activation of Neural Networks” is the result of my own work and that I have only used sources or materials listed and specified in the dissertation.

Munich, 22.12.2017



Lee Simon-Vermot

DECLARATION OF AUTHOR CONTRIBUTIONS

Project 1:

Intrinsic and episodic memory-task related networks in elderly subjects

Lee Simon-Vermot, Alexander N.W.Taylor, Miguel À Araque Caballero, Nicolai Franzmeier, Katharina Buerger, Lana M. Kambeitz-Ilankovic, Birgit Ertl-Wagner, Marco Duering and Michael Ewers. (2017), in preparation.

The author of this thesis is the first author of the manuscript. ME, MD, LMKI, ANWT & LSV conceived and designed the experiment. ANWT, MÀAC, NK & LSV conducted the fMRI data acquisition. LSV and ANWT analyzed the behavioral and fMRI data. LSV and ME wrote the manuscript, which was commented on and reviewed by ANWT, MÀAC, NK, KB, LMKI, BEW & MD.

Project 2:

FDG-PET metabolism and resting-state network connectivity are associated in early Alzheimer's disease

Lee Simon-Vermot, Nicolai Franzmeier, Yifei Zhang, Jinyi Ren, Miguel Á. Araque Caballero, and Michael Ewers, for the Alzheimer's Disease Neuroimaging Initiative (ADNI). (2017). Under review.

The author of this thesis is the first author of the manuscript. ME & LSV designed the research experiment. LSV analyzed fMRI. LSV & MÀAC analyzed the FDG-PET data. LSV conducted the statistical analysis with the help of YZ & JR. LSV, NF & ME wrote the manuscript, which was commented on and reviewed by MÀAC, NK, YZ & JR.

Munich, 21 December 2017

Michael Ewers